Mechanisms of PROX1 mediated regulation of the lymphatic endothelial cell cycle

By

Shannon A. Baxter

A Thesis submitted to the

Faculty of Graduate Studies of the

University of Manitoba

in partial fulfilment of the requirements of the degree of

MASTER OF SCIENCE

Department of Biochemistry and Medical Genetics

University of Manitoba

Institute of Cardiovascular Sciences

St. Boniface Hospital Research Centre

Winnipeg, MB

Canada

To my parents, Kerry and Lynda Baxter, sister Daron, and Kurt.

You are wonderful, and it means so much to have you as my cheering section!

ACKNOWLEDGEMENTS

This has been quite the ride, with highs, lows, and everything in between. I would first like to thank my advisor, Dr. Jeffrey Wigle for sharing his scientific expertise, guidance, patience, support and encouragement throughout my entire tenure in his lab. I have learned a ton, ranging from techniques in the lab, to effectively reading papers and presenting in front of a large group, to managing multiple tasks and getting them done. You've supported me through some tricky decisions, and I appreciate the time and effort that you've put into my education. I hope that someday you will discover how kinda, sorta, maybe, really fantastic pumpkin coffee truly is!

I would also like to thank my committee members: Dr. David Eisenstat, Dr. Spencer Gibson, Dr. Michael Mowat and Dr. Ian Dixon. You've been super in attending committee meetings, reading through drafts and rewrites of my paper, writing reference letters, and allowing me access to equipment and lab resources that weren't readily available at St. B. Thank you for your hard work, input and participation. David, your lab turned into my home away from home at CancerCare, and I spent lots of time getting to know your crew and poaching either expertise or space…or sharing corny jokes and trading Coldplay and music repertoires with Mario and Vanessa. I always felt welcome, and your door was always open if I needed a second opinion to weigh in on anything. I also need to thank Dr. Louise Simard, who provided me with space in her lab when I needed it, and great feedback on troubleshooting and interpreting experiments, as well as Dr. Steve Pind for all of his support and encouragement along the way.

I used many, many instruments and pieces of equipment that didn't belong to our lab directly throughout my tenure. Most of which came to be when I turned up on the lab's doorstep, introduced myself, and informed them I was there to do whatever it took to learn how to use whatever instrument I had my eye on. I have to thank Robert Fandrich, Dr. Elissavet Kardami (St. B), and Liz Henson (MICB) for spending hours with me training and helping me get my driver's licence to use their confocal microscopes. I also need to thank Ludger Klewes (MICB) for his guidance and expertise in getting me up and rolling with the flow cytometer. He truly is the Pope of flow cytometry, and always had an answer to my questions, be it a technical issue or simply booking time on the cytometer. I was fortunate to receive a graduate studentship from the Manitoba Health Research Council for most of my time in the lab, and thank them for their support.

And then, there were the instruments, space and equipment that belonged to Jeff's lab. I have to thank all of my lab mates for their expertise, help, and fun times throughout my time in the lab. Davio, the multitalented, who is the resident lunch inspector, radio, luciferase master and saved the day for any cloning experiment (I'm specifically thinking about E2F cloning and the 60+ minipreps); Teri who cultured cells and was the lab mother keeping all of the kids in the playpen in line; Patty who helped me learn the tricks of the trade in the beginning and passed me a great project to work on; Mehdi who still hasn't figured out what the half-life of PROX1 is; and Joe, Marino, Trisha and Eman who had the best laughs and one liners to keep things interesting.

Finally, to my friends and family who patiently waited for me to “call when I was done in the lab”: your support and encouragement has been amazing, and I honestly would not have been able to accomplish this without you. Joyo and Selena, who left the pinkest cake I’ve ever seen on my doorstep, we’ve come a long way from sitting in first year chimie wondering if it was a toupee or if it was M. Boisvert’s real hair. Pamela, Jill and Jennifer who have been part of organizing and instigating knitting and perogy nights and are the best part of the Morden Corn and Apple Festival, Vanessa for constantly one up-ing me with her nerdiness and pop culture, and to Cheryl, my dear, who held the cattle prod with a kind but stern heart. You went above and beyond the call to keep me from joining the circus, and it means a lot to me.

I’m fortunate to belong to a close, supportive, incredible family in which we are very much each other’s fan club. They have all set quite the example of how to enjoy life to the fullest, and have been supportive of any activity or crazy idea that I’ve had. There has never been any question that I could do whatever I wanted in life, but the bottom line was always that although I would need to lead the charge to get there, they’d be following closely behind to live vicariously and keep pushing. I have yet to choose the easy road to do anything, but my family is always there to celebrate the successes, commiserate and re-strategize near misses, and encourage every step along the route. You were my roadie’s when I just needed to run in for a sec to change media, my practice audience for all of my posters and presentations, spent countless hours waiting in front of the Research Centre, and my sounding board. From Lac Heney and Ottawa, to California, to Shunzhen, China, and back to Gull

Lake and Winnipeg, thank you so much for all of your support and encouragement; it has been so much fun to share the adventure with all of you so far. I'm almost done in the lab, and will be free to put in the dock whenever you're ready!

S. A. B, 2012

TABLE OF CONTENTS

ABSTRACT

The homeobox transcription factor PROX1 is the mammalian ortholog of the *Drosophila* gene *Prospero*. Expression of PROX1 in a subset of venous endothelial cells changes their fate to lymphatic endothelial cells (LEC). PROX1 is required for lymphatic development as *Prox1* null mice lack all lymphatic vasculature. PROX1 has been shown to have cell-type dependent roles in regulating the cell cycle. We hypothesize that PROX1 functions as a key cell cycle regulator in LECs and promotes their cell cycle progression. In this study, immunocytochemistry, western blotting and luciferase assays were used to characterize PROX1 mediated activation of the mouse *Ccne1* promoter. Following deletion of the Prospero 1 domain (PD1Δ), the resulting PROX1 protein is localized to both the nucleus and the cytoplasm. We have determined that PROX1 requires both E2F binding sites located in the *Ccne1* promoter to activate transcription of the gene. We observed that siRNA knockdown of *Prox1* reduced CYCLIN E1 protein levels as well as decreased cellular proliferation in LECs. In contrast, overexpression of a version of PROX1 in which the homeodomain and Prospero domain 2 (HDPD2Δ) were deleted increased CYCLIN E1 protein levels in human umbilical vein endothelial cells (HUVEC), but resulted in the arrest of cells in the G_1 phase. We have also established that PROX1 is phosphorylated in primary human LECs. We have shown a role for the PD1 domain in mediating PROX1 subcellular localization and we have observed that the expression of the HDPD2Δ version of PROX1 blocks proliferation in HUVECs. We are the first to demonstrate a role for PROX1 as a transcriptional co-activator and to establish that PROX1 is phosphorylated in LECs.

LIST OF FIGURES AND TABLES

Literature Review

Results

LIST OF COPYRIGHT MATERIAL FOR WHICH PERMISSION WAS OBTAINED

Figure 5-7, 9, 14-20, 24-30. (Baxter *et al.* 2011) Elsevier

LIST OF ABBREVIATIONS

µ	microunits
7-AAD	7-aminoactinomycin-D
AF-2	Nuclear receptor co-activator 2
Ang2	Angiopoietin 2
APC	Adenomatous polyposis coli
BEC	Blood endothelial cell (either arterial or venous)
bFGF	Beta fibroblast growth factor
BrdU	5-bromo-2'-deoxyuridine
CCL21	Chemokine C-C motif ligand 21
CCNE1	Cyclin E1 protein
Ccne1	Cyclin E1 gene
CCR7	C-C chemokine receptor type 7
Cdk	Cyclin dependent kinase
CDKI	Cyclin dependent kinase inhibitor
CIAP	Calf intestine alkaline phosphatase
CLEC-2	C-type lectin receptor
CMV	Cytomegalovirus
CO_2	Carbon dioxide
COUP-TFII	Chicken ovalbumin promoter transcription factor II
CYP7A1	Cholesterol 7 alpha hydroxylase gene
CYP7α1	Cholesterol 7 alpha hydroxylase protein
Da	Dalton
DAPI	4',6-diamidino-2-phenylindole

Dll4	Delta-like ligand 4
DMEM	Dulbecco's modified Eagle's medium
DNA	Deoxyribonucleic acid
EBM-2	Endothelial basal medium
EGF	Epidermal growth factor
EMSA	Electrophoretic mobility shift assay
EPHB2	Ephrin B2
ESAM	Endothelial specific adhesion molecule
Ets	E-twenty six transcription factor
FBS	Fetal bovine serum
FGFR-3	Fibroblast growth factor receptor 3 gene
FGFR-3	Fibroblast growth factor receptor 3 protein
FOXC2	Forkhead box protein C2
g	grams
HD	Homeodomain
HEK 293	Human embryonic kidney 293 cell line
HepG2	Human hepatocellular carcinoma cell line
HLTS	Hypotrichosis-lymphedema-telangiectasia syndrome
HUVEC	Human umbilical vein endothelial cells (primary)
ICAM	Intercellular adhesion molecule
IGF	Insulin-like growth factor
kDa	kiloDalton
L	Litres
LD	Lymphedema distichiasis
LEC	Lymphatic endothelial cell

LMB	Leptomycin B
LYVE-1	Lymphatic vessel endothelial hyaluronan receptor
m	milliunits
M	moles/litre
Mac-1	Macrophage antigen 1
MOI	Multiplicity of infection
n	nanounits
N	Normals
NEM	N-ethylmalimide
NES	Nuclear export signal
NF-κB	Nuclear factor kappa B
NKX2.1	NK2 homeobox 1
NLS	Nuclear localization signal
NR box	Nuclear receptor box
NRP	Neuropilin
p	picounits
PBS	Phosphate buffered saline
PCNA	Proliferating cell nuclear antigen
PCR	Polymerase chain reaction
PD1	Prospero domain 1
PD2	Prospero domain 2
PDGF-β	Platelet derived growth factor beta
PDX1	Pancreatic and duodenal homeobox 1
PGC-1α	Peroxisome proliferator-activated receptor gamma co-activator 1α
PI	Propidium iodide

pRB	Retinoblastoma protein
Prox1	Prospero related homeobox gene 1
PROX1	Prospero related homeodomain protein 1
RaOp	Ragged Opossum
RNA	Ribonucleic acid
SDS-PAGE	Sodium dodecyl sulfate polyacrylamide gel electrophoresis
siRNA	Small interfering RNA
SIX1	SIX homeobox 1
SLP76	Lymphocyte cytosolic protein
Sox18	SRY- box 18 gene
SOX18	SRY- box 18 protein
SUMO	Small ubiquitin-like modifier
Syk	Spleen tyrosine kinase
TCF	T-cell specific HMG-box
Tie2	Tunica internal endothelial cell kinase 2
U2OS	Human U2 osteosarcoma cell line
VEGF-C/D	Vascular endothelial growth factor C or D protein
VEGFR-3	Vascular endothelial growth factor receptor 3 gene
VEGFR-3	Vascular endothelial growth factor receptor 3 protein
VSMC	Vascular smooth muscle cell

I. LITERATURE REVIEW

1. Discovery and characterization of the lymphatic system

1.1. History

The lymphatic system is composed of the lymphatic vasculature and the lymphoid organs, namely the spleen and the lymph nodes. During embryonic development, the lymphatic and blood vasculature systems share some common features, although the two systems are functionally and molecularly distinct (Hirakawa *et al.* 2003). The lymphatic vasculature was first characterized in 1627 by an Italian scientist, Gasparo Aselli, who described “milky veins” (lacteals) in the mesentery of a recently fed dog. In 1902, Florence Sabin proposed a model of the development of the lymphatic vasculature, which is the basis of current studies of lymphatic development (Sabin 1902; Wigle and Oliver 1999). She injected pig embryos with dye and observed that the lymphatic vasculature budded off from the developing blood vasculature and these sacs continued to grow and develop into the mature lymphatic system (Sabin 1902). An alternative model was proposed in 1910 in which mesenchymal cells formed the primary lymph sacs independently from the blood vasculature and then eventually merged with the venous circulation (Huntington 1910). Sabin’s hypothesis has been supported by studies of different molecular markers that are crucial to specific steps and processes during lymphatic development (Wigle and Oliver 1999; Hirakawa *et al.* 2003).

1.2. General properties of the lymphatic vasculature

The main functions of the lymphatic system are to: 1) return excess extracelluar fluid from the tissues to the venous circulation; 2) ensure efficient trafficking of immune cells; and 3) aid in the absorption of fatty acids from the gut (Tammela and Alitalo 2010; Wang and Oliver 2010). The lymphatic system is fully independent of the blood vascular network with the exception of two junctions with the venous system, which are at the junction of the left or right subclavian veins and the respective internal jugular veins. The lymphatic system is composed of thin-walled, blunt-ended vessels that are found in most tissues with the exception of the bone marrow and the central nervous system. These capillaries are found adjacent to blood capillary beds and connect back to larger collecting lymphatic vessels. Lymphatic capillaries are composed of a single layer of endothelial cells that are linked together by specialized cell-cell junctions. These structures, known as "button-like" junctions, create a discontinuous seal between two neighbouring endothelial cells, which facilitates leukocyte extravasation and passage of lymph through the spaces created between the junction sites (Baluk *et al.* 2007). This structural organization accounts for the high permeability of lymphatic capillaries and is essential for their overall function. The capillaries are also linked to the surrounding tissue by specialized anchoring filaments (Rossi *et al.* 2007). These anchoring filaments project into the neighbouring tissue and allow the vessel to expand and contract in response to changes in tissue interstitial pressure. If there is a low volume of excess fluid and the interstitial pressure is decreased, the vessel will collapse and be unable to accept lymph. In contrast, if there is increased interstitial pressure in the

tissue, the vessel will open and be able to accept lymph (Baluk *et al.* 2007; Wang and Oliver 2010). This pressure sensing mechanism is essential for the regular functioning of the vessel and allows it to rapidly adapt to changes in interstitial pressure.

Lymphatic circulation is unidirectional and flows from the tissues back into the venous circulation. In humans, the left side, encompassing the lower limbs and the abdomen, drains into the thoracic duct, which is the largest lymphatic vessel in the body (Tammela and Alitalo 2010). The right side, including the head, neck and right arm, drains into the right lymphatic trunk. These two collecting vessels connect to the blood circulation via the left and right subclavian veins, respectively (Tammela and Alitalo 2010). In contrast to the blood vasculature, there is no central pump for the lymphatic vasculature. As such, flow of lymph through the vessels and nodes of the system is achieved by a combination of: 1) muscle contractions from surrounding skeletal muscle; 2) presence of unidirectional valves inside the collecting vessels; and 3) the spontaneous contractile activity of collecting vessels. These collecting vessels, in contrast to the highly permeable capillaries, are surrounded by a smooth muscle layer and pericytes, which is an organization more similar to veins. Each section of collecting vessel that spans between two valves is referred to as a lymphangion and forms a single uni-directional pumping unit (Quick *et al.* 2007). Increased volume and pressure on one side of the valve causes it to open and allows lymph to flow from one lymphangion into the next. Increased pressure on the other side of the valve causes it to close and maintains proper uni-directional flow. Once in the neighbouring lymphangion, spontaneous contractions of the surrounding smooth muscle cells push

the lymph into the next lymphangion (Quick *et al.* 2007). This allows the vessel to pump more frequently under conditions where there is a high volume of lymph (Tammela and Alitalo 2010; Wang and Oliver 2010).

2. Diseases affecting the lymphatic system

2.1. Role of lymphatics during inflammation

One of the main functions of the lymphatics is to provide a conduit for immune cells (Wang *et al.* 2010). This role can be divided into two categories: 1) to transport immune cells such as leukocytes, including T and B lymphocytes to sites of injury or inflammation; and 2) to remove these same cells from sites following successful wound healing. Immune cells are able to readily pass across the walls of lymphatic capillaries, through the spaces between the button-like junctions of adjacent lymphatic endothelial cells (LEC). Lymph naturally contains a basal level of circulating immune cells ready to mobilize in the event of an injury requiring their function. Following an injury, LECs will secrete pro-inflammatory cytokines such as chemokine C-C motif ligand 21 (CCL21), which is a ligand for the C-C chemokine receptor type 7 (CCR7) receptor found on the surface of T cells, that will attract immune cells to the affected area (Forster *et al.* 2008). LECs play a role in the maturation of dendritic cells by expressing intercellular adhesion molecule (ICAM) receptors that can interact with macrophage antigen 1 (Mac-1) receptors on the immature dendritic cells preventing their differentiation into mature cells and slowing

the inflammatory response (Podgrabinska *et al.* 2009). VEGFR-3 also has a role in mediating the inflammatory response in LECs (Flister *et al.* 2010). Both PROX1 and nuclear factor kappa B (NF-κB) bind to the *VEGFR-3* promoter following an inflammatory cue and synergistically activate transcription. This same group (Flister *et al.* 2010) also demonstrated that PROX1 levels increase following NF-κB stimulation and propose that NF-κB has a role in regulating PROX1 expression during inflammation. In turn, this promotes lymphangiogenesis through VEGFR-3 up-regulation and increases sensitivity of the affected vessels to the vascular endothelial growth factor C (VEGF-C) and VEGF-D signals that increase as part of the inflammatory response (Flister *et al.* 2010; Tammela and Alitalo 2010). Taken together, these observations provide a mechanism whereby PROX1 regulates the most common form of adult lymphangiogenesis (Mouta *et al.* 2003).

Alternatively, under circumstances of chronic inflammation such as rheumatoid arthritis or psoriasis, increased lymphangiogenesis has a negative effect and exacerbates the symptoms of the disease. In this instance, strategies to block lymphangiogenesis will be beneficial for slowing or preventing continued inflammation. Inflammatory lymphangiogenesis has also been observed in transplant rejection. Increased lymphangiogenesis following kidney transplant allows access for host immune cells and promotes an immune response, leading to eventual destruction and rejection of the allograft (Kerjaschki *et al.* 2004).

2.2. Lymphedema

Lymphedemas are the result of insufficient drainage of the extremities by the lymphatics (Warren *et al.* 2007). This reduced function causes swelling of the affected limbs due to accumulation of the excess fluid in the lymphatic capillaries. This swelling can be painful and lower the overall quality of life of an affected individual. Secondary effects caused by the pooled lymph in the extremities include chronic inflammation due to the rich protein concentration in lymph, reduced immune response and poor circulation of immune cells, and accumulations of subcutaneous fat deposits (Wang and Oliver 2010). Treatment for lymphedema remains limited to manual massage to move the lymph through the vessels and into the collecting system, compression bandages and surgery to remove fat deposits and fluid. Lymphedema is classified into two different types: primary lymphedema, which is of genetic origin, and secondary lymphedema, which is caused by damage to or blockage of existing lymphatic vessels (Warren *et al.* 2007; Wang and Oliver 2010).

2.2.1. Primary Lymphedema

The genetic origins of lymphedema are caused by mutations in various genes that are crucial for developmental lymphangiogenesis (Wang and Oliver 2010). Milroy's disease is caused by a heterozygous missense point mutation in the tyrosine kinase region of the *VEGFR-3* gene (Karkkainen *et al.* 2004; Spiegel *et al.* 2006; Warren *et al.* 2007). VEGFR-3 is one of the key signaling pathways involved in both development of the blood and lymphatic vasculature (Dumont *et al.* 1998). The

Milroy mutation abolishes the kinase activity of the domain and as such creates a dominant negative version of the receptor, which competes for stimulation by VEGF-C with the wild-type receptors (Karkkainen *et al.* 2004).

Lymphedema-distichiasis (LD) is caused by mutations in the *forkhead box protein* (*FOXC2)* gene (Fang *et al.* 2000; Erickson *et al.* 2001; Dagenais *et al.* 2004). FOXC2 is important for valve formation and vascular smooth muscle cell recruitment in the collecting lymphatics (Petrova *et al.* 2004). Onset of LD symptoms occurs after puberty and a particular feature of this type of hereditary lymphedema is the presence of distichiasis or a second row of eyelashes on affected individuals (Fang *et al.* 2000). Unlike Milroy's disease, there is not one particular mutation that is associated with development of LD. Instead there are multiple mutations and insertions associated with this disease that cause either premature truncations or missense mutations of the FOXC2 protein (Fang *et al.* 2000; Erickson *et al.* 2001). In LD patients, the collecting lymphatics are leaky and inefficient at returning lymph to the venous circulation (Petrova *et al.* 2004).

Hypotrichosis-lymphedema-telangiectasia syndrome (HLTS) is characterized by the presence of little or no hair at birth and the further progressive loss of hair, no eyebrows, severe lymphedema of the extremities into childhood and multiple subcutaneous hemorrhages on the palms of the hands and soles of the feet (Irrthum *et al.* 2003). This form of hereditary lymphedema is extremely rare and has currently been documented in only three families (Irrthum *et al.* 2003). HLTS is caused by a mutation in the coding region of the *SRY-box 18* (*SOX18)* gene, which results in a frame-shift and results in the production of a dominant negative version of the wild-

type protein (Irrthum *et al.* 2003). The mouse model of this familial lymphedema is the Ragged Opossum model (*RaOp*) and shows similar characteristics as the human disease, but also has defects in pericyte recruitment to both blood and lymphatic vessels and multiple dermal hemorrhages due to endothelial cell hyperplasia (Downes *et al.* 2009).

2.2.2. Secondary Lymphedema

Secondary lymphedemas are also known as acquired lymphedema because they are caused by either damage or blockage to a normally functioning lymphatic vasculature (Tammela and Alitalo 2010). These diseases are much more common than primary lymphedemas, accounting for the majority of cases (Warren *et al.* 2007). In the developing world, infection from the parasitic worm *Wuchereria bancrofti* (filariasis) is often the cause of secondary lymphedema (Pfarr *et al.* 2009). The worms live and reproduce in the lymphatics, but the disease does not occur until adult worms die and lodge in the lymphatics where they block lymph flow. This results in a local increase in VEGF-C/D production which leads to an inflammatory response that produces pro-lymphangiogenic growth factors and dilates the existing vessels in an attempt to re-establish flow (Pfarr *et al.* 2009). This immune response causes the dilated vessels to weaken and become inefficient at transporting lymph, specifically from the legs, which causes fluid accumulation (lymphedema) (Pfarr *et al.* 2009).

Alternatively, secondary lymphedema is common following therapy for breast, ovarian, or prostate cancer and is prevalent in developed countries (Paskett *et al.* 2012). Following surgical removal of breast tumours, approximately 42% of women report symptoms of lymphedema within five years (Norman *et al.* 2009). Radiation is highly damaging to the vessels and impairs their ability to efficiently transport lymph from the extremities (Cormier *et al.* 2010). This results in accumulation of fluid and swelling of the affected limb and requires massage or compression bandages to manually drain the lymph (Cormier *et al.* 2010; Norman *et al.* 2009). As well, lymph nodes adjacent to the primary tumour site are often removed and biopsied to determine if there is evidence of metastases (Paskett *et al.* 2012; Cormier *et al.* 2010). This surgical destruction of tissue can also impair the flow of lymph and result in secondary lymphedema. Further studies into the molecular mechanisms required to regenerate or repair damaged lymphatic vessels will provide new strategies to treat secondary lymphedemas.

2.3. Tumour metastasis: role of the lymphatic vessels

A key step in the progression of a variety of solid tumours is the invasion of tumour cells into the lymphatic vasculature and subsequent spread to neighbouring lymph nodes (Sahai 2007). Once a tumour has entered the lymphatics, it can disseminate and form secondary tumours that are often more difficult to treat than the original primary tumour (Sahai 2007; Wang and Oliver 2010). Further studies to

better understand how tumours invade the lymphatic system will be beneficial in designing approaches to slow cancer progression.

The lymphatics are an accessible conduit for metastasizing tumour cells due to their high permeability, specialized intercellular junctions and generally low shear stress (Sahai 2007; Wang and Oliver 2010). These features of the lymphatics are crucial for the normal function of the vessels, but renders them susceptible to invasion by neighbouring tumour cells. Detection of tumour cells in the lymph nodes is an important diagnostic tool used for both disease staging and creation of a treatment plan (Qiao *et al.* 2012). The implication of tumour cells in neighbouring lymph nodes is currently unclear but could be: 1) the cells are trapped in the dense lymph node and this creates a lag phase in disease spread; 2) the cells are an indicator of active tumour spread; or 3) the cells colonize the lymph node and form a secondary tumour which can function as a staging area for future spread (Joyce and Pollard 2009; Sleeman and Thiele 2009; Tammela and Alitalo 2010). Invasion of tumour cells into the lymphatics can occur by tumour cell migration and entry into either pre-existing lymphatic capillaries or into tumour induced newly formed lymphatics (lymphangiogenesis) (Figure 1) (Tammela and Oliver, 2010). Tumour cells, tumour associated activated macrophages and stromal cells can secrete pro-lymphangiogenic growth factors such as VEGF-C/D and C-C chemokine receptor type 7 (CCR7), which promotes peri-tumoural lymphangiogenesis (Christiansen *et al.* 2011). These growth factors also cause neighbouring pre-existing lymphatic vessels to expand and dilate which makes them more susceptible to migrating tumour cells (Christiansen *et al.* 2011). Blocking VEGFR-3 signaling with neutralizing antibodies

or soluble VEGFR-3 significantly decreases peri-tumoural lymphangiogenesis. Similarly, neuropilin 2 (NRP-2) is often over-expressed in solid tumours and its blockade with neutralizing antibodies prevents cell migration and slows metastasis (Christiansen *et al.* 2011). Interestingly, molecular differences between tumour associated lymphatic capillaries and normal lymphatic capillaries have been identified (Clasper *et al.* 2008). In this study, the expression profiles between LECs isolated from tumour associated vessels versus LECs isolated from normal vessels were compared and significant changes in approximately 800 genes were observed. Notably, genes that are involved in the formation of intercellular junctions, extracellular matrix deposition and vessel growth and patterning were up-regulated in the tumour associated vessels. Specifically, endothelial specific adhesion molecule (ESAM) expressing vessels showed a positive correlation with metastasis to neighbouring lymph nodes (Clasper *et al.* 2008). Understanding the molecular differences between these two populations of LECs may provide clues as to which pathways are being altered to promote metastasis and will lead to novel strategies to block these pathways.

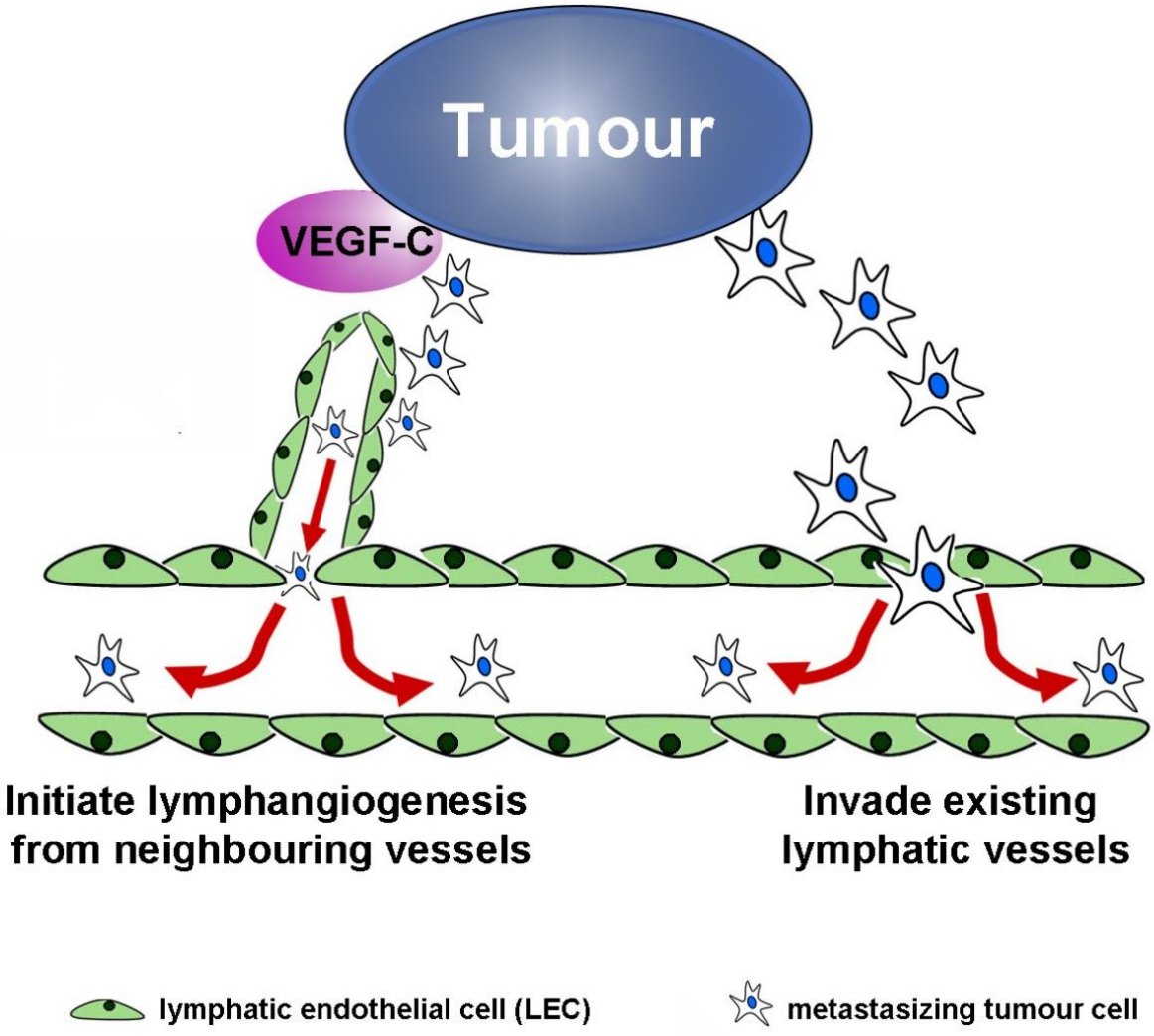
Tumour
VEGF-C
Initiate lymphangiogenesis from neighbouring vessels
Invade existing lymphatic vessels
lymphatic endothelial cell (LEC)
metastasizing tumour cell

Figure 1: Role of peri-tumoural lymphangiogenesis in metastasis. A common step in cancer progression is the invasion of metastasizing cells into the lymphatic vessels. This step leads to formation of secondary tumours. Generally, there are two methods used by metastatic tumours to invade the lymphatic vasculature. First, it has been shown that tumours are capable of inducing sprouting lymphangiogenesis from adjacent lymphatic vessels by producing pro-lymphangiogenic growth factors such as VEGF-C. Second, tumour cells can migrate through the extracellular matrix and directly invade neighbouring lymphatic capillaries. Once in the lymphatics, the metastatic cells will migrate towards afferent lymph nodes and continue the progression of the disease.

2.4. Obesity and Metabolism

The lymphatics play a prominent role in normal fat absorption (Harvey *et al.* 2005; Lim *et al.* 2009; Wang and Oliver 2010). Lacteals, which are found in the intestinal microvilli, contain specialized lymphatic vessels that are responsible for the uptake of dietary fats from the gut. These vessels are often white in appearance and are filled with fat. They are connected to the mesentery and are the "milky veins" that were originally characterized by Aselli in 1627. *Prox1*$^{+/-}$ mice have been demonstrated to have leaky vessels due to reduced vessel integrity, which results in adult onset obesity in the affected mice (Harvey *et al.* 2005). Similarly, the frequently used *Apolipoprotein* (*ApoE)* knockout mouse model has swollen and leaky lymphatic vessels (Lim *et al.* 2009). Loss of *ApoE* affects lymph transport, and the same group proposes a potential link between increased cholesterol levels and decreased lymphatic function (Lim *et al.* 2009). As well, subcutaneous fat accumulation is a common symptom of prolonged lymphedema and lymph promotes the maturation of adipocytes (Warren *et al.* 2007). Taken together, the lymphatics have a crucial role in mediating fat absorption, metabolism and storage.

3. *Prospero*-related homeobox protein 1 (PROX1)

3.1. General features of PROX1

PROX1 is the mammalian ortholog of the *Drosophila melanogaster* gene *Prospero* and was first identified in the mouse in 1993 (Oliver *et al.* 1993). In

Drosophila, *Prospero* is involved in asymmetric cell division in the developing nervous system and gets its name from Prospero, the wizard in the Shakespearean play *The Tempest,* as it similarly dictates the fate of the cells which express it (Chu-Lagraff *et al.* 1991). Prospero works together with Numb to control a binary switch during development of the central and peripheral nervous system (Choksi *et al.* 2006). Numb is a potent inhibitor of Notch signaling and is often down-regulated in human cancers. Loss of Numb function leads to aberrant activation of Notch signaling and increased proliferation. In fly neuroblasts, Numb and Prospero are localized to the cytoplasm and form a crescent shaped band just below the cell membrane at one end of the cell. When the neuroblast divides, it undergoes asymmetric division to produce a self-renewing stem cell like daughter cell, which does not contain Numb or Prospero, and a ganglion mother cell, which expresses both Numb and Prospero. Prospero translocates into the nucleus and the ganglion mother cell further differentiates and divides asymmetrically to generate either neuronal or glial cells. In the fly, both Numb and Prospero repress cell cycle genes such as Cyclin E, E2F, and Cyclin A (Li *et al.* 2000) and block proliferation. Loss of either Numb or Prospero in the ganglion mother cell results in uncoordinated proliferation, differentiation, and improper development of the nervous system. The ganglion mother cell is not produced and the self-renewing daughter cells that are produced continue to proliferate in an uncontrolled manner and eventually form a mass. To this end, both Numb and PROX1 are proposed to function as tumour suppressors (Choksi *et al.* 2006).

PROX1 is widely expressed and can be found in the lens, liver, pancreas, spinal cord, and lymphatic vasculature (Wigle *et al.* 1999; Wigle and Oliver 1999; Sosa-Pineda *et al.* 2000; Wang *et al.* 2005; Misra *et al.* 2008). In mammals, *Prox1* encodes a 737 amino acid protein, which has a predicted molecular weight of 83 kDa. In the N-terminus of the protein, there is the nuclear localization signal (NLS), which directs the protein to the nucleus and two nuclear receptor boxes (NR1 and NR2). These nuclear receptor boxes have been shown to be crucial for PROX1's role as a transcriptional co-activator at the *cholesterol 7α hydroxylase* (*CYP7A1*) promoter, a key regulator of bile acid synthesis *(Qin et al.* 2004). Following the NR boxes, there is an evolutionary conserved region known as the Prospero domain 1 (PD1), which shares homology with the recently characterized PROX2 protein (Pistocchi *et al.* 2008). The function of this domain remains unknown although it is highly evolutionarily conserved from humans through to zebrafish. The C-terminus of PROX1 encodes the DNA binding domain that is composed of the highly conserved homeodomain and the Prospero domain 2 (PD2). The homeodomain (HD) encodes the canonical helix-turn-helix binding motif, but PROX1 contains a three amino acid insertion between helices 2 and 3, which defines it as an atypical homeodomain protein (Ryter *et al.* 2002). The PD2 domain is common among all PROX1 orthologs and masks a nuclear export signal (NES) in the homeodomain, which results in PROX1 being retained in the nucleus. Rather than binding to the ATTA/TAAT site that is common for other homeobox transcription factors, PROX1 binds to a specific DNA consensus sequence C(A/T)(C/T)NNC(T/C) (Hassan *et al.* 1997; Cook *et al.* 2003).

3.2. Biochemical functions of PROX1

PROX1 has a diverse set of functions that are dependent on the cell type and microenvironment in which PROX1 is being expressed. As a transcription factor, PROX1 has been shown to function as a co-repressor (Qin *et al.* 2004), an activator (Shin *et al.* 2006), a repressor (Chang *et al.* 2012) and, in this study, a co-activator (Baxter *et al.* 2011). In the adult liver, PROX1 functions as a co-repressor of the *CYP7A1* promoter (Qin *et al.* 2004). CYP7α1 is the rate limiting enzyme during bile acid synthesis and contains a liver receptor homolog-1 response element (LRE). PROX1 binds directly to either the DNA-binding domain or the ligand-binding domain of liver receptor homolog 1 (LRH-1) and inhibits transcription of the *CYP7A1* promoter. Qin *et al.,* proposed that PROX1 functions either by destabilizing LRH-1 binding to DNA or by sequestering LRH-1 from binding to the promoter to block transcription (Qin *et al.* 2004). Interestingly, PROX1 also interacts with another regulator of the *CYP7A1* promoter, hepatocyte nuclear factor 4α (HNF4α) (Song *et al.* 2006). In this instance, PROX1 binds directly to the AF2 domain in HNF4α via its NR boxes and again functions as a co-repressor to block transcription of the *CYP7A1* promoter. In contrast to the mechanism used for LRH-1 mediated repression, PROX1 does not affect HNF4α DNA-binding and instead competes with a transcriptional co-activator, peroxisome proliferator-activated receptor gamma co-activator-1α (PGC-1α) for the same nuclear receptor co-activator 2 (AF-2) binding site (Song *et al.* 2006). To support the cell-type specificity of PROX1, in murine fetal hepatoblasts, which are a type of hepatic progenitor cells, PROX1 over-expression following retrovirus infection increased the transcription of the *Lrh-1* gene, but

inhibited its function at the *p16*^{ink4a} promoter, and had no effect on the levels or the function of *Hnf-4α* (Kamiya *et al.* 2008).

PROX1 binds directly to DNA to function as a transcriptional activator at the *βB1-crystallin* promoter in the lens (Cui *et al.* 2004; Chen *et al.* 2008) and the *fibroblast growth factor receptor-3* (*FGFR-3*) promoter in the lymphatic endothelial cells (LECs) (Shin *et al.* 2006). In the lens, the *βB1-crystallin* promoter contains two types of PROX1 binding sites. The first type of site is an OL2 element that contains the previously mentioned consensus PROX1 binding site (**CA**CTTCC), which is required for PROX1 activation of transcription from the *βB1-crystallin* promoter (Cui *et al.* 2004). This site has a CA dinucleotide group that is necessary for PROX1 binding and is also found in the *FGFR-3* promoter (Shin *et al.* 2006). The second type of binding sites contain an AG dinucleotide motif that is necessary for PROX1 mediated repression (Chen *et al.* 2008). Two of these PROX1 binding sites (AA**AG**TGG) were identified in the *βB1-crystallin* promoter that following PROX1 binding represses transcription of the promoter (Chen *et al.* 2008). Again, this result supports the hypothesis that the cell type, available binding partners, and microenvironment modulate PROX1 function. PROX1 binds directly to the *FGFR-3* promoter to activate transcription of the lymphatic specific isoform *FGFR-3* IIIc (Shin *et al.* 2006). Shin *et al.* identified a nine nucleotide consensus sequence and determined that this putative binding site was both necessary and sufficient for PROX1 mediated induction of *FGFR-3* transcription (Shin *et al.* 2006). They also identified *FGFR-3* as a specific lymphatic marker and demonstrated that although knockdown of *FGFR-3* did not affect LEC cell fate, it significantly reduced LEC proliferation (Shin *et al.* 2006). They

propose a potential role for PROX1 mediated transcriptional activation of *FGFR-3* in the proliferation of LECs during developmental lymphangiogenesis (Shin *et al.* 2006).

3.3. PROX1 binding partners and post-translational modifications

PROX1 has been demonstrated to interact with a number of different proteins such as the orphan nuclear receptor chicken ovalbumin upstream promoter transcription factor II (COUP-TFII) *(*Lee *et al.* 2009; Yamazaki *et al.* 2009). COUP-TFII is important for venous specification and represses the expression of key arterial endothelial cell specific genes, namely *Neuropilin-1* (*NRP1*) and *Notch* (You *et al.* 2005; Kume 2010). Knockdown of *COUP-TFII* in venous endothelial cells causes an up-regulation of *NRP1* and *Notch* and a phenoconversion to an arterial endothelial cell phenotype. Though much is known about the factors that are responsible for arterial specification, COUP-TFII remains one of the few required proteins required for venous specification (You *et al.* 2005). The interaction between PROX1 and COUP-TFII is of particular interest as COUP-TFII is the first PROX1 binding partner that is also involved in the regulation of cell fate (Lee *et al.* 2009). Together, PROX1 and COUP-TFII up-regulate two known PROX1 target genes, *FGFR-3* and *Vascular Endothelial Growth Factor Receptor 3 (VEGFR-3)*, both of which are specific markers of the lymphatic vasculature. They also bind together at the *Ccne1* promoter despite the absence of consensus binding sites for either factor. PROX1 itself has been shown to be a direct transcriptional target of COUP-TFII (Srinivasan *et al.* 2010).

Further studies into this area will identify details into the initial steps of the fate switch occurring from blood endothelial cell to lymphatic endothelial cell.

Another lymphatic relevant binding partner of PROX1 is a member of the E-twenty six (Ets) family of transcription factors, Ets-2 (Yoshimatsu *et al.* 2011). The Ets transcription factors play a crucial role in angiogenesis with up to 19 isoforms identified to date in endothelial cells (Hollenhorst *et al.* 2007). In blood endothelial cells, Ets-1 promotes angiogenesis by up-regulation of transcription of *VEGFR-2* and the angiopoietin receptor Tunica internal endothelial cell kinase 2 (*Tie2)* (Hashiya *et al.* 2004). This mechanism is repeated in lymphatic endothelial cells with Ets-2 interacting directly with PROX1 via the NR boxes to promote transcription of *VEGFR-3*, suggesting a pro-lymphangiogenic role for Ets-2 (Yoshimatsu *et al.* 2011).

Finally, PROX1 has been shown to co-localize and interact directly with histone deacetylase 3 (HDAC3) (Steffensen *et al.* 2004). HDACs remove acetyl groups from lysine side chains of histone tails and thereby induce chromatin compaction (Barneda-Zahonero *et al.* 2012). Interestingly, PROX1's interaction with HDAC3, both *in vitro* and *in vivo*, is dependent on PROX1 being modified by the addition of the small ubiquitin-like modifier (SUMO) (Shan *et al.* 2008; Pan *et al.* 2009). Four putative SUMOylation sites have been identified in PROX1 and one (K556) was shown to be modified by the addition of SUMO-1 (Shan *et al.* 2008). SUMOylation destabilized the interaction of PROX1 with HDAC3 and reduced its function as a co-repressor (Shan *et al.* 2008). As well, SUMOylation increases PROX1's affinity for DNA. Mutation of the SUMOylation site K556R decreased PROX1's DNA-binding affinity and decreased its activation of both the *FGFR-3* and

VEGFR-3 promoters. This mutation of PROX1 also decreased vessel formation and migration of LECs in culture in response to VEGF-C (Pan *et al.* 2009).

In a mass spectrometry scan of phosphoproteins in the adult mouse liver, many phosphorylation sites were identified in PROX1 (Villen *et al.* 2007). Various homeobox transcription factors such as pancreatic and duodenal homeobox 1 (PDX1) (Frogne *et al.* 2012), SIX homeobox 1 (SIX1) (Ford *et al.* 2000). , and NK2 homeobox 1 (NKX2.1) (Silberschmidt *et al.* 2011) are phosphorylated. Phosphorylation of these transcription factors can affect protein subcellular localization, DNA-binding affinity, or other protein-protein interactions (Walsh *et al.* 2005). Interestingly, phosphorylation and SUMOylation have been shown to modulate protein function through phosphorylation dependent SUMO motifs in which phosphorylation in a consensus sequence provides a stable docking site for the E2 conjugation enzyme and facilitates modification (Gareau *et al.* 2010). Taken together, this adds a new dimension of regulation and further studies in this area will elucidate the role that post-translational modifications play in regulating PROX1's role as a transcription factor.

4. Molecular mechanism of lymphatic development

Lymphangiogenesis, or the growth of new lymphatic vessels, generally occurs during embryonic development of the lymphatic system, and during wound healing or disease conditions in the adult organism. The entire lymphatic vasculature develops

from the blood vasculature at embryonic day E9.5 in mice and at 6-7 weeks gestation in humans (Tammela and Alitalo 2010). Lymphatic development (Figure 2) begins when a subset of venous endothelial cells that are polarized to one side of the cardinal vein begin to express PROX1 (Wigle and Oliver 1999; Wigle *et al.* 2002). Upon expression of PROX1, these cells will bud out of the cardinal vein, migrate towards a VEGF-C signal and continue to grow and proliferate to form the primary lymph sacs. Following the expression of PROX1, these cells undergo a "fate-switch" and actively down-regulate blood endothelial cell markers such as CD45, E-selectin and CD34 and up-regulate lymphatic endothelial cell markers such as VEGFR-3 and Podoplanin (Hong and Detmar 2003; Podgrabinska *et al.* 2002). Without expression of PROX1, the molecular switch from blood endothelial cell to lymphatic endothelial cell does not occur. *Prox1* null mice have severe edema and die at approximately embryonic day E14.5 (Wigle and Oliver 1999). The correct gene dosage of PROX1 is also important in assuring development of a fully functional lymphatic system. *Prox1* heterozygous mice (*Prox1*$^{+/-}$) are haploinsufficient and present with adult onset obesity caused by poorly formed, leaky vessels in the mesentery (Harvey *et al.* 2005). As well, these mice have underdeveloped lymphovenous valves at the two sites where the lymphatics rejoin the venous circulation (Srinivasan *et al.* 2011). PROX1 is also crucial for maintaining the lymphatic endothelial cell phenotype in adult cells. Following siRNA mediated knockdown of *Prox1* in adult LECs in culture, it was observed that the affected cells began to return to a venous endothelial cell phenotype in that LEC markers were selectively down-regulated and BEC markers were once again up-regulated (Johnson *et al.* 2008). Taken together, PROX1 is

essential for the normal growth, development, and maintenance of the lymphatic vascular network.

Other key molecular players of lymphangiogenesis have been recently identified namely SRY-box 18 (SOX18) and COUP-TFII. SOX18 was identified as a regulator of lymphatic development as *Sox18* null mice have many of the same characteristics of *Prox1* null mice; they lack a lymphatic vasculature and die at E14.5 (Francois *et al.* 2008). SOX18 is activated in the subset of vein endothelial cells in the cardinal vein that are destined to become lymphatic endothelial cells at approximately embryonic day E9.0, before PROX1 expression is observed in these cells. The *Prox1* promoter contains two putative SOX18 binding sites and is activated by direct SOX18 binding. Francois *et al.* demonstrated that SOX18 binding to the *Prox1* promoter is unique to the context of lymphangiogenesis (Francois *et al.* 2008). In other tissues, such as the sympathetic ganglia, SOX18 does not bind to the *Prox1* promoter and does not activate transcription of the gene (Francois *et al.* 2008). Interestingly though, SOX18 expression is not crucial for maintaining the lymphatic endothelial cell phenotype in adult lymphatics and is down-regulated as the lymphatics mature (Francois *et al.* 2008). Mutations in SOX18 have also been associated with HLTS syndrome, which again outlines its importance in normal lymphatic development (Irrthum *et al.* 2003). The *RaOp* mouse model of HLTS syndrome is a naturally occurring model which is caused by a missense mutation in the *Sox18* allele (Downes *et al.* 2009). This mutation causes severe edema as well as blood vascular defects and similar symptoms observed in human HLTS syndrome. Matrix metalloproteinase 7, interleukin receptor 7 and N-cadherin expression is reduced as these are likely

downstream effectors of SOX18 (Downes *et al.* 2009). This mouse model is a powerful tool used to study the molecular origins of HLTS, and will provide further insight into the role of SOX18 in both blood and lymphatic vascular development.

The other key player in the fate switch from blood endothelial cell to lymphatic endothelial cell is COUP-TFII. COUP-TFII is consistently expressed in venous endothelial cells, as well as lymphatic endothelial cells, throughout the entire process of developmental lymphangiogenesis and into adulthood (Lee *et al.* 2009). Together with PROX1, it activates downstream lymphatic specific genes. COUP-TFII binds directly to PROX1 and together they both bind to the *Ccne1* promoter to promote proliferation of LECs (Yamazaki *et al.* 2009). It has also been demonstrated that PROX1 and COUP-TFII bind together to activate transcription of the *VEGFR-3*, *FGFR-3* and *Nrp-1* promoters all of which are involved in promoting cell growth and proliferation following lymphatic specification (Lee *et al.* 2009). COUP-TFII is required for SOX18 mediated activation of PROX1 at E9.5 (Figure 2), but COUP-TFII also binds to consensus binding sites in the *Prox1* promoter to activate its transcription following lymphatic specification (Srinivasan *et al.* 2010). Further studies investigating the cross-talk that occurs between these three transcription factors are required to fully elucidate the mechanism behind the BEC to LEC cell fate switch.

Following lymphatic specification, PROX1 up-regulates expression of *VEGFR-3* and *Ccne1* to promote growth and proliferation of the newly formed lymphatic endothelial cells. These cells will bud out from the cardinal vein and migrate towards a VEGF-C signal (the ligand for VEGFR-3) to form the primary lymph sacs. Further

lymphatic specific markers such as podoplanin and lymphatic vessel endothelial hyaluronan receptor (LYVE-1) will be up-regulated, but proper separation of the primary lymph sacs from the venous vasculature depends on the expression of spleen tyrosine kinase/lymphocyte cytosolic protein (Syk/SLP76) (Abtahian *et al.* 2003). The lymphatic vasculature in *Syk/SLP76* null mice has multiple aberrant connections with the veins and is often blood filled (Abtahian *et al.* 2003). Interestingly, C-type lectin receptor (CLEC-2) expressed by platelets in the blood circulation binds to podoplanin on the surface of LECs when in contact with blood (at the points where the lymphatics join the venous system) (Bertozzi *et al.* 2010). In turn, this binding activates expression of Syk/SLP76 in the affected LECs and maintains blood/lymphatic separation. In platelet deficient mice, this mechanism is impaired and blood circulates in their lymphatics (Bertozzi *et al.* 2010).

Following separation from the blood vasculature, the lymphatics mature and remodel to form the collecting vessels and capillaries. A key player in this process is the forkhead transcription factor FOXC2 (Dagenais *et al.* 2004; Wu and Liu 2011). It is important for recruiting vascular smooth muscle cells (VSMCs) to the walls of collecting vessels and for regulating other downstream remodelling factors such as platelet derived growth factor β (PDGF- β), angiopoietin-2 (Ang2) and Delta-like ligand 4 (Dll4) (Wu *et al.* 2011). Remodelling continues until the entire lymphatic vasculature is formed (Figure 2).

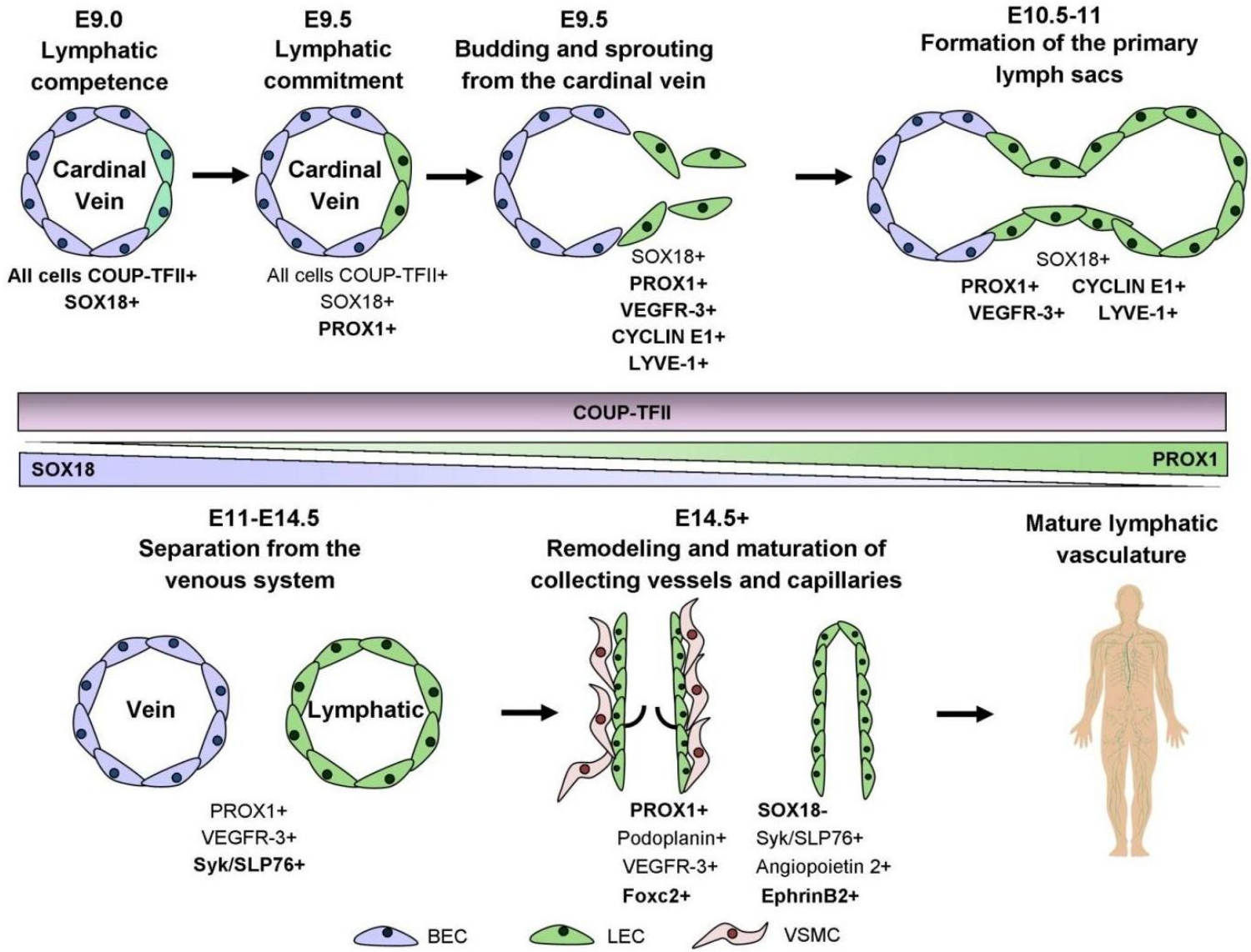
E9.0
Lymphatic competence
Cardinal Vein
All cells COUP-TFII+
SOX18+
E9.5
Lymphatic commitment
Cardinal Vein
All cells COUP-TFII+
SOX18+
PROX1+
E9.5
Budding and sprouting from the cardinal vein
SOX18+
PROX1+
VEGFR-3+
CYCLIN E1+
LYVE-1+
E10.5-11
Formation of the primary lymph sacs
SOX18+
PROX1+ CYCLIN E1+
VEGFR-3+ LYVE-1+
COUP-TFII
PROX1
SOX18
E11-E14.5
Separation from the venous system
Vein
Lymphatic
PROX1+
VEGFR-3+
Syk/SLP76+
E14.5+
Remodeling and maturation of collecting vessels and capillaries
PROX1+
Podoplanin+
VEGFR-3+
Foxc2+
SOX18-
Syk/SLP76+
Angiopoietin 2+
EphrinB2+
Mature lymphatic vasculature
BEC
LEC
VSMC

Figure 2: Mechanism of developmental lymphangiogenesis. At E9.0, a subset of venous endothelial cells on one side of the cardinal vein begin to express SRY-box 18 (SOX18). By E9.5, these cells also express PROX1, which down-regulates expression of blood endothelial cell markers, up-regulates expression of lymphatic endothelial cell (LEC) markers and leads to a cell fate switch. The cells continue to grow and proliferate and bud out of the cardinal vein towards a vascular endothelial growth factor C (VEGF-C) signal. These cells form the primary lymph sacs and continue to express LEC markers. Spleen tyrosine kinase/lymphocyte cytosolic protein 2 (SYK/SLP76) is required to ensure proper separation from the blood vasculature. Once separated, the expression of forkhead box protein C2 (FOXC2), Ephrin B2 (EPHB2), and Podoplanin is up-regulated to ensure vascular smooth muscle cell recruitment and valve formation in collecting vessels and remodeling of capillaries. The vasculature continues to develop and grow into adulthood. The entire process is dependent on the expression of PROX1 in the original subset of venous endothelial cells and PROX1 expression increases as the system develops. Chicken ovalbumin upstream promoter transcription factor II (COUP-TFII) expression is maintained at a constant rate throughout the process whereas SOX18 is crucial for the initiation of PROX1 expression, but diminishes in the latter stages of embryonic development. Adapted from (Duong *et al.* 2012) and (Wang and Oliver 2010).

5. PROX1 and the mammalian cell cycle

5.1. General overview of the mammalian cell cycle

The mammalian cell cycle is composed of four phases: gap 1 (G_1), synthesis (S), gap 2 (G_2) and mitosis (M) (Figure 3) (Reed 2003). The cycle is unidirectional and progression through the cycle is tightly regulated. It is based on cycles of phosphorylation and dephosphorylation of key transcription factors by cyclin- cyclin dependent kinase (Cdk) complexes that are expressed in specific phases of the cell cycle, and the precisely timed degradation of these same factors by the ubiquitin proteosome pathway (Glotzer *et al.* 1991; Reed 2003; Fasanaro *et al.* 2009). This coordinated system ensures the quick, concise transitions between phases, and minimizes the risk of error. The cycle also has four key checkpoints, which require certain criteria for the cycle to proceed (Figure 3). The first is located in G_1 phase and requires optimal growth conditions, a successful mitotic exit and no DNA damage for the cycle to proceed. The next is located in mid-S phase following DNA replication and requires replication to be complete with no lingering DNA damage. Following successful passage through S phase, there is a checkpoint at the G_2/M transition that ensures no DNA damage is present before entering mitosis and the final checkpoint during anaphase in mitosis verifies that the spindle assembly is correctly organized (Schnerch *et al.* 2012). In the event of cell or DNA damage, the cell has the option to initiate either DNA repair or apoptosis at these built in checkpoints (Schnerch *et al.* 2012). Mutations of the cell cycle machinery lead to deregulation of

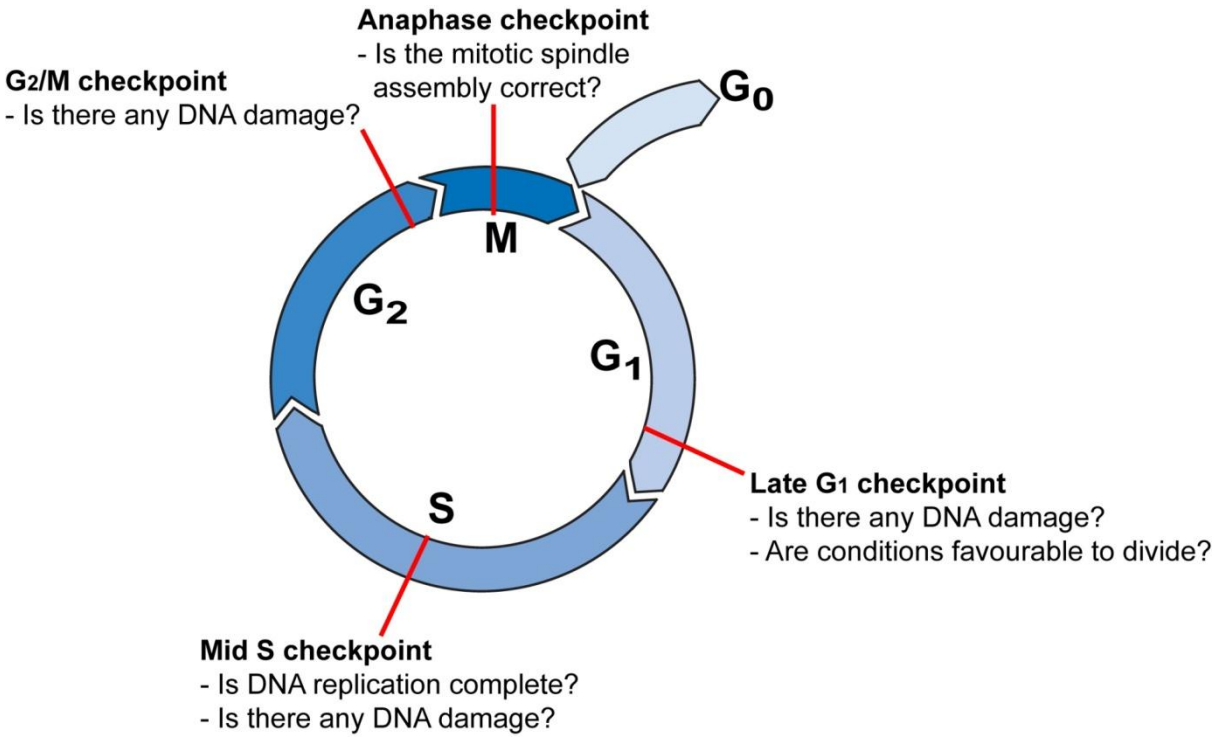

Figure 3: Overview of the eukaryotic cell cycle. The cell cycle contains four phases: gap 1 (G_1), synthesis (S), gap 2 (G_2) and mitosis (M). The cycle is unidirectional and to ensure proper passage through each phase, there are four built-in checkpoints. Passage through these checkpoints is dependent on specific criteria and any defects have a chance to be either repaired or the cell can initiate apoptosis.

cellular proliferation followed by aneuploidy or genomic instability, and as such, are often observed in a variety of different cancers (Schnerch *et al.* 2012).

5.2. The role of CCNE1 in the G_1/S transition

CCNE1 is expressed in a tight window of the cell cycle that spans from late G_1 phase through the transition into S phase and abruptly ends at the beginning of S phase (Le Cam *et al.* 1999; Polanowska *et al.* 2001). CCNE1 forms a complex with Cdk2 and together they phosphorylate key effectors of the G_1/S transition (Dulic *et al.* 1992). The CCNE1-Cdk2 complex is bound by cell cycle inhibitors $p21^{cip1}$, $p27^{kip1}$ and $p57^{kip2}$ in late G_1 phase (Dulic *et al.* 1992). Once the cell commits to transition into S phase, the amount of CCNE1-Cdk2 complexes surpasses the pool of cell cycle inhibitors. This results in their degradation by the ubiquitin proteosome pathway and release of the active CCNE1-Cdk2 complex thereby pushing the cell from G_1 to S phase (Clurman *et al.* 1996; Won and Reed 1996). Once the transition is complete, the CCNE1-Cdk2 complexes autophosphorylate, which targets them for degradation via the ubiquitin proteosome pathway (Clurman *et al.* 1996; Won and Reed 1996).

Transcription of CCNE1 is regulated by the E2F-retinoblastoma protein (pRB) pathway. The *Ccne1* promoter contains multiple transcription factor binding sites, but is primarily controlled by two E2F binding sites located on either side of the transcriptional start site (Le Cam *et al.* 1999; Cobrinik 2005). Interestingly for our study, the *Ccne1* promoter also contains a response element for LRH-1, which has

been shown to interact with PROX1 (Figure 25) (Qin *et al.* 2004). The upstream E2F site, E2F-Sp1, is constitutively bound by a complex containing an activating E2F protein (1-3a) and other chromatin remodelers and transcription factors (Figure 4) (Cobrinik 2005). The downstream E2F site, E2FX-AT rich, is bound by a repressive complex, including an E2F protein and pRB, but only when the promoter is inactive. During late G_1 phase, pRB is phosphorylated and releases the E2F protein bound to the E2FX-AT rich site. E2F release allows the assembly of the pre-initiation complex and transcription of the *Ccne1* gene (Figure 4) (Le Cam *et al.* 1999; Cobrinik 2005). Deregulation of the machinery that assures precise expression and timing of CCNE1 is frequently observed in cancers and leads to aneuploidy and genomic instability (Siu *et al.* 2012).

5.3. PROX1 in the cell cycle

Paradoxically, PROX1 has been shown to have both anti-growth and pro-growth roles depending on the tissue and physiological context in which it is being expressed (Table 1). On the anti-growth side, over-expression of PROX1 inhibits proliferation in hepatocellular carcinoma cells (Shimoda *et al.* 2006). Shimoda *et al.* knocked down PROX1 expression using siRNA in three cell lines as well as human patient samples and observed a decrease in cell proliferation (Shimoda *et al.* 2006). They also observed in their patient samples that low PROX1 expression correlated with a lower degree of differentiation, and increased proliferation leading to progression of the disease and poorer prognosis (Shimoda *et al.* 2006). Similarly, in neuroblastoma

cells, PROX1 blocks cell cycle progression by down-regulating expression of Cyclin D1, A and B1 as well as up-regulating expression of the CDKI $p27^{kip1}$ (Foskolou *et al.* 2012). Interestingly, expression of CCNE1 is increased in this cell type but this increased expression is not correlated with cell cycle progression. Foskolou *et al.* propose that this disconnect could be caused by the lack of induction of other pro-growth co-factors required for G_1/S progression and up-regulation of $p27^{kip1}$ (Foskolou *et al.* 2012). In the developing central nervous system, PROX1 is expressed in spinal interneurons and causes them to exit the cell cycle and differentiate (Misra *et al.* 2008).

On the pro-growth side, PROX1 has been shown to have a role in mediating colon cancer progression through interactions with adenomatous polyposis coli (APC) and the T-cell specific HMG-box transcription factor (TCF)/β-catenin pathway (Petrova *et al.* 2008). High levels of PROX1 expression were observed in colon cancer cells and resulted in increased dysplasia and favoured the formation of carcinoma *in situ*. Petrova *et al.* proposed that loss of APC caused nuclear translocation of β-catenin that in turn increased Wnt signaling, which through a presently unknown mechanism lead to over-expression of PROX1 (Petrova *et al.* 2008). In fetal hepatoblasts, PROX1 works in opposition to LRH-1 to up-regulate expression of Cyclin D2, CCNE1 and CCNE2. PROX1 also down-regulates expression of the cyclin dependent kinase inhibitor (CDKI) $p16^{INK4}$ (Kamiya *et al.* 2008). In this cell type, increased PROX1 levels promote proliferation whereas increases in LRH-1 levels decrease cell proliferation (Kamiya *et al.* 2008).

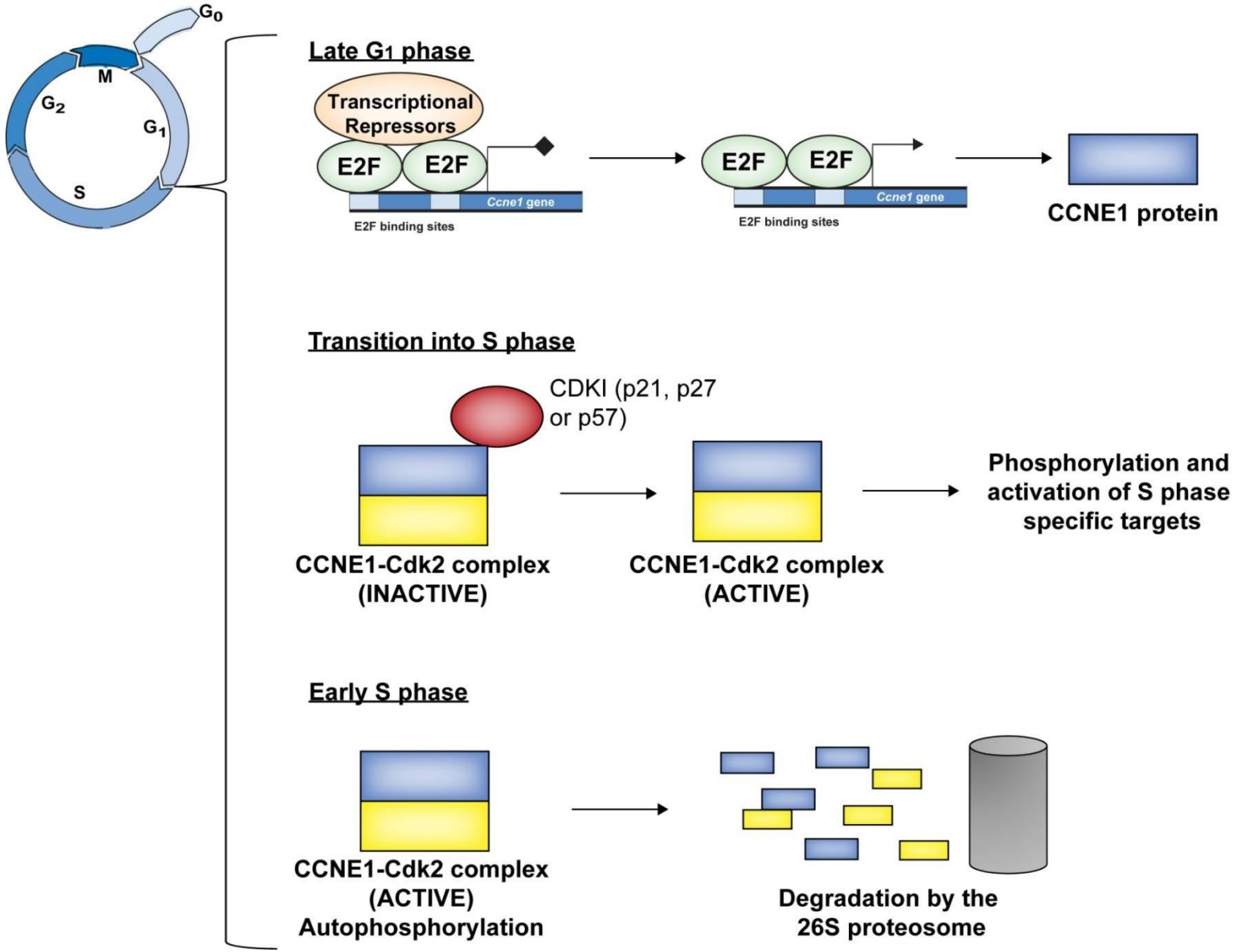
G0
M
G2
G1
S
Late G1 phase
Transcriptional Repressors
E2F
E2F
Ccne1 gene
E2F binding sites
E2F
E2F
Ccne1 gene
E2F binding sites
CCNE1 protein
Transition into S phase
CDKI (p21, p27 or p57)
CCNE1-Cdk2 complex (INACTIVE)
CCNE1-Cdk2 complex (ACTIVE)
Phosphorylation and activation of S phase specific targets
Early S phase
CCNE1-Cdk2 complex (ACTIVE) Autophosphorylation
Degradation by the 26S proteosome

Figure 4: The role of CCNE1 in the G_1/S transition. Progression from one phase to the next in the cell cycle depends on the precisely timed expression and degradation of cyclins. During G_1 phase, the *Ccne1* promoter is bound by E2F proteins and is repressed by a group of transcriptional repressors including the retinoblastoma protein (pRB) and histone deacetylases (HDAC). In late G_1 phase, pRB is phosphorylated which destabilizes the repressive complex and allows for the transcription of *Ccne1*. CCNE1 binds to Cyclin dependent kinase 2 (Cdk2), but is inhibited by a pool of cyclin dependent kinase inhibitors (CDKI). To transition into S phase, sufficient CCNE1 is required to overwhelm the pool of CDKI's which allows active CCNE1-Cdk2 complexes to activate S phase specific targets. In early S phase, CCNE1-Cdk2 complexes autophosphorylate, which targets them for ubiquitination by the Skp, Cullin, F-box containing complex (SCF^{Fbw9}) and degradation by the 26S proteosome. This ensures the unidirectional nature of the cell cycle and prevents aneuploidy and genomic instability.

Pro-growth	
Colon cancer cells: promotes dysplastic phenotype and cancer progression	Petrova *et al.* (2008) *Cancer Cell*, 13 (5), 407-19.
Fetal hepatoblasts: increases cell growth	Kamiya *et al.* (2008) *Hepatology*, 48 (1), 252-64.
Anti-growth	
Neuroblastoma cells: blocks cell cycle progression by upregulating Cyclin D1, A, B1 and $p27^{kip1}$	Foskolou *et al.,* (2012) *Oncogene*, epub April 16.
Primary hepatocellular carcinoma cells: suppresses cell growth	Shimoda *et al.* (2006) *Clin Cancer Res*, 12 (20 pt 1), 6005-11
Lens: up-regulates $p57^{kip2}$ which is important for cell cycle arrest and differentiation	Dyer *et al.* (2003) *Nat Genetics*, 34 (1), 53-8.
Spinal cord: Causes cell cycle exit in interneuron precursor cells in the developing chick spinal cord	Mishra *et al.* (2008) *Dev Dyn*, 237, 393-402.

Table 1: Known pro-growth and anti-growth roles of PROX1. PROX1 has varied roles in cell cycle regulation depending on the cell type that is being studied. This is a summary of the known roles of PROX1 in cell cycle regulation that are either pro-growth or anti-growth.

In *Drosophila melanogaster*, the PROX1 ortholog Prospero also has conflicting roles in cell cycle regulation. In glial precursor cells, Prospero up-regulates CycE to maintain the mitotic potential of a specific subset of longitudinal glia (Griffiths and Hidalgo 2004). In contrast, Prospero up-regulates expression of Dacapo ($p27^{kip1}$ homolog) in embryonic neuroblasts and promotes cell cycle arrest (Colonques *et al.* 2011). Our study supports a pro-growth role for PROX1 through promoting cell cycle progression in LECs (Baxter *et al.* 2011).

5.4. PROX1 and CCNE1

PROX1 has been shown to up-regulate expression of CCNE1 in both endothelial cells and non-endothelial cells (Petrova *et al.* 2002). Petrova *et al.* postulated that PROX1 activates transcription of CCNE1 through binding directly to the E2F binding sites located in the *Ccne1* promoter (Petrova *et al.* 2002). Prospero, the *Drosophila* ortholog of PROX1, also regulates *CycE* in the developing nervous system. It controls the timed expression of *CycE* in the longitudinal glia ensuring that the correct number of cells are produced (Griffiths and Hidalgo 2004). PROX1 works together with COUP-TFII to activate expression of CCNE1 in LECs (Yamazaki *et al.* 2009). This study demonstrates that PROX1 functions as a co-activator of *Ccne1* transcription, which promotes cell cycle entry in LECs (Baxter *et al.* 2011).

II. RATIONALE

PROX1 is required for both the development and maintenance of the lymphatic vasculature (Wigle and Oliver 1999; Wigle *et al.* 2002; Johnson *et al.* 2008). In *Prox1* null mice, lymphatics fail to develop and the embryos die at E14.5. One of the key steps during lymphatic vessel development is the active proliferation of newly formed lymphatic endothelial cells, which is initiated by PROX1 expression in the cardinal vein (Petrova *et al.* 2002). These cells are actively proliferating in response to pro-growth stimuli through the up-regulation of *Cyclin E1* and activation of the VEGF-C/VEGFR-3 pathway (Petrova *et al.* 2002). CYCLIN E1 is a regulator of the G_1 to S transition in the cell cycle (Dulic *et al.* 1992). In *Drosophila*, Prospero has been shown to up-regulate *CycE* in the developing nervous system and in mammalian cells, PROX1 has been shown to increase levels of *Ccne1* both in endothelial and non-endothelial cells (Petrova *et al.* 2002; Griffiths and Hidalgo 2004). PROX1 has also been demonstrated to be involved in either promoting or inhibiting cell growth in a cell-type and context specific manner (Dyer *et al.* 2003; Shimoda *et al.* 2006; Kamiya *et al.* 2008; Misra *et al.* 2008; Petrova *et al.* 2008; Foskolou *et al.* 2012). Further study of the role of PROX1 in mediating the lymphatic endothelial cell cycle will contribute to the understanding of how PROX1 promotes proliferation during developmental and adult lymphangiogenesis. It will also identify potential mechanisms to control the growth of lymphatic capillaries. In the context of lymphedema where vessels are unable to support normal lymph flow and proper drainage, promoting lymphatic vessel growth and remodeling could restore normal

lymphatic function. In contrast, one of the hallmarks of cancer progression is the aggressive spread of tumour cells from their primary site to other regions of the body where they form secondary tumours (Hanahan *et al.* 2011). Cancer related deaths are frequently caused by organ failure due to these secondary tumours and not by the primary tumour itself (Van den Eynde 2009). Malignant cells often enter neighbouring lymphatic vessels and metastasize via the lymphatic vasculature (Hanahan *et al.* 2011). Lymphatic vessels are particularly susceptible to invading tumour cells due to their highly permeable nature. Recent studies suggest that inhibiting of tumour associated lymphangiogenesis (growth of new lymphatic vessels) is more a potent approach to block tumour spread than is inhibiting of angiogenesis (growth of new blood vessels) (Pytowski *et al.* 2005; Tammela *et al.* 2008). Further study of lymphatic vessel biology will provide us new techniques with which to inhibit the spread of a broad spectrum of solid cancers.

III. HYPOTHESIS

We hypothesize that PROX1 is a key regulator of the lymphatic endothelial cell cycle and activates *Ccne1* transcription in a DNA-binding independent manner, which leads to increased lymphatic endothelial cell proliferation.

IV. OBJECTIVES

To determine the role of PROX1 in mediating the LEC cell cycle we sought to identify the mechanism by which it promotes transcription of the *Ccne1* promoter.

1) To establish the functional domains of PROX1 necessary for transcriptional activation of the *Ccne1* promoter.

2) To identify the regions of the *Ccne1* promoter that are required for PROX1 mediated transcriptional activation.

3) To determine the overall effect of PROX1 on the LEC cell cycle through gain of function and loss of function studies.

V. MATERIALS AND METHODS

1. Generation of Prox1 expression constructs

A plasmid containing a full-length mouse *Prox*1 cDNA (clone 6490801, Invitrogen) was digested with *EcoRI/SacII* and the insert containing the *Prox1* coding sequence was ligated into the *EcoRI/SacII* sites of the pBluescript II KS+ vector (Stratagene, (Baxter *et al.* 2011)). This plasmid was used as a template for all of the various *Prox1* constructs used in this study. The FailSafe PCR kit (Epicentre) was used to amplify these constructs in combination with the PCR splice overlap extension technique (Horton *et al.* 1989) to generate the different *Prox1* deletions or mutations used in this study (Refer to Table 2). All versions of *Prox1* were cloned into the *SacII/XhoI* sites of the pCMV-Tag4A vector (Stratagene) and therefore all constructs contained a carboxyl termini FLAG epitope. Prior to use in experiments, all versions of *Prox1* were sequenced at the University of Calgary core sequencing facility to verify that there were no inadvertent mutations incorporated during PCR amplification.

2. Luciferase Reporter Constructs

A 1 Kb portion of the mouse *Ccne1* promoter, upstream of the transcription start site (BAC genomic clone RP2377J9, Invitrogen), was amplified (Refer to Table 3) as previously described (Le Cam *et al.* 1999) and cloned into the pCRBlunt vector (Invitrogen, (Baxter *et al.* 2011)). All of the deletion versions of the *Ccne1* promoter

were cloned into the *KpnI/BglII* sites of the pGL3 basic reporter vector (Promega) and the sequence was verified at the University of Calgary core sequencing facility. The 220 bp mouse *FGFR-3* promoter in pGL2 was a kind gift from Dr. Ornitz, Washington State University Medical School (McEwen *et al.* 1999).

3. Cell culture

Human embryonic kidney (HEK) 293A cells (ATCC) were grown in Dulbecco's Modified Eagle's medium (DMEM) with high glucose supplemented with L-glutamine,sodium pyruvate (HyClone),5% fetal bovine serum (Invitrogen) and 1% Penicillin/Streptomycin (HyClone). U2-Osteosarcoma (U2OS) cells (ATCC, HTB-96) were grown in McCoy's 5A medium (Invitrogen) supplemented with 10% fetal bovine serum and 1% Penicillin/Streptomycin. Cells were transiently transfected using the Lipofectamine 2000 reagent (Invitrogen) and were harvested for experiments 48 hours post-transfection. Leptomycin B was purchased from Sigma-Aldrich and U2OS cells were treated with a final concentration of 1ng/mL in normal growth media for 20 hours at 37°C as previously described (Kojima *et al.* 2007; Glover-Collins and Thompson 2008). Control cells were treated with the same volume (3.6 µL) of vehicle (70% methanol). Human Umbilical Vein Endothelial Cells (HUVEC) (Lonza) were grown in endothelial basal media (EBM-2) supplemented with growth factors (epidermal growth factor (EGF), vascular endothelial growth factor (VEGF), insulin like growth factor (IGF), beta fibroblast growth factor B (bFGF), heparin, ascorbic acid, hydrocortisone, gentamicin sulphate and amphotericin-B) and 2% fetal bovine serum (Lonza). Cells were infected with adenovirus (human adenovirus serotype 5,

E1/E3 deleted pAdEasy Adenoviral Vector System, Agilent Technologies) encoding either WT *Prox1* or a version in which the homeoprospero domain had been deleted (HDPD2Δ) at a multiplicity of infection (MOI) of 250. The cells were then harvested 48 hours post-infection. Human neonatal dermal microvascular lymphatic endothelial cells (LEC) (Lonza) were grown in EBM-2 supplemented with growth factors (EGF, VEGF, IGF, FGF-B, ascorbic acid, hydrocortisone, gentamicin sulphate and amphotericin-B) and 10% fetal bovine serum (Lonza). Cells were transfected with 100 μM of either ON-TARGETplus siCONTROL non-targeting or PROX1 ON-TARGETplus SMART pool siRNAs (Dharmacon) using DharmaFECT1 transfection reagent for 48 hours as per the manufacturer's instructions. Human hepatocellular carcinoma cells (HepG2) were cultured in DMEM (Hyclone) supplemented with 10% FBS (Invitrogen) and 1% penicillin/streptomycin (Hyclone). HepG2 cells were plated 48 hours prior to being harvested for experiments.

Table 2: Primers used to generate PROX1 constructs

PROX1 Version	Primer Sequence	Primer Name	Restriction Enzyme site added
WT	F: 5'-GC***ggatcc***TAATACGACTCACTATAGGGC-3' R: 5'-CC***ctcgag***CTCGTGAAGGAGTTCTTGTAG-3'	Mx10 Mx49	*BamHI* *XhoI*
dblNRΔ	F: 5'- GC***ggatcc***TAATACGACTCACTATAGGGC-3' R: 5'- **CTCGGTGCCACCGTTTTTGTTCATGTTATTTTTT ACGTTCGACTTTTCCCCATCTGCGTGTTG** -3' F: 5'- **CAACACGCAGATGGGGAAAAGTCGAACGTAA AAAATAACATGAACAAAAACGGTGGCACCGAG**-3' R: 5'-CC***ctcgag***CTCGTGAAGGAGTTCTTGTAG-3'	Mx10 Px46 Px47 Mx49	*BamHI* *XhoI*
PD1Δ	F: 5'-GC***ggatcc***TAATACGACTCACTATAGGGC-3' R: 5'-**GCTGTCTTCAGACAGGTCGCCATCGCGATC-CACATCAAACTGGC**-3' F: 5'-**GCCAGTTTGATGTGGATCGCGATGGCGACC-TGTCTGAAGACAGC** -3' R: 5'-CC***ctcgag***CTCGTGAAGGAGTTCTTGTAG-3'	Mx10 Px106 Px107 Mx49	*BamHI* *XhoI*
HDΔ	F: 5'-GC***ggatcc***TAATACGACTCACTATAGGGC-3' R: 5'-**GGCTTGGCGCGCATACTTCTCCTGCATTG-CGCTTCCTGAATAAGGTG**-3' F: 5'-GATGTGGATCGCTTATGTGATGAGCACC-3' R: 5'-CC***ctcgag***CTCGTGAAGGAGTTCTTGTAG-3'	Mx10 Px3 Px4 Mx49	*BamHI* *XhoI*
PD2Δ	F: 5'-GC***ggatcc***TAATACGACTCACTATAGGGC-3' R: 5'-CC***ctcgag***TCCATCATTGATGGCTTGACGCGC-3'	Mx10 Px7	*BamHI* *XhoI*
HDPD2Δ	F: 5'-GC***ggatcc***TAATACGACTCACTATAGGGC-3' R: 5'-CC***ctcgag***CTGCATTGCGCTTCCTGAATAAGG-3'	Mx10 Px8	*BamHI* *XhoI*
^{623}WF**EE**FR^{628} DBDmut	F: 5'-GC***ggatcc***TAATACGACTCACTATAGGGC-3' R: 5'-GTAAAACTCACG***GAATTC***CTCGAACCACTT-GATGAGCTGCGAGG-3' F: 5'-GATGTGGATCGCTTATGTGATGAGCACC-3' R: 5'-CC***ctcgag***CTCGTGAAGGAGTTCTTGTAG-3'	Mx10 Px1 Px2 Mx49	*BamHI* *EcoRI* *XhoI*
^{623}WFS**A**F**A**^{628} DBDmut	F: 5'-GC***ggatcc***TAATACGACTCACTATAGGGC-3' R: 5'-CTGAATGTAGTAAAACTC**GGC**GAAA**GC**GCTAAACCACTTG-3' F: 5'-CTCATCAAGTGGTTT*agc**GC**t*TTC**GCC**GAGTTTTACTAC-3' R: 5'-CC***ctcgag***CTCGTGAAGGAGTTCTTGTAG-3'	Mx10 Px54 Px55 Mx49	*BamHI* *HaeII* *XhoI*
NterPD1Δ	F: 5'-GC***ggatcc***TAATACGACTCACTATAGGGC-3' R: 5'-**CTGCTGCTGGGGCAGCTTCTGTAAGCGATCCACATCAAACTG**-3' F: 5'-**CAGTTTGATGTGGATCGCTTACAGAAGCTGCCCCAGCAGCAG**-3' R: 5'-CC***ctcgag***CTCGTGAAGGAGTTCTTGTAG-3'	Mx10 Px96 Px97 Mx49	*BamHI* *XhoI*
CterPD1Δ	F: 5'-GC***ggatcc***TAATACGACTCACTATAGGGC-3' R: 5'-**CTTCAGACAGGTCGCCATCTTCCTGGTAGAACTTCTCCTGCAG**-3' F: 5'-**CTGCAGGAGAAGTTCTACCAGGAAGATGGCGACCTGTCTGAAG**-3' R: 5'-CC***ctcgag***CTCGTGAAGGAGTTCTTGTAG-3'	Mx10 Px98 Px99 Mx49	*BamHI* *XhoI*

Note: Restriction enzyme sites are shown in lowercase *italics*, inserted mutations are shown in **bold and are highlighted in red**, and deletion primers used for splice-overlap extension PCR are shown in **bold**.

Note: All constructs were cloned into the *SacII* and *XhoI* sites of pCMV-Tag4A via an endogenous *SacII* site. The *BamHI* site was used for cloning into pBluescript II KS+.

Table 3: Primers used to generate *Ccne1* promoter luciferase constructs

***Ccne1* promoter Version**	**Primer sequence**	**Primer name**	**Restriction enzyme site added**
1 kb	F: 5'- CCTTCAAGTTTTCCGGAAGCACAAACAGCTGGAATGGG-3' R: 5'-GGAGTCCAGGCAGCCCGTACCCGAAGCTGTGTCC-3'	Px15 Px16	Primers were used to amplify from BAC clone
1 kb	F: 5'- CTT***ggtacc***GCCCCCACCAGAGCTCCTCGCTGGTC-3' R: 5'-GCG***ggatcc***GCGCCTGCCCCCTACACCGC-3'	Px18 Px19	*KpnI* *BamHI*
206 bp	F: 5' ***ggtacc***GCCCCCACCAGAGCTCCTCGCTGGTC-3' R: 5'-GGAGTCCAGGCAGCCCGTACCCGAAGCTGTGTCC-3'	Px32 Px19	*KpnI*
206 bp mut E2FI	F: 5'- CTT***ctcgag***GCCCCCACCAGAGCTCCTCGCTGGTC-3' R: 5'-AAAAATCCCAGCGC**TA**GGCACCGG**TA**CCGTCCCG**TA** CTCGCG**TA**CCG**TA**CCGAGGGCTGCGAG-3' F: 5'- CTCGCAGCCTCGG**TA**CGG**TA**CGCGAGTACGGAC ***ggTAcc***GGTGCC**TA**GCGCTGGGATTTTT -3' R: 5'- GCG***ggatcc***GCGCCTGCCCCCTACACCGC-3'	Px63 Px61 Px62 Px19	*XhoI* *KpnI* *BamHI*
206 bp mut E2FX	F: 5'- CTT***ctcgag***GCCCCCACCAGAGCTCCTCGCTGGTC-3' R: 5'- GGCTTCGAGC**TCT**ACATT**GC**A**G**AA-3' F: 5'- TT**C**T**GC**AATGT**AGA**GCTCGAAGCC-3' R: 5'- GCG***ggatcc***GCGCCTGCCCCCTACACCGC-3'	Px63 Px69 Px68 Px19	*XhoI* *BamHI*

Note: Restriction enzyme sites are shown in lowercase *italics*, inserted mutations are shown in **bold and are underlined**.

4. Immunocytochemistry

6-8x10^4 HEK 293 or U2OS cells were grown on uncoated glass coverslips in 6-well tissue culture plates (Becton Dickinson). After 48 hours, the cells were transfected with various *Prox1* constructs in the pCMV-Tag4A vector by using Lipofectamine 2000 and following the manufacturer's instructions (Invitrogen). 48 hours post-transfection, cells were fixed in 4% paraformaldehyde (EM Science) for 30 minutes. Coverslips were then washed with 1x Phosphate Buffered Saline (PBS) followed by washes with 1x PBT (PBS with 0.3% Triton X-100) and were blocked in a 5% normal goat serum-PBT solution. The cells were then incubated overnight with anti-FLAG M2 monoclonal primary antibody (Sigma, 1:1000). The coverslips were washed in PBT and incubated with a goat-anti-mouse secondary antibody coupled to Alexa Fluor 488 (Molecular Probes). The coverslips were then washed with 2x SSC (0.3M sodium chloride, 0.03M sodium citrate, pH 7.0) and treated with 100 µg/mL of RNase A (Sigma) for 30 minutes. The coverslips were stained with propidium iodide (1:1000, Molecular Probes) for 15 minutes and mounted onto glass slides. Images were captured with either an Olympus light scanning confocal microscope (Manitoba Institute for Cell Biology) equipped with FluoView imaging software (Olympus) or a Zeiss 200M light scanning confocal microscope (St. Boniface Research Centre) equipped with a digital camera and Pascal 5 imaging software (Zeiss). Where immunocytochemistry results were quantified, the observer was blinded to the identity of the slides.

5. Cell cycle analysis

$5x10^5$ HUVECs were infected at 250 MOI and grown in 175 cm^2 tissue culture flasks for 48 hours prior to analysis. Alternatively, $3x10^5$ LECs were transfected with siRNA and allowed to grow for 24 hours on fibronectin (Sigma) coated 6-well tissue culture plates. The cells were then trypsinized and re-plated onto fibronectin coated 6-well tissue culture plates at a lower density ($1.5x10^5$ cells per well) and incubated for 24 hours prior to harvest. Cells were trypsinized and fixed in ice-cold 70% ethanol for 2 hours and centrifuged at 200 x g for 5 minutes at 4^oC. The cell pellets were then washed once with 1xPBS, centrifuged at 200 x g and stained for 30 minutes at room temperature in PI staining solution (0.1% PBT, 0.5 mg/mL RNase A, 0.5 mg/mL propidium iodide). 10^4 gated cells were counted using a BD FACSCalibur (Manitoba Institute for Cell Biology) and the gates were arranged using the FL2-A vs FL2-W plot to exclude doublets. The data was analyzed using FlowJo software (Tree Star, Inc) and quantified using Origin 8 software.

6. Bromodeoxyuridine (BrdU) labelling

We employed 5'-bromo-2'-deoxyuridine (BrdU) (Fisher) labelling in conjunction with DNA staining and measured the proportion of S phase cells using flow cytometry. $2.5x10^5$ HUVECs were infected at 250 MOI with different adenoviral vectors and grown in 10 cm tissue culture plates for 48 hours prior to analysis. Alternatively, $3x10^5$ LECs were transfected with siRNA and allowed to grow for 24 hours on fibronectin (Sigma) coated 6-well tissue culture plates. The cells were then

trypsinized and re-plated on fibronectin coated 6-well tissue culture plates at a lower density ($1.5x10^5$ cells per well) and incubated for 24 hours. Forty-five minutes prior to harvest, BrdU was added to each well to a final concentration of 100 µM and the plates were incubated at 37°C, 5% CO_2. Cells were trypsinized and fixed in ice-cold 70% ethanol overnight at 4°C. The cells were then centrifuged at 200 x g for 5 minutes at 4°C and the cell pellets resuspended in 1 mL of freshly prepared 2N HCl (Fisher) and allowed to stand at room temperature for 25 minutes. 2 mL of 3% fetal bovine serum (FBS) in 1xPBS was added to each sample and the cells were centrifuged at 200 x g for 5 min at 4°C. The pellets were resuspended in 1 mL of sodium borate (Fisher) pH 8.5 and incubated at room temperature for 2 minutes. 2 mL of 3% FBS in 1xPBS was added to each sample and the cells were centrifuged at 200 x g for 5 minutes at 4 °C. This step was repeated, after which the cell pellets were resuspended in 100 µL of 1xPBS containing 3% FBS and 10 µL of anti-BrdU Alexa Fluor 488 conjugated antibody (Molecular Probes) and incubated for 2 hours at room temperature. 2 mL of 3% FBS in 1xPBS was added and the cells were centrifuged at 200 x g for 5 minutes at 4 °C. The pellets were subsequently resuspended in 500 µL of 3% FBS in 1xPBS containing 20 µL of 7-aminoactinomycin-D (7-AAD, Sigma) and allowed to stand at room temperature for 15 minutes prior to measuring on a BD FACSCalibur. Ten thousand gated cells were counted and the gates were arranged using the FL3-A vs FL3-W plot to exclude doublets. The data was analyzed using CellQuest Pro software (BD Biosciences) and quantified using Origin 8 software.

Alternatively, 5 x 10^4 HUVECs were infected and plated onto rat tail collagen type 1 coated glass coverslips (BD Biosciences) in 6-well tissue culture plates (Becton Dickinson). 48 hours post transfection, BrdU (Fisher) was added to each well to a final concentration of 100 μM and the plates were incubated at 37°C for three hours. The cells were then fixed and stained using the cell proliferation kit (GE Healthcare Life Sciences) according to the manufacturer's instructions. Briefly, cells were washed twice with 1xPBS and were fixed using 4% paraformaldehyde. The coverslips were rinsed with 0.07 N NaOH and were then incubated overnight at 4°C with a nuclease solution containing an anti-BrdU primary antibody supplied with the kit. Following three 1xPBT washes, the coverslips were then incubated with a goat anti-mouse secondary coupled to Alexa Fluor 546 (Molecular Probes) and mounted onto slides using mounting media containing 4',6-diamidino-2-phenylindole DAPI (Molecular Probes). Three images were taken at random of each slide using a Zeiss Axioskop 2 Fluorescent microscope equipped with a digital camera (Axiocam HR, Zeiss) and Axiovision imaging software. The observer was blinded to the identity of the slides during imaging and quantification.

7. Proliferating cell nuclear antigen (PCNA) staining

HUVECs were plated as described for BrdU staining and infected with adenovirus encoding either WT or HDPD2Δ Prox1. For detection of chromatin bound PCNA, cells were fixed and stained using a PCNA antibody (Abcam ab18197). Briefly, cells were washed twice with 1xPBSS (phosphate buffered saline with 0.5 mM

$MgCl_2$ and 0.5 mM $CaCl_2$) followed by one wash with CSK (10 mM PIPES pH 7.0, 100 mM NaCl, 300 mM sucrose, 3 mM $MgCl_2$). Cells were then incubated in 0.2% Triton-X for five minutes and fixed with 2% paraformaldehyde. Methanol (100%) was then added to the coverslips and they were fixed for 20 minutes at -20°C. The coverslips were stained using the anti-PCNA antibody (1:3000 Abcam) followed by a goat-anti-rabbit Alexa Fluor 546 conjugated secondary antibody (1:400, Molecular Probes). Cells displaying uniform staining in the nucleus were scored as positive. The observer was blinded to the identity of the slides before counting and the percentage of PCNA positive cells was determined by dividing the number of uniformly stained PCNA cells by the total number of cells in each field. Three random fields for each slide were counted and each sample was imaged in triplicate.

8. Western blotting

$2x10^5$ cells grown in 6 cm (28.3 cm^2) plates were either transfected with 4 µg of DNA or infected with 250 MOI of adenovirus 48 hours after plating. These cells were lysed at 4°C using New RIPA lysis buffer (50 mM Tris, 150 mM NaCl, 1 mM EDTA, 1 mM EGTA, 1% Triton X-100, 1% sodium deoxycholate, 0.1% SDS, pH 7.4) with a cocktail of protease inhibitors (Complete Mini, Roche) as well as phosphatase inhibitors (PhoSTOP, Roche) and centrifuged at 16,100 x g for 5 minutes to pellet cell debris. To detect SUMOylated PROX1, N-ethylmalimide (NEM, Sigma) was added at a final concentration of 20 mM to the lysates. A standard protein assay was then performed using the DC standard protein assay kit (Biorad) to ensure equal loading.

To evaluate the phosphorylation status of PROX1, 10-20 µg of whole cell lysate was treated for 3 hours at 30°C with 2 µL (100 U) of protein lambda phosphatase (New England Biolabs) as per the manufacturer's instructions. The samples were then prepared and denatured by heating at 95˚C for five minutes and loaded onto 8% SDS-polyacrylamide gels. After electrophoresis, the proteins were transferred to a 0.45 µM nitrocellulose membrane and the membranes were then blocked in a 5% skim milk powder-Tris buffered saline (TBS) solution (5% Carnation Brand skim milk powder, 50 mM Tris, 140 mM NaCl, 2.7 mM KCl, pH 8) and probed with either the anti-FLAG M2 monoclonal antibody (1:10000, Sigma), anti-PROX1 polyclonal antibody (1:1000, Millipore) or an anti-CYCLIN E1 monoclonal antibody (1:200, Santa Cruz Biotechnology). The blots were then probed with a rabbit anti-actin antibody (1:10000, Sigma) to assess for normalization of protein loading. Images were captured using a western blot chemiluminescence kit (Santa Cruz Biotechnology) and either a Fluor-S Max Imager (BioRad) or CL-Xposure blue x-ray film (Thermo Scientific).

9. Luciferase reporter assays

$1x10^5$ cells were co-transfected with 1 µg of luciferase reporter plasmid, 1 µg of pCMV-Tag4A encoding a version of *Prox1* and 1 µg of pcDNA3.1-*lacZ* (gift from Dr. Mesaeli, Weill Cornell Medical College in Qatar). Cells were harvested 48 hours post-transfection using Nonidet P-40 (NP-40) lysis buffer (1 M Tris, 10% NP-40, 50 mM dithiothreitol (DTT), pH 7.8), and the luciferase activity was measured in

luciferase assay buffer (20 mM Tricine, 1.07 mM $MgCO_3$, 2.67 mM $MgSO_4$, 0.1 mM EDTA, 33.3 mM DTT, 270 µM coenzyme A, 470 µM beetle luciferin (Promega), 530 µM ATP) using a Lumat LB 9507 luminometer. β-galactosidase activity was measured using a spectrophotometer (MRX TC Revelation plate reader, Dynex Technologies) at 410 nm and was used to normalize the luciferase results to the transfection efficiency.

10. Electrophoretic mobility shift assays (EMSA)

Recombinant versions of WT PROX1, ^{623}WF**EE**FR^{628} PROX1 and HDΔ PROX1 protein were made using the pMal fusion protein system (New England Biolabs, (Baxter *et al.* 2011). EMSA oligonucleotide probes (Sigma Genosys) were annealed and terminally labelled with γ^{32}P dATP (GE Healthcare Life Sciences) at the 5' end using T4 polynucleotide kinase (refer to Table 4 for probe sequences (Song *et al.* 2006)). The labelled probes were then diluted to 0.05 pmol/µL and mixed with 400 ng of recombinant protein. The reactions were incubated at room temperature for 30 minutes in binding buffer (20% glycerol, 5 mM $MgCl_2$, 2.5 mM EDTA, 2.5 mM DTT, 250 mM NaCl, 50 mM Tris-HCl pH 7.5, 0.25 mg/mL poly(dI-dC);poly(dI-dC)). The samples were then run on a 6% polyacrylamide gel for 20 minutes at 300V. The gels were dried and exposed to autoradiographic film overnight at -80°C.

11. Statistical Analysis

Statistical analysis for all experiments was performed using Origin 8 software. A paired Student's t-test was used to analyze groups containing two samples whereas a one-way ANOVA analysis was used to analyze groups containing multiple samples. Significant differences for ANOVA analyses were determined using the Tukey post-hoc analysis test at a p-value of less than 0.05.

Table 4: EMSA probes (Shin *et al.* 2006).

Probe name	Probe sequence
FGFR-3 sense PROX1 binding site	5'- CTGGGCTCCCACGCCTCTGGGACCGCCCG-3'
FGFR-3 anti-sense PROX1 binding site	5'- CGGGCGGTCCCAGAGGCGTGGGAGCCCAG-3'
FGFR-3 sense PROX1 binding site mutant	5'- CTGGGCTCCACTTAAGCTGGGACCGCCCG-3'
FGFR-3 anti-sense PROX1 binding site mutant	5'-CGGGCGGTCCCAGCTTAAGTGGAGCCCAG-3'

VI. RESULTS

1. Identification of the functional domains of PROX1 required for activation of *Ccne1* transcription

To identify the functional domains in PROX1 required for activation of the 1 kb *Ccne1* promoter, we first generated expression constructs encoding various versions of mouse PROX1 in which potential functional domains were either mutated or deleted (Figure 5). We transfected HEK 293 and U2OS cells and used immunocytochemistry and western blotting to determine whether each version of PROX1 was localized to the nucleus in transfected cells and to compare the expression levels of each construct. We observed that the WT version of PROX1 was uniformly distributed throughout the nucleus (Figure 6). We noted that the HDΔ and HDPD2Δ versions of PROX1 were also similarly localized to the nucleus, but in contrast to WT PROX1, these mutant proteins were localized in a more punctate pattern (Figure 6). Additionally, we harvested whole cell lysates from transfected cells and used western blotting to establish whether the different versions of PROX1 were equally expressed (Figure 7). We observed that all of the versions were equivalently expressed, with the exception of the HDPD2Δ version, which was expressed at a significantly higher level than WT PROX1 (Figure 7).

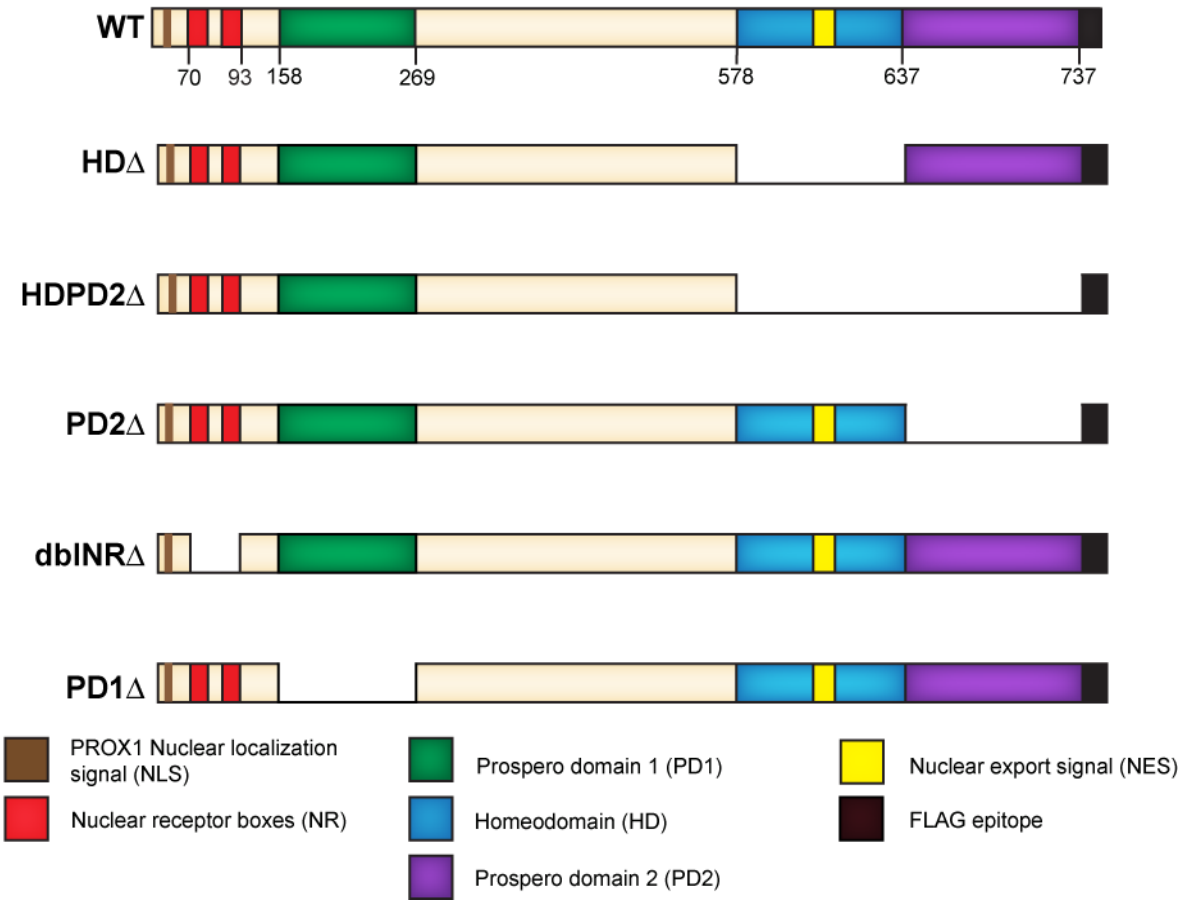

Figure 5: Known functional domains of PROX1 and mutation or deletion versions used in this study. PROX1 is a 737 amino acid atypical homeobox protein. In the N-terminal region of the protein, there are two nuclear receptor boxes (NR), nuclear localization signal (NLS) and a highly conserved Prospero domain 1 (PD1). The C-terminal region is composed of the homeodomain (HD) and the Prospero domain 2 (PD2), which together bind directly bind to DNA. PROX1 also contains a nuclear export signal (NES) in the homeodomain. All constructs used in this project were cloned into the pCMV-Tag4A vector (Stratagene) and are FLAG tagged at the C-terminus.

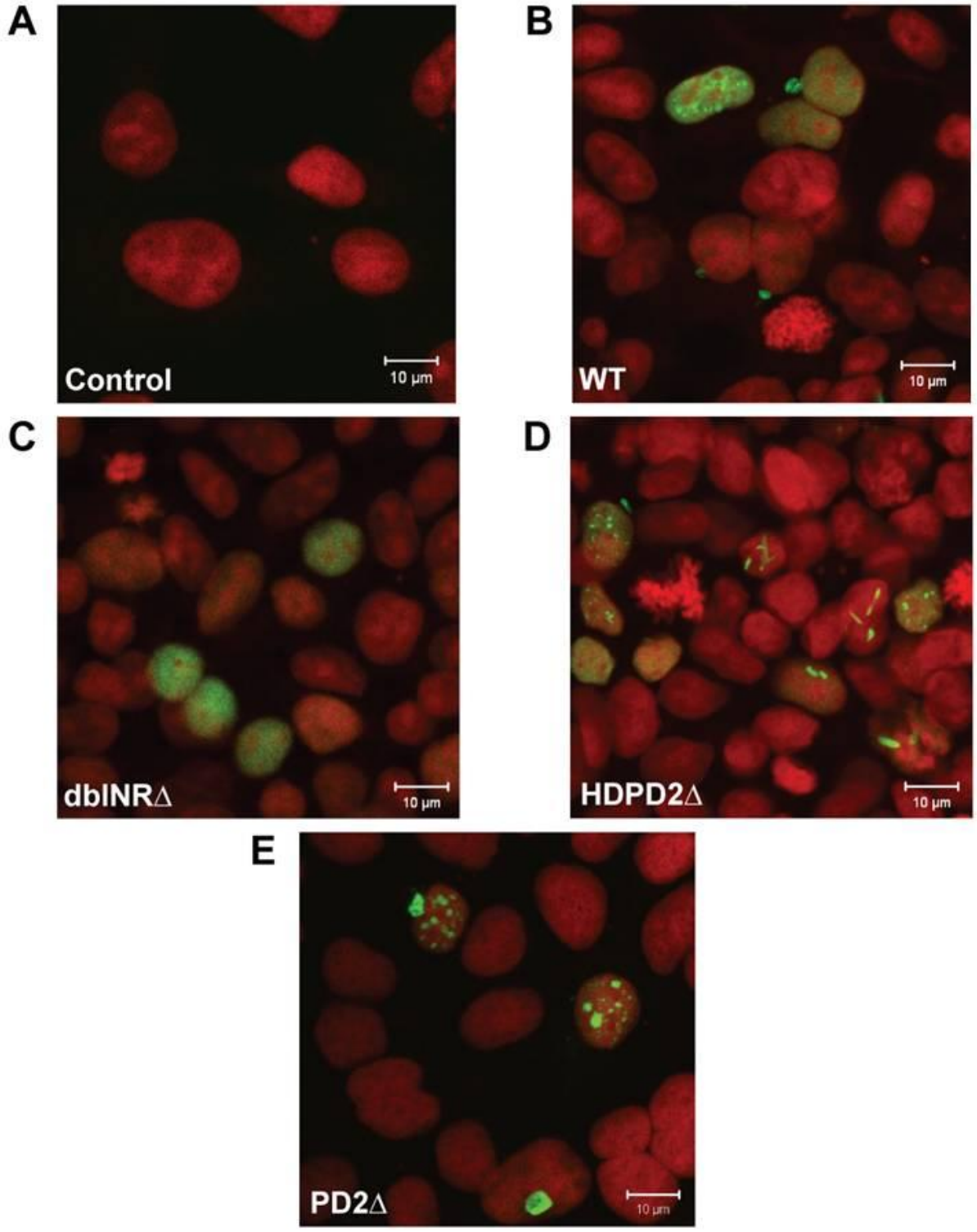
A
Control
10 µm
B
WT
10 µm
C
dblNRΔ
10 µm
D
HDPD2Δ
10 µm
E
PD2Δ
10 µm

Figure 6: Subcellular localization of PROX1 versions in HEK 293 cells. HEK 293 cells were transiently transfected with A) Empty pCMV-Tag4A vector (Control), B) wild-type PROX1 (WT), C) nuclear receptor boxes deleted PROX1 (dblNRΔ), D) homeodomain and Prospero domain 2 deleted (HDPD2Δ) and E) Prospero domain 2 deleted (PD2Δ). Scale bars represent 10μM, nuclei were labelled with propidium iodide (red) and exogenous PROX1 was detected with an anti-FLAG monoclonal antibody (green).

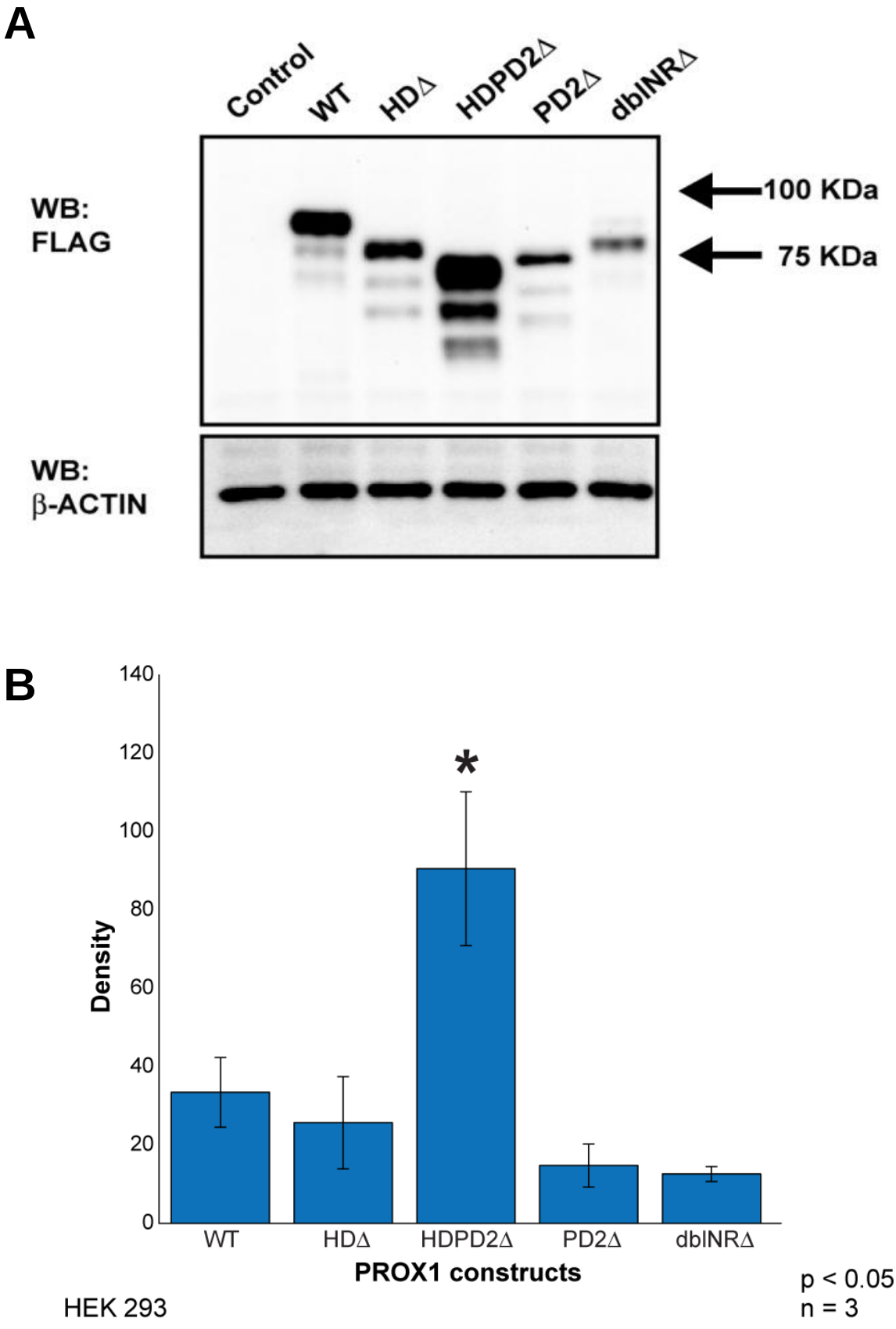
A
Control
WT
HDΔ
HDPD2Δ
PD2Δ
dblNRΔ
WB:
FLAG
100 KDa
75 KDa
WB:
β-ACTIN
B
140
120
100
80
60
40
20
0
Density
*
WT
HDΔ
HDPD2Δ
PD2Δ
dblNRΔ
PROX1 constructs
HEK 293
p < 0.05
n = 3

Figure 7: Protein expression levels of the different versions of PROX1 used for this project. HEK 293 cells were transfected with expression vectors encoding different versions of PROX1 and harvested for western blot. A) A representative blot showing the protein expression levels of an assortment of PROX1 deletion versions. B) Quantification of western blots normalized to the β-ACTIN loading control of PROX1 versions in HEK 293 cells. Empty pCMV-Tag4A vector was used for the control lane and the other PROX1 versions tested were wild-type (WT), homeodomain deleted (HDΔ), homeodomain and Prospero domain 2 deleted (HDPD2Δ), Prospero domain 2 deleted (PD2Δ) and both nuclear receptor boxes deleted (dblNRΔ). (*) denotes significance from WT at a p value of less than 0.05.

2. The PD1 domain mediates PROX1 subcellular localization

Surprisingly, during our analysis of the different PROX1 constructs, we discovered that the PD1Δ version of PROX1 was localized to both the nucleus and the cytoplasm in HEK 293 and in U2OS cells (Figure 9C). The PD1 domain (AA 158-269) is an evolutionarily conserved region of PROX1, although its function remains unknown (Figure 8). The unexpected finding of PD1Δ being localized to the cytoplasm suggested a potential role for the PD1 domain in either mediating PROX1 nuclear import or nuclear export. A nuclear localization signal (NLS) is predicted in the N-terminus of the protein spanning amino acids 14-18. The PROX1 ortholog Prospero has been shown to have a nuclear export signal (NES) in the homeodomain and this sequence is conserved in PROX1 (Demidenko *et al.* 2001). The Prospero NES is hidden or masked by the Prospero domain, which makes it inaccessible to the nuclear exportins and results in Prospero being retained in the nucleus. Although this has not been directly shown in PROX1, it is possible that the PD2 domain or another known domain in the protein functions in a similar manner in mammalian cells.

To distinguish between a role of the PD1 domain in controlling PROX1 nuclear import or PROX1 nuclear export, we treated U2OS cells with 1 ng/mL of the nuclear export inhibitor Leptomycin B (LMB) for 20 hours and used immunocytochemistry to measure the effects on WT and PD1Δ subcellular localization. We observed that PD1Δ was predominantly localized to the nucleus following LMB treatment (compare Figure 9C and 9F). This result supported a role for the PD1 domain in preventing PROX1 nuclear export potentially via acting as a NES mask (Demidenko *et al.* 2001; Ryter *et al.* 2002).

We then compared the PD1Δ version of PROX1 with another version of PROX1 that had been previously generated in our lab. This version, glutamine rich region deletion (QrichΔ), contains a deletion of amino acids 211-260 and is localized solely to the nucleus and significantly activates the 1 kb *Ccne1* promoter to the same extent as WT PROX1 (Bocangel 2006). In comparing this version to PD1Δ, which had a pronounced effect on PROX1 subcellular localization, we realized that there were two regions left intact in the QrichΔ version that may be responsible for the effects we observed with the PD1Δ deletion version of PROX1 (Figure 11). We deleted these two areas to make two new variants of PD1Δ PROX1, which we designated NterPD1Δ (deletion of residues 158 to 211) and CterPD1Δ (deletion of residues 260-269) (Figure 11). We used western blotting in HEK 293 cells and determined that the proteins were expressed (Figure 12). We then used immunocytochemistry to characterize the subcellular localization of the proteins. We observed that CterPD1Δ was localized to the nucleus in a similar fashion as the WT PROX1 protein (Figure 13). In contrast, NterPD1Δ was localized both to the nucleus and the cytoplasm as seen with the PD1Δ version (Figure 13). We used luciferase assays in both HEK 293 and U2OS cells with the 220 *bp FGFR-3* promoter and observed that similar to PD1Δ in HEK 293 cells, NterPD1Δ did not significantly activate the promoter to the same extent as did WT PROX1 (Figure 14). In U2OS, there was no difference between different versions of PROX1 in activating the the 220 *bp FGFR-3* promoter (Figure 14). These findings indicate that the NterPD1 region spanning amino acids 158-211 is involved in mediating PROX1 subcellular localization and function.

```
Human          DEHLRAKRARVENIIRGMSHSPSVALRGNENEREMAPQSVSPRESYRENKRKQKLPQQQQ
Mouse          DEHLRAKRARVENIIRGMSHSPSVALRGNENEREMAPQSVSPRESYRENKRKQKLPQQQQ
Chicken        DEHLRAKRARVENIIRGMSHSPRVALRGNENEREIRPQSVSPRESYRENKRKQNWPQQQQ
Zebrafish      DEHLRAKRARVENIIRGMSHSPSVTLRAGDNDREGAAQPPSPRENYRENKRKQKLPQQQQ
               ********************** *:**..:*:**  .*. ****.********: *****

Human          QSFQQLVSARKEQKREERRQLKQQLEDMQKQLRQLQEKFYQIYDSTDSEND
Mouse          QSFQQLVSARKEQKREERRQLKQQLEDMQKQLRQLQEKFYQVYDSTDSEND
Chicken        QSFQQLVSARKEQKREERRQLKQQLEDMQKQLRQLQEEFYQIYDSTDSEND
Zebrafish      QSFQQLVSARKEQKHEERRQLKLQLEDMQKQLRQLQEKFYQIYDSTDSEND
               **************:******* **************:***:*********
```

Figure 8: Sequence comparison of the PD1 domain (amino acids 158-269). CLUSTALw (NCBI) was used to align the PD1 domains of human, mouse, chicken and zebrafish PROX1 to compare the sequence conservation across evolutionarily distant species. (*) indicate conserved residues, (**:**) indicates a conserved strong group and (**.**) indicates a conserved weak group as described in the CLUSTALw search set up (NCBI).

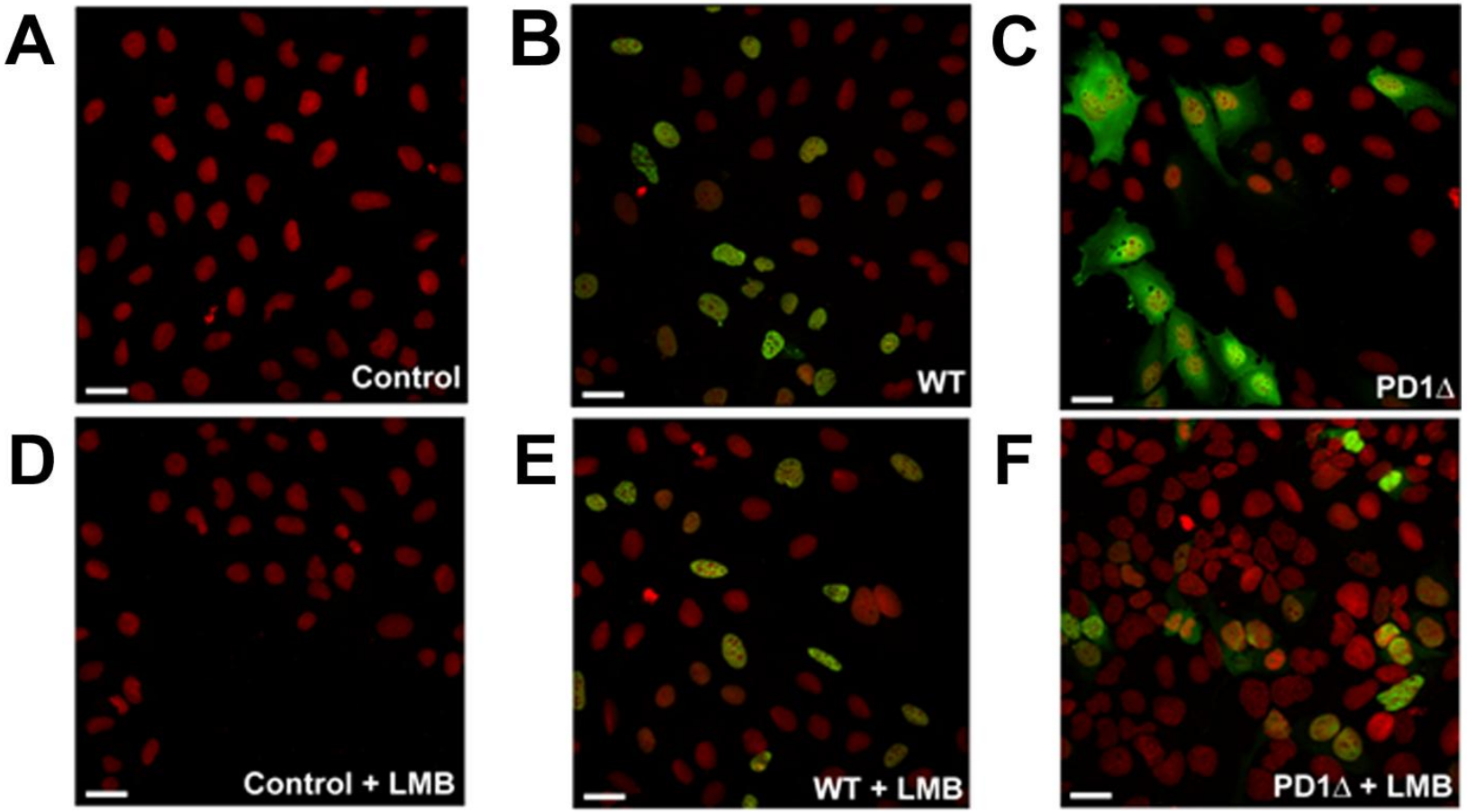
A
Control
B
WT
C
PD1Δ
D
Control + LMB
E
WT + LMB
F
PD1Δ + LMB

Figure 9: The Prospero domain 1 (PD1) is important for PROX1 subcellular localization. To establish whether the PD1 domain was involved in nuclear import or nuclear export, U2OS cells were transfected with empty pCMV-Tag4A vector (Control), wild-type PROX1 (WT) or the PD1 deletion version of PROX1 (PD1Δ) and treated with 1 ng/ml of the nuclear export inhibitor leptomycin B (LMB) for 20 hours. Scale bars represent 20μM, nuclei were labelled with propidium iodide (red) and exogenous PROX1 was detected with an anti-FLAG monoclonal antibody (green).

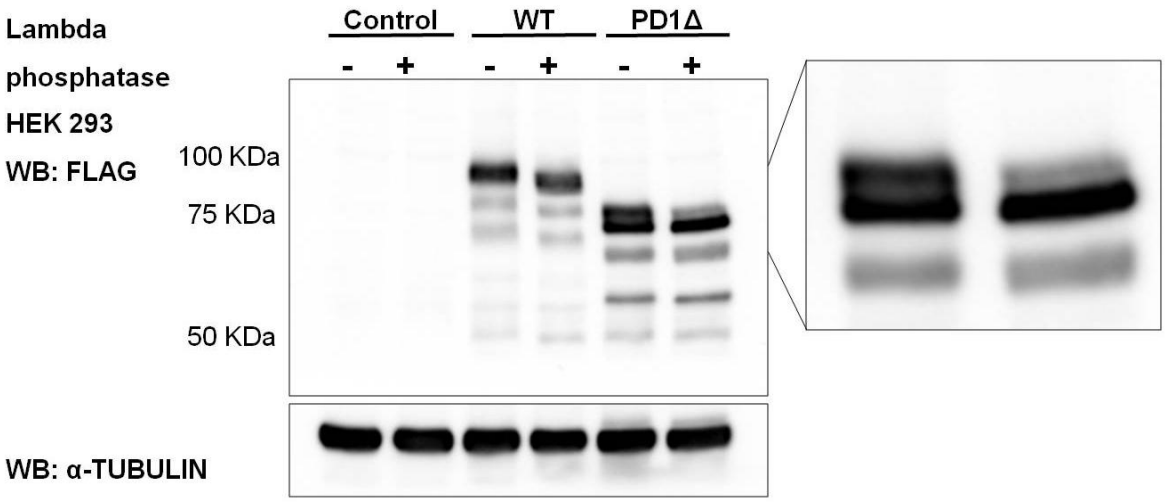

Figure 10: Western blot showing the phosphorylation status of PD1Δ. Whole cell lysates were harvested from HEK 293 cells that were transiently transfected with empty pCMV-Tag4A (Control), wild-type PROX1 (WT) or Prospero domain 1 deleted PROX1 (PD1Δ) and treated with protein lambda phosphatase for three hours prior to SDS-PAGE and western blotting. (+ indicates lanes treated with lambda phosphatase).

A

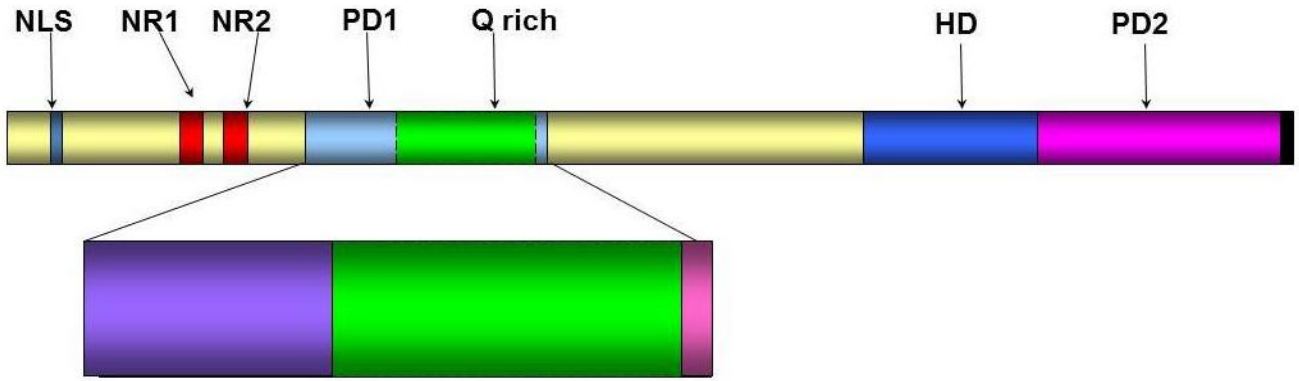

B

```
Human       DEHLRAKRARVENIIRGMSHSPSVALRGNENEREMAPQSVSPRESYRENKRKQKLPQQQQ
Mouse       DEHLRAKRARVENIIRGMSHSPSVALRGNENEREMAPQSVSPRESYRENKRKQKLPQQQQ
Chicken     DEHLRAKRARVENIIRGMSHSPRVALRGNENEREIRPQSVSPRESYRENKRKQNWPQQQQ
Zebrafish   DEHLRAKRARVENIIRGMSHSPSVTLRAGDNDREGAAQPPSPRENYRENKRKQKLPQQQQ
            ********************** *:**..:*:**  .*. ****.********: *****

Human       QSFQQLVSARKEQKREERRQLKQQLEDMQKQLRQLQEKFYQIYDSTDSEND
Mouse       QSFQQLVSARKEQKREERRQLKQQLEDMQKQLRQLQEKFYQVYDSTDSEND
Chicken     QSFQQLVSARKEQKREERRQLKQQLEDMQKQLRQLQEEFYQIYDSTDSEND
Zebrafish   QSFQQLVSARKEQKHEERRQLKLQLEDMQKQLRQLQEKFYQIYDSTDSEND
            **************:******* **************:***:*********
```

Figure 11: Regions of PROX1 that were deleted to make the N-terminal Prospero domain 1 deletion (NterPD1Δ) and C-terminal Prospero domain 1 deletion (CterPD1Δ) versions of PROX1. The Prospero domain 1 sequence was compared with another version of PROX1 previously generated in the lab (QrichΔ) and two areas that were not previously deleted were identified. These two regions were deleted individually to generate two new versions of PROX1 (NterPD1Δ and CterPD1Δ) and used for further experiments.

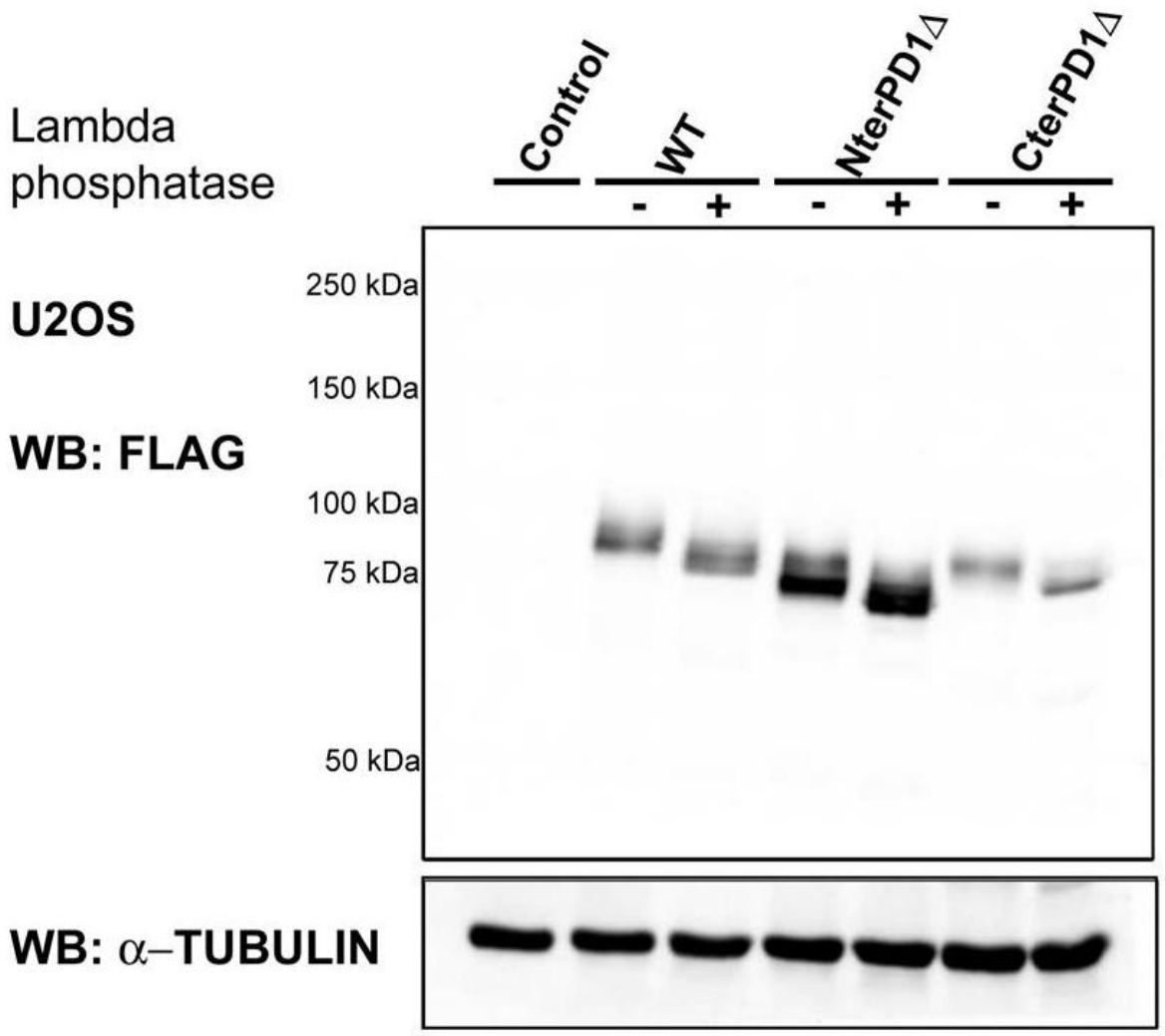

Figure 12: NterPD1Δ and CterPD1Δ deletion versions of PROX1 are phosphoproteins. U2OS cells were transiently transfected with either empty pCMV-Tag4A (control), wild-type (WT), NterPD1Δ or CterPD1Δ and the lysates were treated with or without lambda phosphatase before separation on a SDS-PAGE gel.

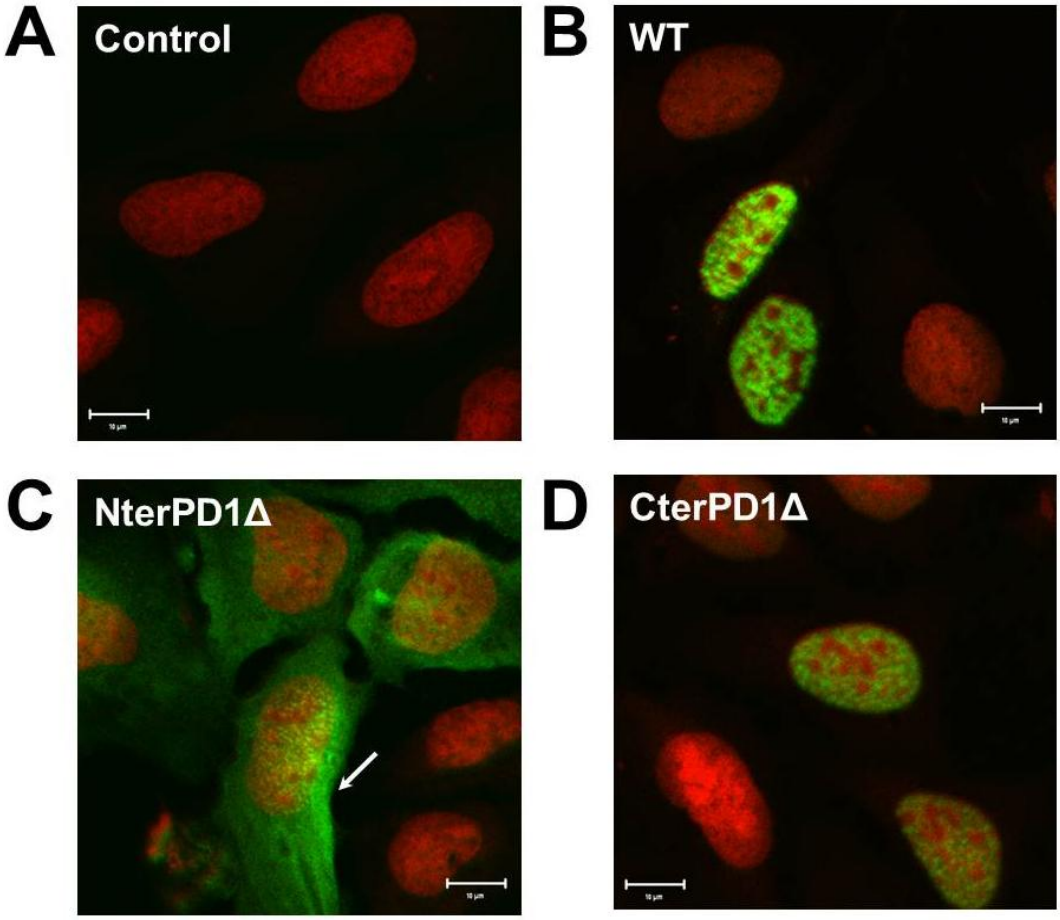

Figure 13: N-terminal region of the Prospero domain 1 (PD1) is essential for proper PROX1 subcellular localization. U2OS cells were transiently transfected with empty pCMV-Tag 4A vector (control), wild-type PROX1 (WT) or N-terminal deletion of the PD1 domain (NterPD1Δ) or C-terminal deletion of the PD1 domain (CterPD1Δ) Prox1. Scale bars indicate 10μM, the nuclei were stained red with propidium iodide and FLAG-PROX1 was stained green with Alexa Fluor 488.

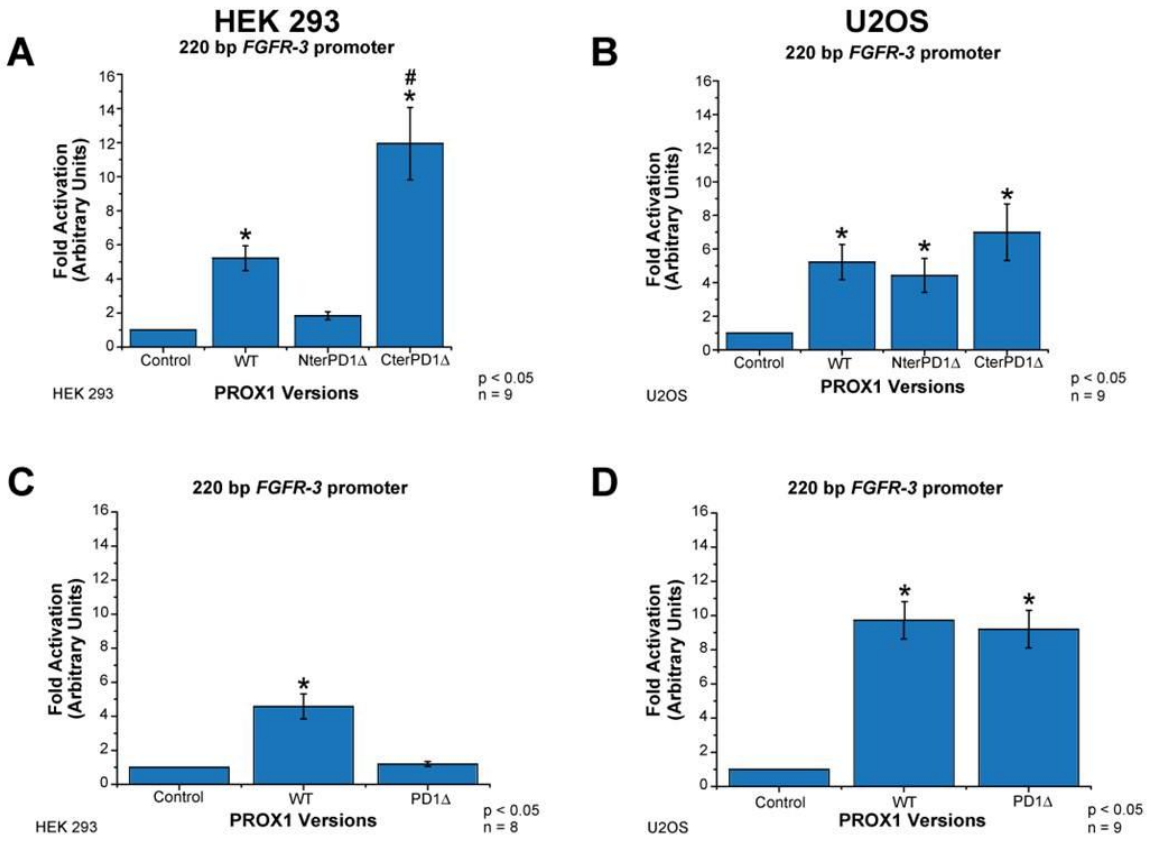

Figure 14: Prospero domain 1 (PD1) deletion alters PROX1 transcriptional potency. Luciferase reporter gene assays were performed with the 220 *bp FGFR-3* promoter to compare the activity of NterPD1Δ , CterPD1Δ and PD1Δ in HEK 293 (A and C) and U2OS (B and D) cells. (*) denotes significance from control and (#) denote significance from WT at a p value of less than 0.05.

3. PROX1 activates *Ccne1* transcription via a DNA-binding independent mechanism.

We next sought to determine the domains of PROX1 which were necessary for activation of the *Ccne1* promoter. We used luciferase reporter gene assays in HEK 293 cells with a 1 kb segment of the mouse *Ccne1* promoter and the various deletion or mutation versions of PROX1 to evaluate the key functional domains. We observed that WT PROX1 activated the 1 kb promoter approximately 4-5 fold (Figure 15). HDΔ and dblNRΔ activated the promoter to levels equivalent to WT (Figure 15 and 16). In contrast, the PD2Δ and HDPD2Δ versions only activated the promoter 2-3 fold which was significantly different from both control and WT (Figure 15). This finding suggests that the HD domain, a known DNA-binding motif, is dispensable for PROX1 mediated activation of *Ccne1*, which would support a role for PROX1 activating *Ccne1* transcription in a DNA-binding independent manner.

To support this hypothesis that our HDΔ version was unable to bind DNA, we first performed luciferase assays using a 220 bp *FGFR-3* promoter (McEwen *et al.* 1999). *FGFR-3* is a known target of PROX1 in which PROX1 functions as a transcriptional activator and directly binds to DNA (Shin *et al.* 2006). As such, we predicted that the HDΔ version should not be able to activate this promoter. WT significantly activated the promoter as expected, whereas both the HDΔ version and our DNA-binding domain mutant (^{623}WF**EE**FR^{628}) did not significantly activate the promoter (Figure 17A). We further confirmed our constructs were incapable of binding DNA by using electrophoretic mobility shift assays (EMSA). We tested if either the HDΔ and or ^{623}WF**EE**FR^{628} recombinant fusion proteins could

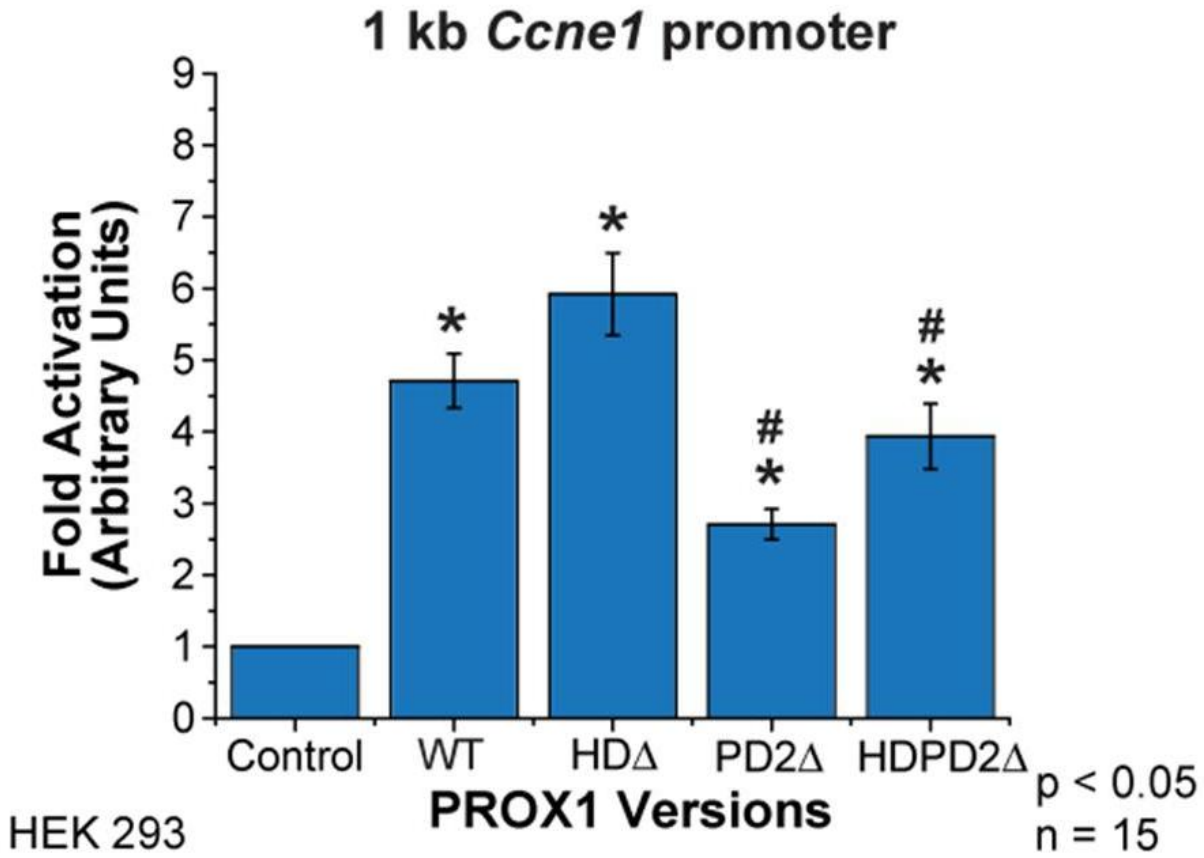

Figure 15: PROX1 activates a 1 kb *Ccne1* promoter via a DNA-binding independent mechanism. Various versions of PROX1 in which either the homeodomain (HD) or the Prospero domain 2 (PD2) were deleted individually or together were generated. The HDPD2 together forms the DNA-binding domain of PROX1 and as such these constructs are not able to bind directly to DNA. Luciferase assays with the 1 kb mouse *Ccne1* promoter were used to assess if these versions could activate the promoter. (*) denotes significance from Control and (#) denotes significance from WT at a p value of less than 0.05.

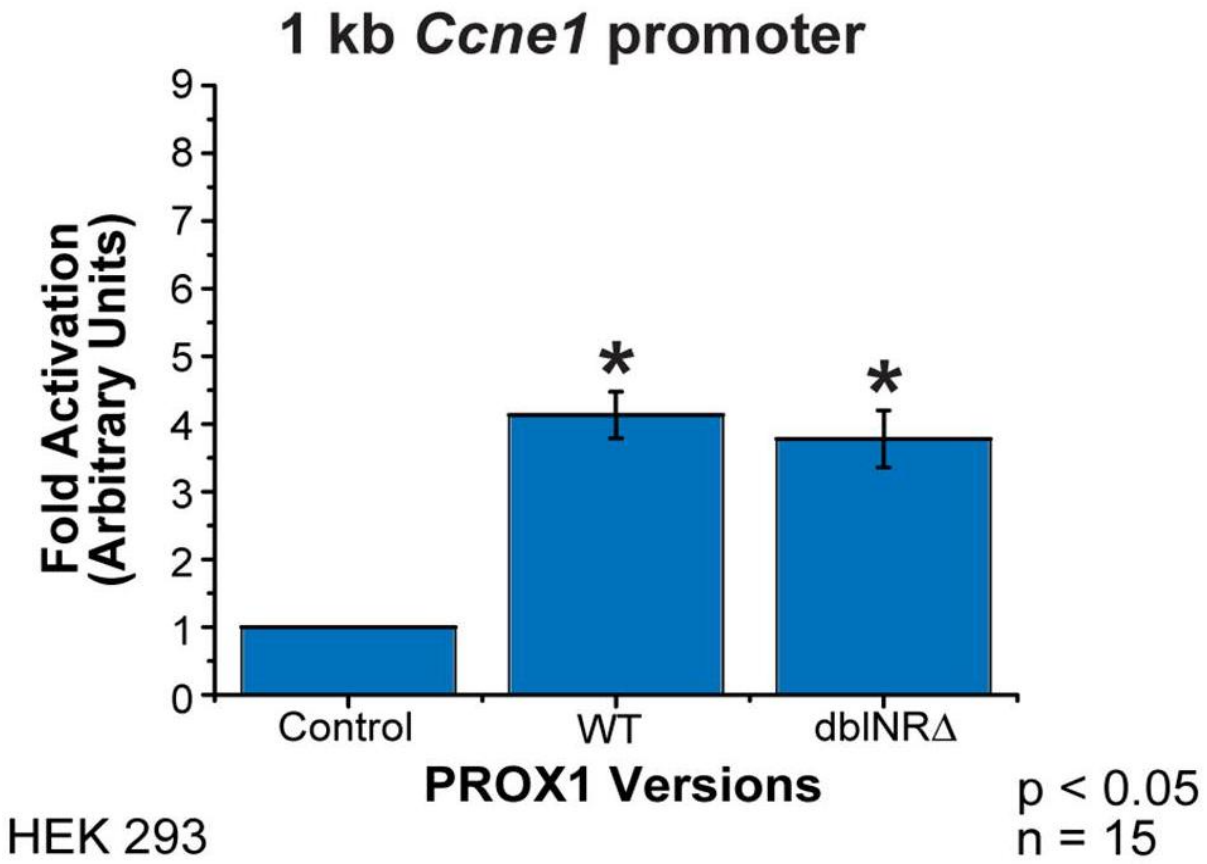

Figure 16: The nuclear receptor (NR) boxes are not required for PROX1 mediated transcriptional activation of the 1 kb *Ccne1* promoter. HEK 293 cells were transfected with a version of PROX1 in which both nuclear receptor boxes had been deleted (dblNRΔ) and luciferase assays were used to determine whether this mutant construct activated the 1 kb *Ccne1* promoter. (*) denotes significance from Control at a p value of less than 0.05.

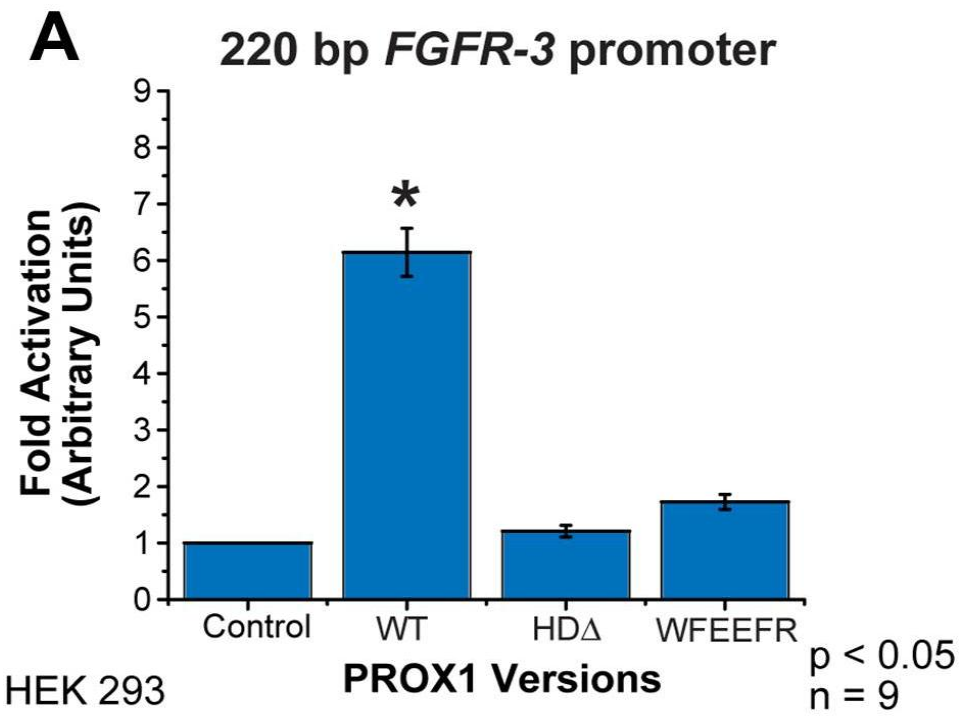
A
220 bp FGFR-3 promoter
Fold Activation (Arbitrary Units)
9
8
7
6
5
4
3
2
1
0
*
Control
WT
HDΔ
WFEEFR
PROX1 Versions
HEK 293
p < 0.05
n = 9

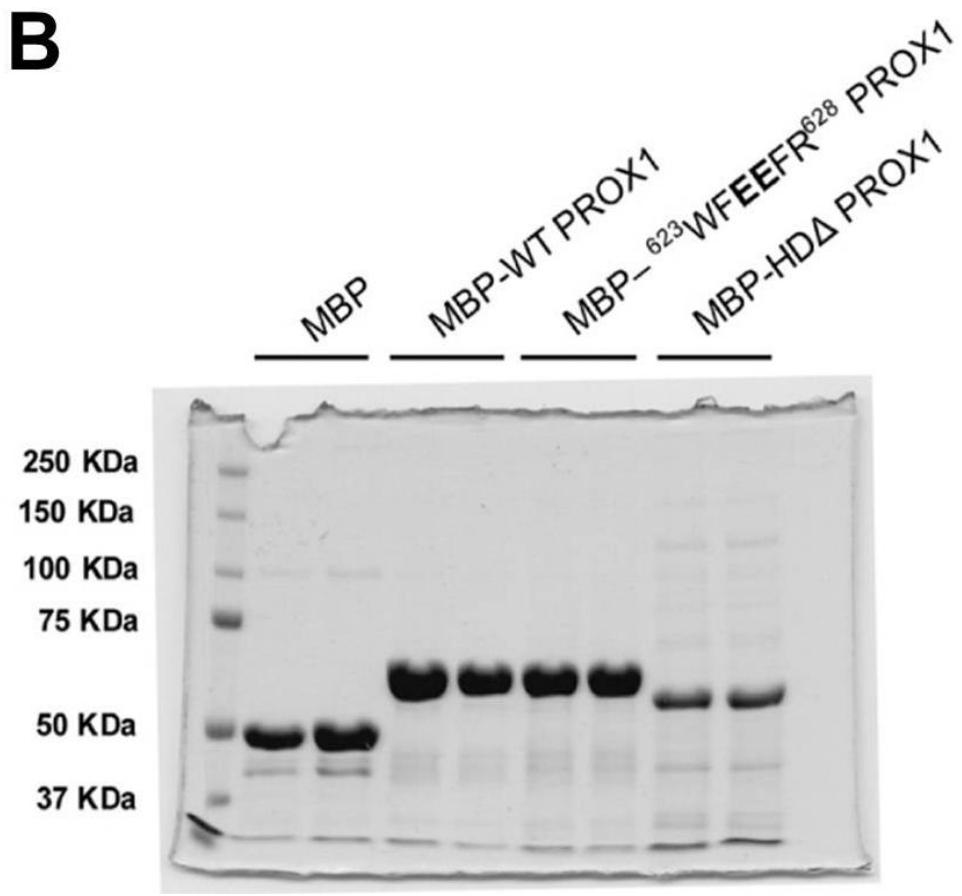
B
MBP
MBP-WT PROX1
MBP–623WFEEFR628 PROX1
MBP-HDΔ PROX1
250 KDa
150 KDa
100 KDa
75 KDa
50 KDa
37 KDa

C

	1	2	3	4	5	6	7	8	9	10
Maltose binding protein (MBP)	-	+	-	-	-	-	-	-	-	-
WT PROX1	+	-	+	+	+	-	-	-	-	-
WFEEFR DBDmut PROX1	-	-	-	-	-	+	-	-	-	-
HDΔ PROX1	-	-	-	-	-	-	+	-	-	-
anti-PROX1	-	-	-	+	-	-	-	-	-	-
Rabbit IgG	-	-	-	-	+	-	-	-	-	-
Unlabelled probe	+	-	-	-	-	-	-	-	-	+
Labelled probe	+	+	+	+	+	+	+	+	+	-

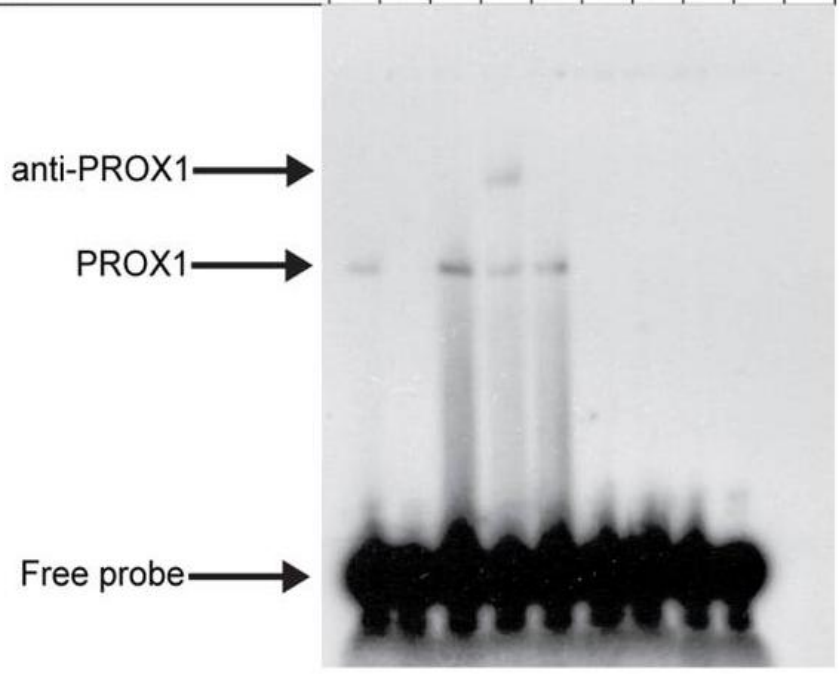

Figure 17: PROX1 DNA-binding is essential for its activation of the *fibroblast growth factor receptor 3 (FGFR3)* promoter. To ensure that the DNA-binding mutants (HDΔ, and ^{623}WF**EE**FR^{628}) were unable to bind DNA A) luciferase assays were performed in HEK 293 cells with a known DNA-binding dependent target of PROX1, the 220 bp *FGFR-3* promoter. B) Purified recombinant protein versions of WT, PROX1 HDΔ, and ^{623}WF**EE**FR^{628} were used to conduct EMSAs. C) Probes encoding the putative PROX1 DNA-binding sites located in the *FGFR-3* promoter (lanes 1, 3, 4, 5) were tested. (*) denotes significance from control at a p value of less than 0.05.

bind to radiolabelled probes encoding the proposed PROX1 binding site in the *FGFR-3* promoter. As expected, WT was the only version of PROX1 that bound the probe and caused a shift (Figure 17C). Upon addition of an anti-PROX1 antibody, we observed a supershift indicating that this result was specific to PROX1. In total, our data supports the hypothesis that PROX1 activates transcription of *Ccne1* through a DNA-binding independent mechanism.

4. Characterization of two DNA-binding domain mutant versions of PROX1.

A previous group (Petrova *et al.* 2002) generated a DNA-binding domain mutant version of PROX1 in which they mutated key residues in the DNA-binding sequence ^{623}WFSNFR^{628} to hydrophobic residues ^{623}WFS**A**F**A**^{628}. Using luciferase reporter gene assays in U2OS cells, they observed that the ^{623}WFS**A**F**A**^{628} mutant did not activate the 1 kb *Ccne1* promoter. As a result, they concluded that PROX1 activated transcription of *Ccne1* through a DNA-binding dependent mechanism. In contrast, we generated a different DNA-binding mutant by replacing two key residues in the DNA-binding sequence with negatively charged glutamate residues which will be repelled by DNA and prevent binding (^{623}WF**EE**FR^{628}) and by deleting the entire homeodomain (HDΔ). We transfected the ^{623}WF**EE**FR^{628} version of PROX1 into HEK 293 cells and observed that it activated the 1 kb *Ccne1* promoter to the same extent as WT supporting a DNA-binding independent mechanism (Figure 18A). As demonstrated in previous sections, we also conducted luciferase assays with PROX1

HDΔ and observed that the activation of the 1 kb *Ccne1* promoter was not significantly different from the WT protein (Figure 15).

To further unravel this discrepancy between our results and that of Petrova *et al.*, we generated the ^{623}WFS**A**F**A**^{628} mutant version of PROX1 and repeated the luciferase reporter gene assays in parallel with our ^{623}WF**EE**FR^{628} mutant version in both HEK 293 and U2OS cell lines. We observed that both DNA-binding domain mutants significantly activated the 1 kb *Ccne1* promoter in HEK 293 cells, but only the ^{623}WF**EE**FR^{628} mutant version significantly activated the *Ccne1* promoter in U2OS cells (Figure 18). We then proceeded to use immunocytochemistry and western blotting to make sure that both proteins were properly localized and expressed in the two different cell lines. To our surprise, we observed that in U2OS cells, a large proportion of cells transfected with the ^{623}WFS**A**F**A**^{628} mutant had PROX1 localized not only in the nucleus but also in the cytoplasm (Figure 19D, arrow). We quantified the extent of this mislocalization by counting three separate fields of view in three separate experiments (the observer was blinded to the identity of the slides both during image acquisition and counting) and determined that 20% of cells transfected with the ^{623}WFS**A**F**A**^{628} mutant showed localization in the nucleus and cytoplasm (Figure 19F). This phenomenon was not as evident in the HEK 293 cells (Figure 19A-C). We proceeded with western blotting to measure the protein expression levels of the DNA-binding mutant proteins as compared to WT. To our surprise, we noticed that the ^{623}WFS**A**F**A**^{628} protein migrated at a smaller apparent molecular weight than either the WT or ^{623}WF**EE**FR^{628} PROX1 proteins in both cell types (Figure 20). Taken together, the altered localization and smaller molecular weight of

the ^{623}WFS**A**F**A**^{628} protein likely accounts for the discrepancies observed between the two DNA-binding mutant versions of PROX1. Our finding supports a role for PROX1 activating *Ccne1* transcription independent of DNA-binding.

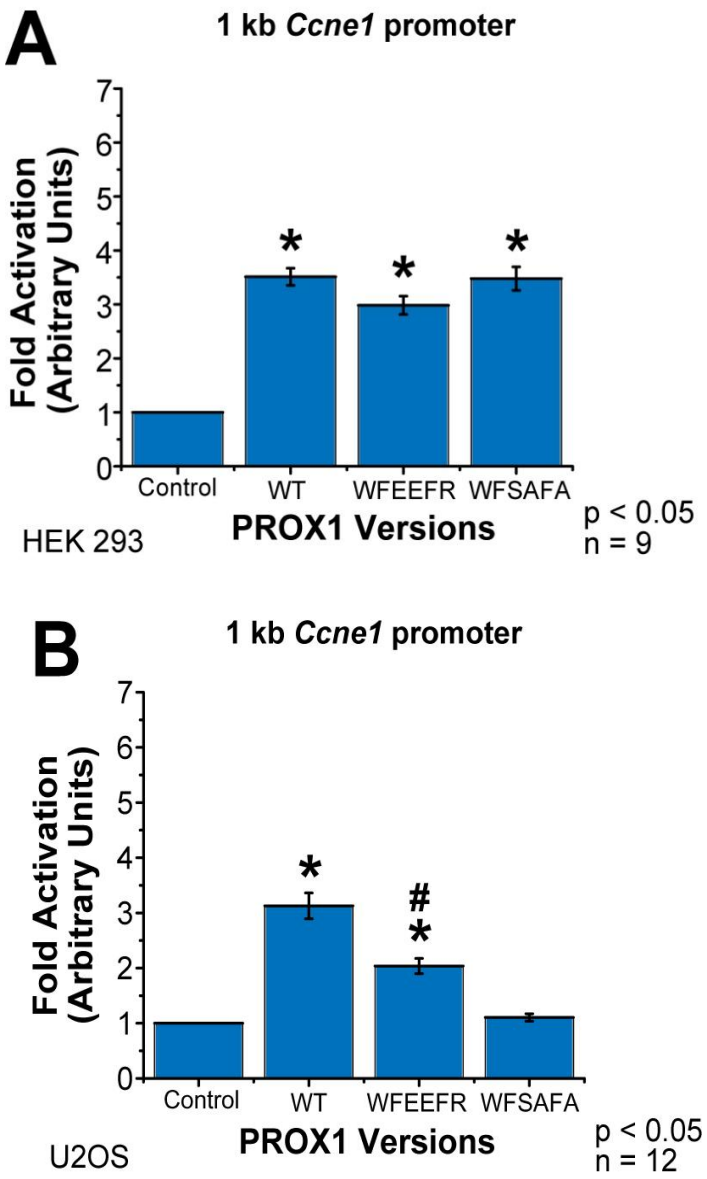

Figure 18: Cell-type specific differences between the DNA-binding domain mutant proteins. The activity of the two DNA-binding domain mutants was compared by conducting luciferase assays with the 1 kb *Ccne1* promoter in A) HEK 293 and B) U2OS cells. (*) denotes significance from control at a p value of less than 0.05.

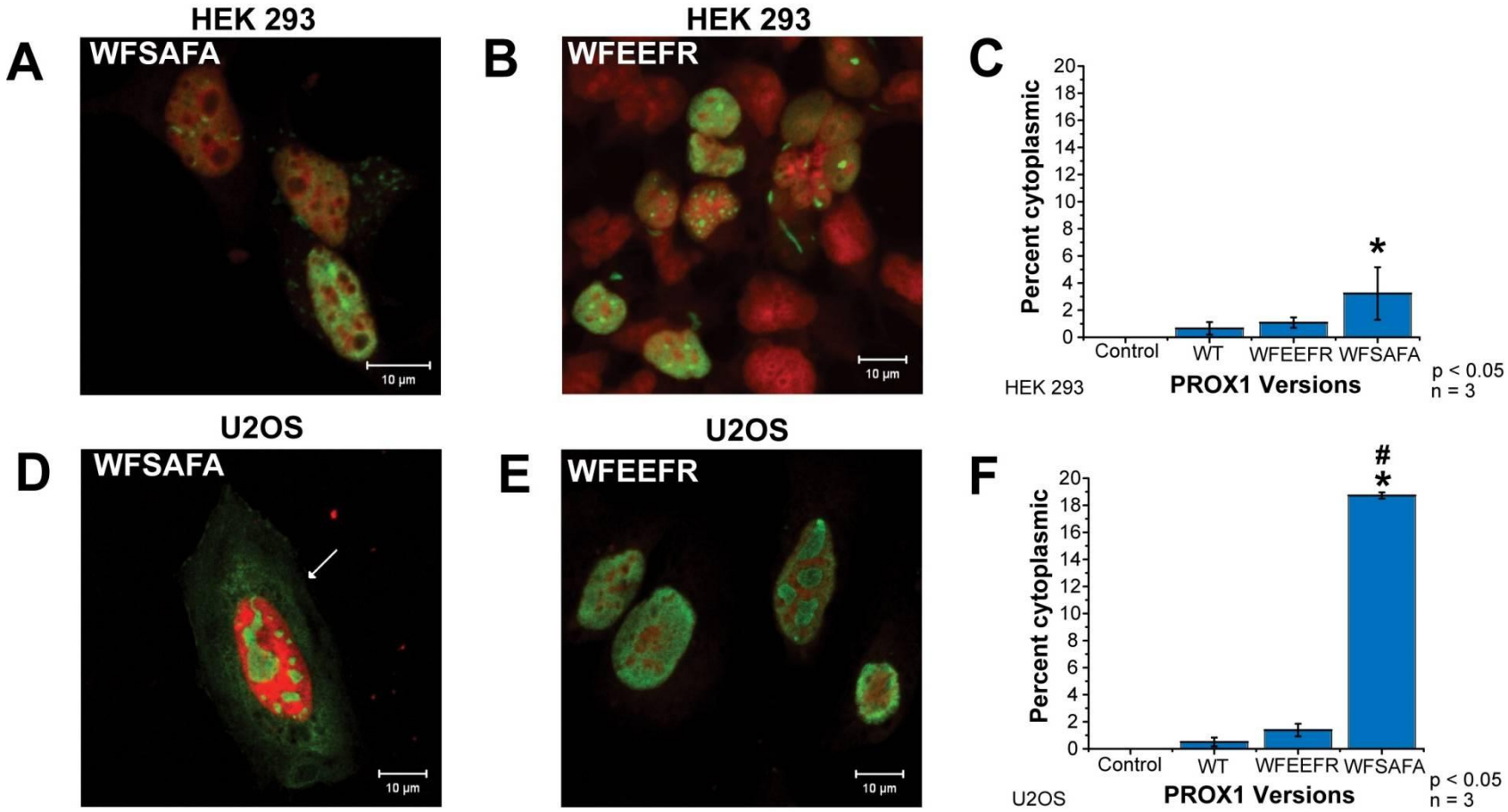
A
HEK 293
WFSAFA
10 µm
B
HEK 293
WFEEFR
10 µm
C
Percent cytoplasmic
20
18
16
14
12
10
8
6
4
2
0
*
Control
WT
WFEEFR
WFSAFA
HEK 293
PROX1 Versions
p < 0.05
n = 3
D
U2OS
WFSAFA
10 µm
E
U2OS
WFEEFR
10 µm
F
Percent cytoplasmic
20
18
16
14
12
10
8
6
4
2
0
#
*
Control
WT
WFEEFR
WFSAFA
U2OS
PROX1 Versions
p < 0.05
n = 3

Figure 19: Comparison of the subcellular localization of the two DNA-binding domain mutants. DNA-binding domain mutant constructs were transiently transfected into A) and D) HEK 293 and B) and E) U2OS cells. Quantification of immunocytochemistry of C) HEK 293 and F) U2OS cells containing PROX1 localization to the cytoplasm. (*) denotes significant from control and (#) denotes significant from wild-type (WT).

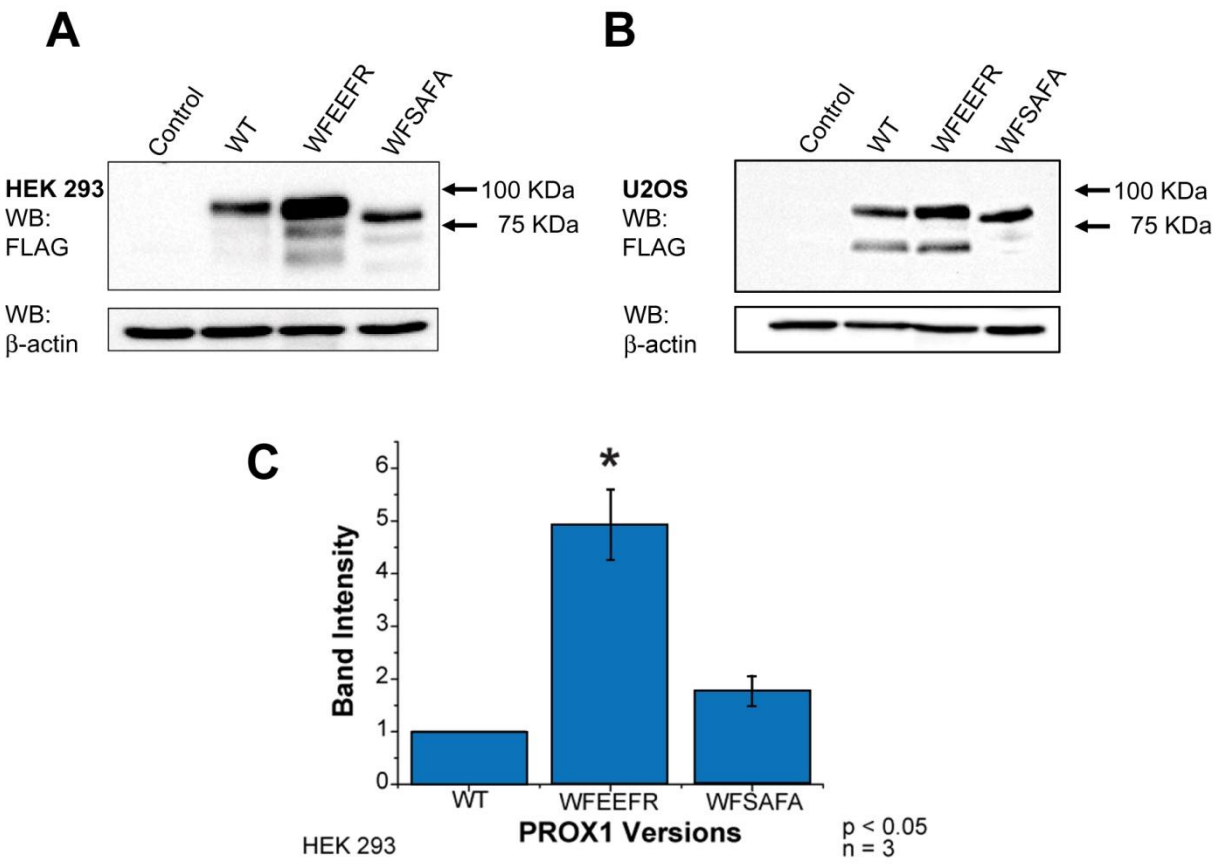

Figure 20: Comparison of the protein expression levels of the DNA-binding domain mutants. A) HEK 293 and B) U2OS cells were transiently transfected with empty pCMV-Tag4A (Control), wild-type (WT) and the two DNA-binding domain mutant proteins (WFEEFR and WFSAFA) and western blotting was performed to measure protein expression levels. C) Blots were normalized to the β-ACTIN control and quantified to evaluate changes in protein expression levels. (*) indicates significant from WT at a p value of less than 0.05.

5. PROX1 is a phosphoprotein

Our observation that the ^{623}WFS**A**F**A**^{628} DNA-binding domain mutant version of PROX1 migrated at a smaller apparent molecular weight was an unexpected, exciting finding. To investigate a cause for this phenomenon, we treated whole cell lysates of HEK 293 (Figure 20A) and U2OS cells (Figure 20B), which were transiently transfected with vectors encoding WT Prox1 and the two DNA mutant versions, with protein lambda phosphatase. Using mass spectrometry, a phosphate group (H_3PO_4) added to a serine or threonine will increase the molecular mass of a protein by 98 Da whereas a phosphate group added to a tyrosine (HPO_4) will increase the molecular mass of a protein by 80 Da (Mann *et al.* 2002). Enzymatic removal of phosphates via a phosphatase enzyme will result in a reduction of the apparent molecular weight of the treated protein. We chose lambda phosphate because it is able to specifically dephosphorylate serine, threonine and tyrosine residues (Zhuo *et al.* 1993), whereas other phosphatases such as calf intestine alkaline phosphatase (CIAP) can have preferences over which type of phosphorylated residues they will recognize. The observed molecular weight of the ^{623}WF**EE**FR^{628} version of PROX1 shifted to a smaller apparent molecular weight following lambda phosphatase treatment (Figure 21). In contrast, the apparent molecular weight of ^{623}WFS**A**F**A**^{628} mutant did not shift to the same extent (Figure 21). We then sought to determine if this effect of lambda phosphatase on the molecular weight of PROX1 was unique to these two cell lines or whether PROX1 was phosphorylated in endothelial cells as well. We treated whole cell lysates from HUVECs infected with adenovirus encoding either WT Prox1 or HDPD2Δ Prox1 at 250 MOI for 48 hours with lambda phosphatase. We observed

that the apparent molecular weight of both WT PROX1 and HDPD2Δ PROX1 was considerably reduced following the addition of the phosphatase (Figure 21). The next question was to determine if this reduction of apparent molecular weight occurred in cells that expressed endogenous PROX1. We used the human liver hepatocellular carcinoma cell line HepG2, which expresses PROX1. In addition, we used primary human dermal lymphatic endothelial cells (LECs). We observed in both cell types that following lambda phosphatase treatment there was a similar change in the apparent molecular weight as we had noted previously for exogenous PROX1 expressed in HEK 293, U2OS and HUVECs (Figure 22, black arrows). We also consistently detected a higher molecular weight version of PROX1 (Figure 22, red arrows). Previous studies had shown that PROX1 is also SUMOylated and the PROX1 band we detected is approximately the same size as the predicted SUMO-PROX1 complex shown by these groups (Shan *et al.* 2008; Pan *et al.* 2009).

We then proceeded to identify putative phosphorylation sites in PROX1. We first used two online prediction tools (MotifScan and PhosSite) to identify potential sites. As well, a previous mass spectrometry scan had been performed of all of the phosphoproteins in the mouse liver (Villen *et al.* 2007).

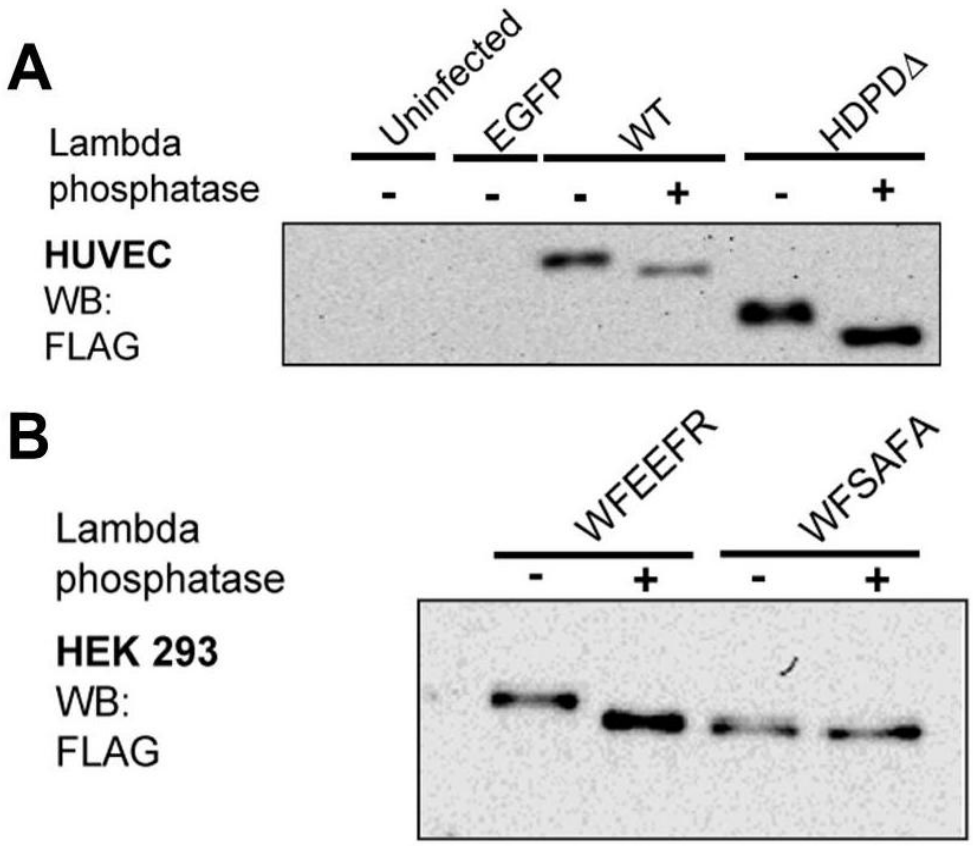

Figure 21: Exogenous PROX1 is phosphorylated. To determine if ectopically expressed versions of PROX1 were phosphorylated, whole cell lysates from either A) HUVECs infected with adenovirus encoding PROX1 or B) HEK 293 cells that were transiently transfected with PROX1 expression plasmids were treated with (+) or without (-) protein lambda phosphatase.

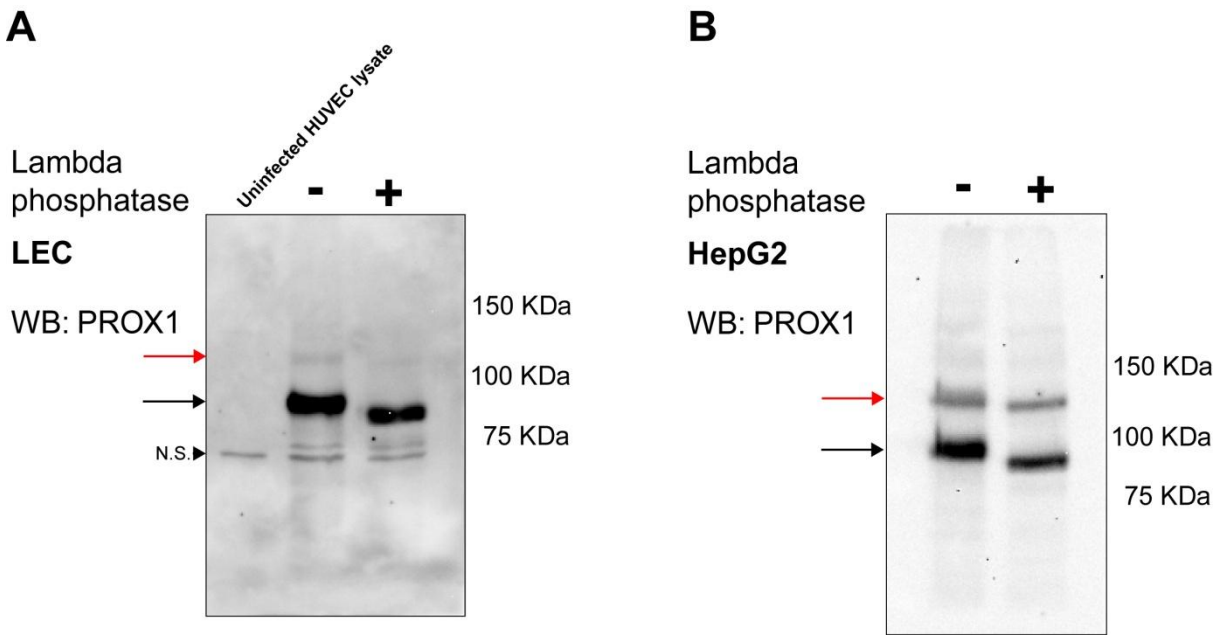

Figure 22: Endogenous PROX1 is phosphorylated. Whole cell lysates of both A) primary Lymphatic Endothelial Cells (LEC) and B) HepG2 human liver hepatocellular carcinoma cells were treated with protein lambda phosphatase and used for western blotting to determine if endogenous PROX1 was phosphorylated. N.S. identifies a non-specific band that was observed in both LEC and Human Umbilical Vein Endothelial Cell (HUVEC) whole cell lysates.

A

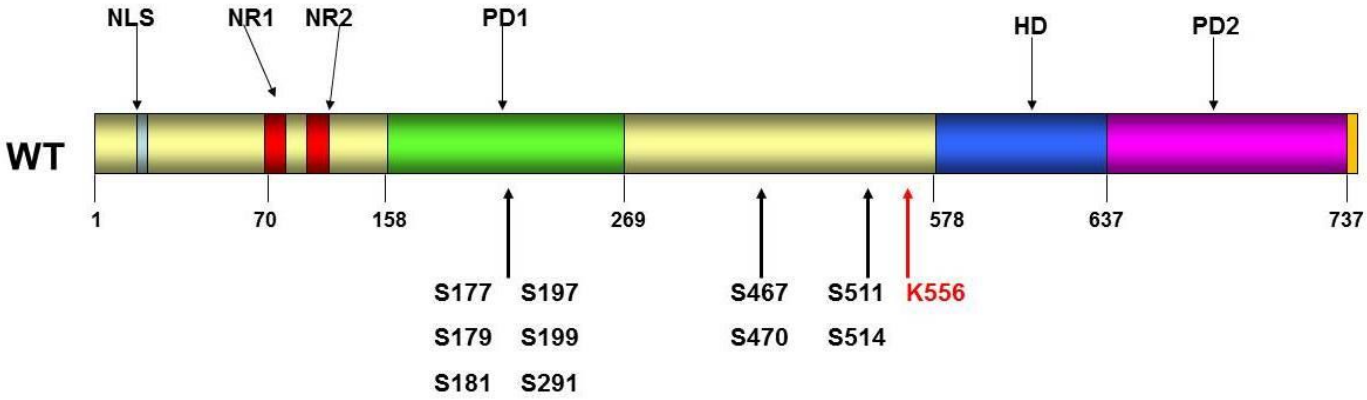

B

Site	Kinase	Frequency	Source
S177	Protein Kinase A (PKA)	3	ScanSite and Villen *et al.*, 2007
S179	Cell Division Cycle 2 (cdc2)	3	ScanSite and Villen *et al.*, 2007
S181	Protein Kinase C (PKC)	1	ScanSite and Villen *et al.*, 2007
S197	?	6	ScanSite and Villen *et al.*, 2007
S199	cdc2	9	ScanSite and Villen *et al.*, 2007
S291	?	2	Villen *et al.*, 2007
S467	?	1	Villen *et al.*, 2007
S470	?	1	Villen *et al.*, 2007
S511	?	3	Villen *et al.*, 2007
S514	Casein Kinase 2 (CK2)	1	ScanSite and Villen *et al.*, 2007

Figure 23: PROX1 contains multiple predicted phosphorylation sites. Using Scansite (an online prediction tool) combined with analysis of a published scan of phosphoproteins detected in the mouse liver (Villen *et al*., 2007), putative phosphorylation sites in PROX1 were identified. A) A diagram of the structure of the PROX1 protein showing the nuclear localization signal (NLS), nuclear receptor boxes (NR1 and NR2), the Prospero domain 1 (PD1), the homeodomain (HD) and the Prospero domain 2 (PD2). The potential phosphorylation sites and their location relative to the known functional domains are indicated in black font below and a predicted SUMOylation site is indicated in red font. Many of the predicted phosphorylation sites are clustered in the N-terminus of PROX1, specifically in the PD1 domain. B) A chart of the predicted phosphorylation sites identified by the online searches along with potential kinases that may be responsible and the frequency which these sites were found (Villen *et al.,* 2007).

PROX1 is highly expressed in the liver. By pooling the data from the three sources, we found that PROX1 has multiple potential phosphorylation sites, many of which are clustered in the PD1 domain (Figure 23). We treated lysates from HEK 293 cells transfected with the PD1Δ version of PROX1 with or without lambda phosphatase. We observed that untreated PD1Δ PROX1 was detected as a doublet by western blotting (Figure 10). This doublet was resolved largely into a single band with lambda phosphatase treatment, indicating that the PD1Δ PROX1 protein is at least still partially phosphorylated (Figure 10). Taken together, our results demonstrate that PROX1 is phosphoprotein.

6. Both E2F sites are required for PROX1 mediated activation of *Ccne1* transcription

Once we had determined which functional domains in PROX1 were important for activating the *Ccne1* promoter, we next wanted to establish which regions in the *Ccne1* promoter were required for PROX1 mediated transcriptional activation. The *Ccne1* promoter is primarily regulated by two protein complexes that bind to the two E2F sites (E2FI and E2FX) that are located on either side of the transcriptional start site (Cobrinik 2005). Our laboratory had previously generated a truncated 206 bp version of the promoter that contains the transcriptional start site and both of these E2F sites were cloned into the pGL3 luciferase reporter vector (Bocangel 2006) (Figure 24). It is

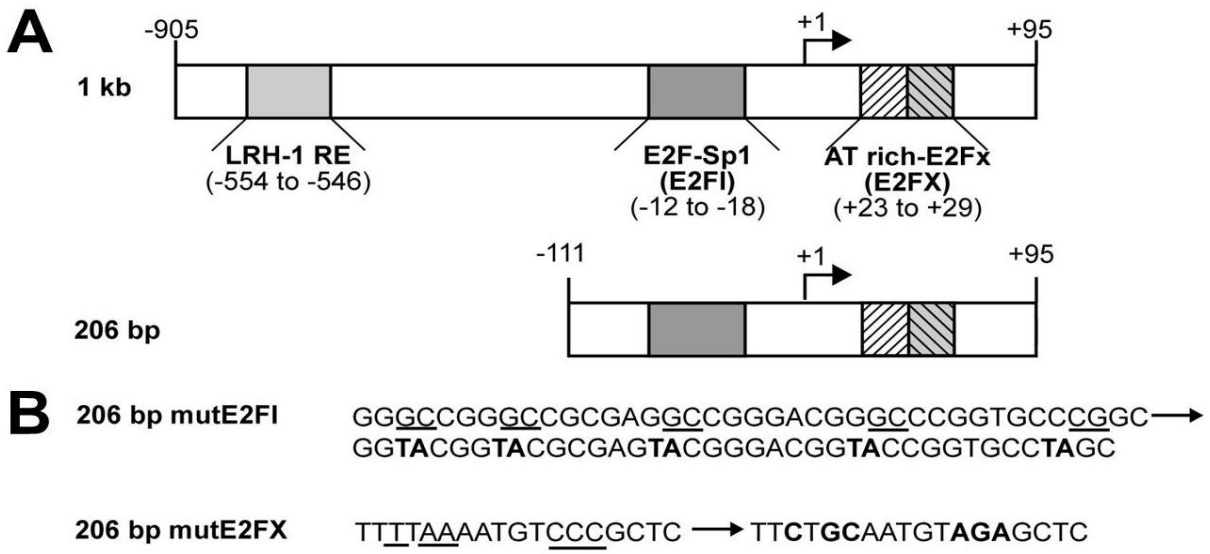

Figure 24: *Ccne1* promoters used in this study. A) The mouse 1 kb *Ccne1* promoter was cloned into the pGL3 reporter vector for use in luciferase reporter gene assays. As well, a truncated 206 bp promoter which contains the transcriptional start site as well as the two key E2F binding sites located on either side of the start site was cloned into the pGL3 vector and used for experiments. B) Two other mutant versions of the 206 bp promoter were generated in which each E2F binding site was mutated individually (the mutations of these sites are highlighted in **bold**).

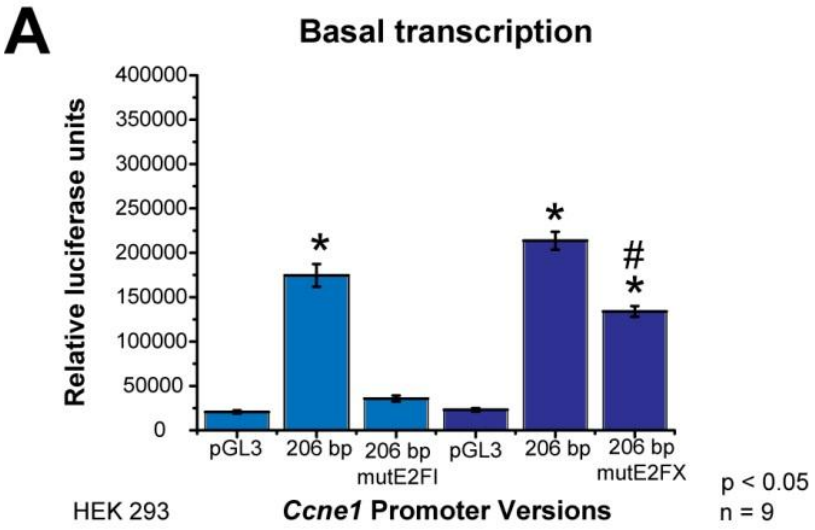
A
Basal transcription
Relative luciferase units
400000
350000
300000
250000
200000
150000
100000
50000
0
*
*
#
*
pGL3
206 bp
206 bp mutE2FI
pGL3
206 bp
206 bp mutE2FX
HEK 293
Ccne1 Promoter Versions
p < 0.05
n = 9

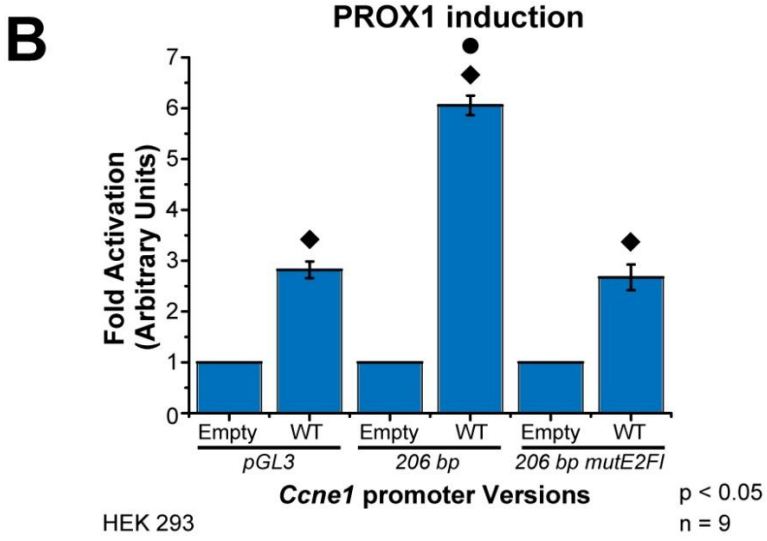
B
PROX1 induction
Fold Activation (Arbitrary Units)
7
6
5
4
3
2
1
0
Empty
WT
Empty
WT
Empty
WT
pGL3
206 bp
206 bp mutE2FI
Ccne1 promoter Versions
p < 0.05
n = 9
HEK 293

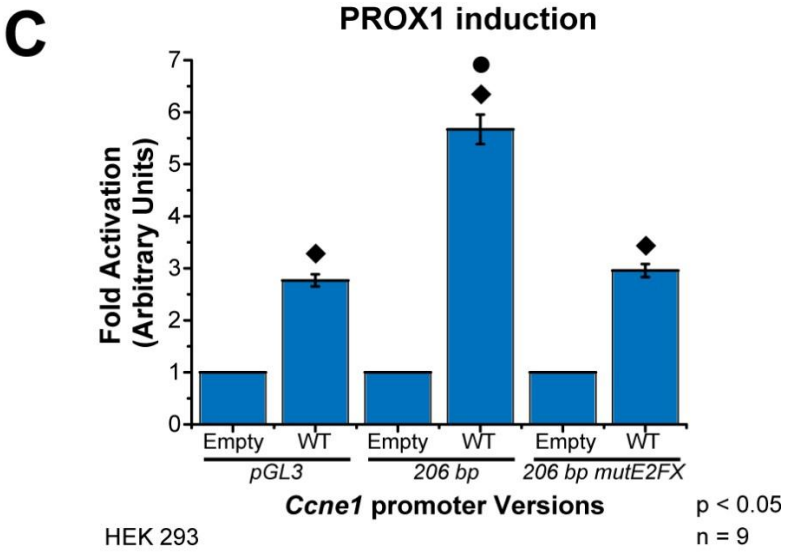
C
PROX1 induction
Fold Activation (Arbitrary Units)
7
6
5
4
3
2
1
0
Empty
WT
Empty
WT
Empty
WT
pGL3
206 bp
206 bp mutE2FX
Ccne1 promoter Versions
p < 0.05
n = 9
HEK 293

Figure 25: PROX1 mediated activation of the Ccne1 promoter requires both E2F binding sites. Luciferase assays in HEK 293 cells were used to assess if the E2F sites in the *Ccne1* promoter were involved in PROX1 mediated transcriptional activation. A) Basal transcription levels of the 206 bp promoter, the mutE2FI 206 bp promoter, and the mutE2FX 206 bp promoter were determined. B) Each of the mutant promoters was then tested with empty pCMV-Tag4A (Empty) and wild-type PROX1 (WT) to determine if there was an effect on PROX1 mediated activation without the E2F site. (*) indicates significance from the pGL3 control, (#) indicates significance from the 206 bp promoter, (◆) indicates significance from empty and (●) indicates significant difference in induction by WT as compared to empty pGL3 or the corresponding mutant promoter at a p value of less than 0.05.

significantly activated by wild-type PROX1 which indicates that the LRH-1 response element, located at position -554 to -546, is not required for PROX1 mediated activation of *Ccne1* (Bocangel 2006). We also mutated each of the E2F binding sites individually to determine whether PROX1 required either binding site to regulate *Ccne1* transcription. The basal transcription level of both the 206 bp promoter and the 206 bp mutE2FX promoter was significantly higher than that of the empty pGL3 control whereas the basal transcription of the 206 bp mutE2FI promoters was not significantly changed (Figure 25A). We next transfected HEK 293 cells with WT PROX1 to determine whether PROX1 induced transcription of these promoters. We noted that WT PROX1 activated the empty pGL3 vector approximately three fold (Figure 25B). We observed a significantly higher level of activation with the 206 bp WT promoter by PROX1. In contrast, we did not observe a significant increase above the three-fold activation observed for the empty pGL3 control for either the 206 bp mutE2FI or 206 bp mutE2FX promoters by WT PROX1 (Figure 25C). This indicates that the 206 bp promoter is sufficient for PROX1 mediated transcriptional activation, provided that both E2F sites are intact.

7. PROX1 regulation of CYCLIN E1 expression.

We next wanted to evaluate the effects of altering PROX1 expression on *Ccne1* expression at the protein level in endothelial cells. We observed that in HUVECs, there was a significant increase in CYCLIN E1 protein levels following infection with adenovirus encoding either WT or HDPD2Δ PROX1 (Figure 26). In

contrast, in LECs transfected with Prox1 siRNA, there was a marked decrease in CYCLIN E1 protein levels (Figure 27).

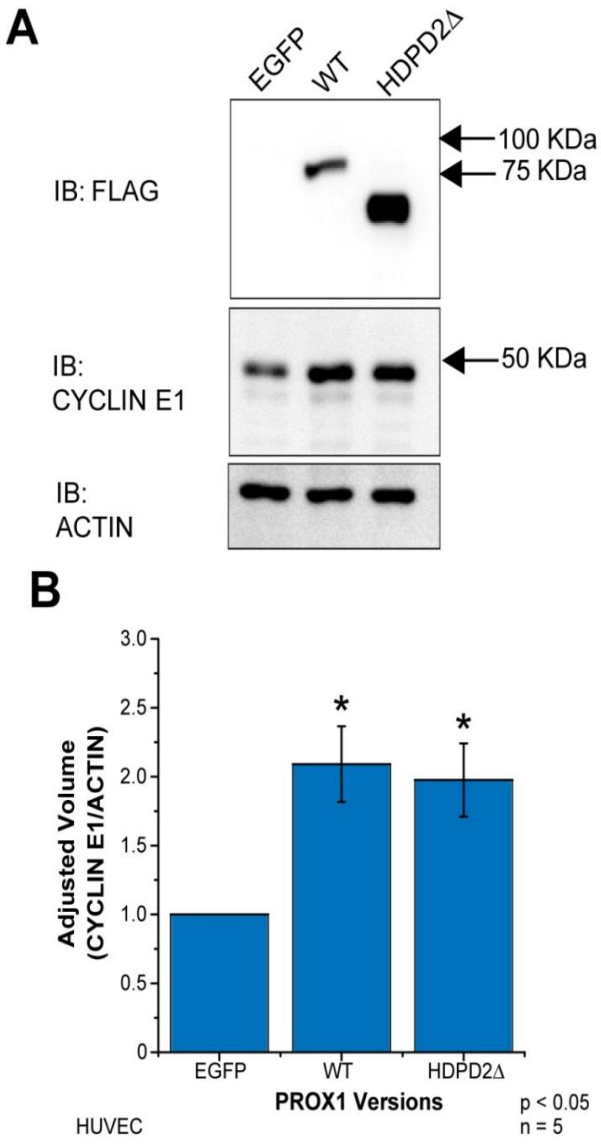

Figure 26: Gain of PROX1 function in endothelial cells results in increased levels of CYCLIN E1. HUVECs were infected with 250 MOI of adenovirus encoding either the WT Prox1 or the HDPD2Δ version of Prox1 for 48 hours. A) The cells were harvested for western blot to assess if there was an effect on the protein expression levels. B) Quantification of CYCLIN E1 protein levels in HUVECs normalized to the β-ACTIN loading control. (*) indicates significant from EGFP at a p value less than 0.05.

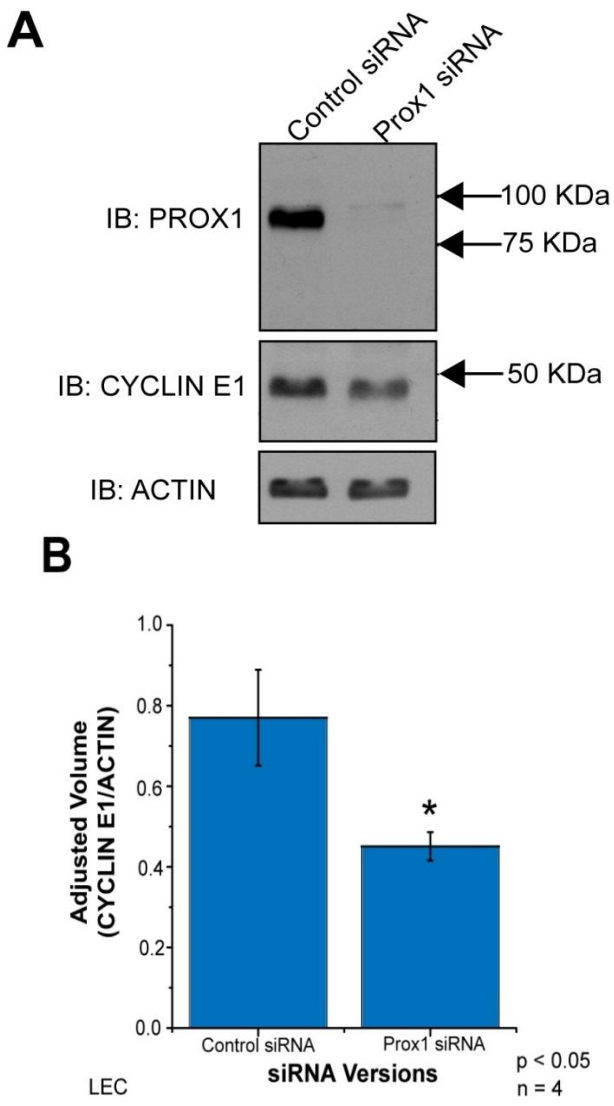

Figure 27: Loss of PROX1 protein expression reduced protein levels of CYCLIN E1 in LECs. Primary LECs were transfected with 100µM of the SMARTpool of PROX1 siRNA for 48 hours and harvested for western blotting to assess the effect on CYCLIN E1 protein levels. A) Western blot showing a decrease in the CYCLIN E1 levels in cells upon knockdown of PROX1. B) Quantification of CYCLIN E1 levels normalized to the β-ACTIN loading control. (*) denotes significance from Control siRNA at a p value of less than 0.05.

8. PROX1 mediates progression through the cell cycle in endothelial cells

Since CYCLIN E1 is a key mediator of the G_1 to S checkpoint (Dulic *et al.* 1992) and PROX1 regulates *Ccne1* transcription, we next determined the effect of PROX1 gain or loss of function on the cell cycle in venous and lymphatic endothelial cells. For the gain of function studies, we infected HUVECs with adenovirus encoding EGFP, WT PROX1 or HDPD2Δ PROX1 at 250 MOI. For loss of PROX1 function studies, we transiently transfected LECs with either a pool of 4 non-targeting control siRNAs or a pool of 4 siRNAs specifically targeting PROX1 (Figure 26). We used flow cytometry with propidium iodide labeling to establish whether the proportions of cells in each phase of the cell cycle were altered by either gain or loss of PROX1 function. In HUVECs, there was no significant change in the proportion of cells in S phase upon PROX1 expression (Figure 28A). Surprisingly, we noted a significant decrease in the proportion of S phase cells in PROX1 HDPD2Δ expressing HUVECs (Figure 28A). In LECs, we observed a significant decrease in S phase cells and a significant increase in the proportion of G_0/G_1 phase cells following knockdown of Prox1 by siRNA (Figure 29A).

To further evaluate the effects on the G_1/S transition, we used two different labeling strategies to identify S phase cells: PCNA labelling and BrdU labelling. For PCNA labelling, we used immunocytochemistry and counted the number of uniformly stained cells present in three random fields on three slides per sample. The PCNA protein has a long half-life in the cell, and as such the majority of cells on a slide will show positive staining; however, chromatin bound PCNA (which occurs only in S phase during DNA replication) displays a uniform staining pattern in the nucleus,

which is distinct from the more punctate pattern observed in other phases of the cell cycle. The observer was blinded to the identity of the slides throughout the entire process. We noted that in HUVECs, following infection with WT Prox1, there was no significant increase in the number of PCNA positive cells (Figure 28C). Again, we observed that HDPD2Δ resulted in a significant decrease of S phase cells (Figure 28C).

For BrdU labeling, we incubated HUVECs or LECs with BrdU for 45 minutes and labelled the cells with 7-AAD (DNA) and Alexa-Fluor488 (BrdU). Flow cytometry was used to measure the proportion of S phase cells. In HUVECs, we observed a similar trend in that WT PROX1 expression did not induce a significant increase in BrdU positive cells (Figure 28B). In contrast, HDPD2Δ expression caused a significant decrease in BrdU positive cells (Figure 28B). In LECs we observed a significant decrease in the amount of BrdU positive cells following siRNA knockdown of PROX1 (Figure 29B). Together, this data indicates that PROX1 is an important regulator of LEC cell cycle progression.

A

HUVEC PI	EGFP	WT	HDPD2Δ
G_0/G_1	51.05%	50.51%	58.59%
S	21.04%	23.22%	*15.40%
G_2/M	24.83%	20.76%	22.86%

B

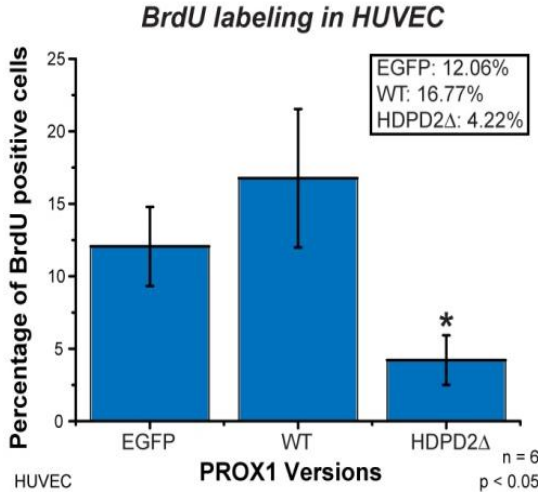

C

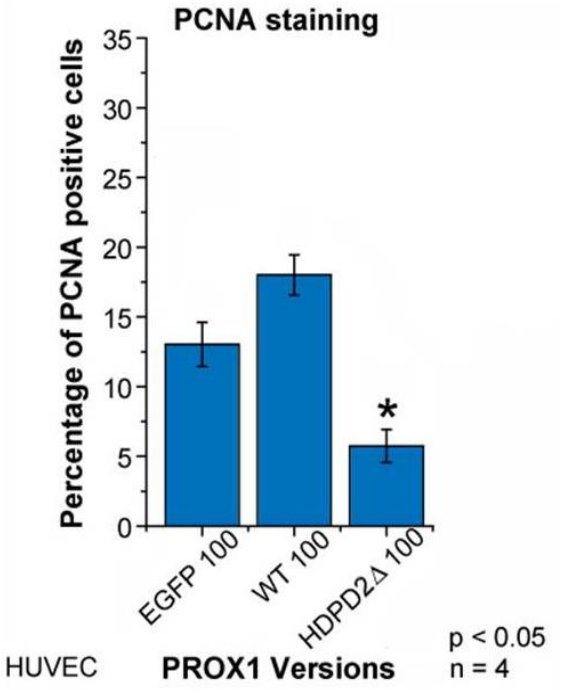

Figure 28: The effects of PROX1 gain of function on the endothelial cell cycle. Human Umbilical Vein Endothelial Cells (HUVEC) were infected with 250 MOI of adenovirus encoding either wild-type (WT) or homeodomain and Prospero domain 2 deleted (HDPD2Δ) Prox1. Flow cytometry was used to measure the proportion of cells in each phase of the cell cycle. A) Cells were first labelled with propidium iodide (PI) and a significant decrease in the proportion of S phase cells in HDPD2Δ infected cells was observed. B) To specifically study the S phase, cells were double labelled cells with 7-aminoactinomycin D (7-AAD) and bromodeoxyuridine (BrdU). A similar trend was observed in that there was a significant reduction in the proportion of S phase cells following infection with HDPD2Δ. C) To study S phase with a different approach, immunocytochemistry was used and infected HUVECs were stained with an antibody specific for proliferating cell nuclear antigen (PCNA). Similar to the patterns observed with both propidium iodide labelling and BrdU staining, there was a significant reduction in the proportion of S phase cells following infection with HDPD2Δ. (*) indicates significance from enhanced green fluorescent protein (EGFP) control at a p value less than 0.05.

A

LEC PI	Control siRNA	Prox1 siRNA
G_0/G_1	54.86%	*62.66%
S	23.07%	*15.52%
G_2/M	16.46%	17.39%

B

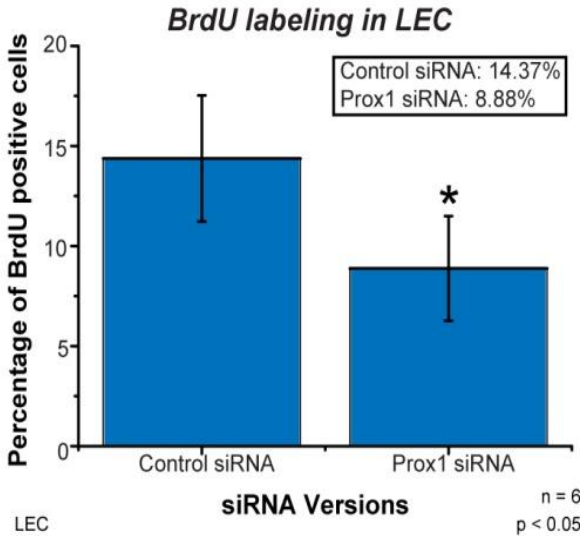

Figure 29: PROX1 knockdown affects progression of lymphatic endothelial cells (LEC) through the cell cycle. LECs were transfected with a SMARTpool of siRNA to knockdown PROX1 expression. Flow cytometry was used to assess the effects of PROX1 knockdown on the LEC cell cycle. A) Cells were first labelled with propidium iodide (PI) and analyzed by flow cytometry. B) To further confirm the S phase results, cells were double labelled with 7-aminoactinomycin D (7-AAD) and bromodeoxyuridine (BrdU) followed by flow cytometry. (*) indicate significance from control siRNA at a p value of less than 0.05.

VII. DISCUSSION

PROX1 is a key cell fate switch that is essential for the development of the lymphatic system (Wigle and Oliver 1999; Wigle, Harvey *et al.* 2002). Besides lymphatic endothelial cells, PROX1 is expressed in many other organs and cell types such as the colon, brain, spinal cord, lens and the retina (Wigle *et al.* 1999; Wigle and Oliver 1999; Sosa-Pineda *et al.* 2000; Wang *et al.* 2005; Misra *et al.* 2008). A potential role for PROX1 in regulating the cell cycle has been identified in many of these cell types. PROX1 induces cell cycle exit in the retina and lens via a mechanism involving the cell cycle inhibitors CDKN1B ($p27^{kip1}$) and CDKN1C ($p57^{kip2}$) (Dyer *et al.* 2003). As well, PROX1 promotes cell cycle arrest and differentiation in the spinal cord and hepatocellular carcinoma (Shimoda *et al.* 2006; Misra *et al.* 2008). In contrast to its' role as "brake" on the cell cycle, PROX1 promotes cellular growth in colon cancer and fetal liver hepatoblasts (Kamiya *et al.* 2008). Taken together, PROX1 has cell type specific roles in controlling the cell cycle. A connection between PROX1 and the G_1/S phase protein CYCLIN E1 has been previously established both in *Drosophila* and mammalian endothelial cells (Petrova *et al.* 2002; Griffiths and Hidalgo 2004; Yamazaki *et al.* 2009). Therefore, we sought to determine the role of PROX1 in mediating the lymphatic endothelial cell cycle and determine if this regulation involved regulating expression of CYCLIN E1.

1. Identification of the functional domains of PROX1 required for activation of *Ccne1.*

We first determined which of the known functional domains in PROX1 were important for transcriptional activation of the 1 kb mouse *Ccne1* promoter. We cloned a set of deletion or mutation constructs and transiently transfected them into HEK 293 cells for immunocytochemistry, western blotting and luciferase assays to compare their subcellular localization, expression level and activity, respectively. We observed that all of the various versions were localized to the nucleus with the exception of the PD1Δ version of PROX1. However, even with the PROX1 versions localized to the nucleus we did note different patterns of localization within the nucleus. For example, the WT generally was uniformly localized throughout the nucleus with exclusion from the nucleoli. We did occasionally observe a more punctate localization of WT PROX1, but a uniform pattern was most often seen. In contrast, many of the DNA-binding deficient versions such as HDΔ, PD2Δ and HDPD2Δ were localized into larger aggregates in the nucleus. In an attempt to establish if these aggregates or speckles co-localized with any known nuclear bodies, we co-stained HEK 293s transiently transfected with different versions of PROX1 for FLAG and the nuclear speckle marker SC35 (data not shown). We did not observe any co-localization and the nuclear speckles were much smaller than the PROX1 aggregates. The limitation to our study is that all of the constructs were expressed at a high level following transient transfection or adenoviral infection (expression driven by the cytomegalovirus promoter) and this supraphysiological level of expression may result in the aberrant aggregation or mislocalization of the PROX1 proteins. Characterizing

the expression of endogenous PROX1 in lymphatic endothelial cells would establish its localization in a more physiologically relevant model and support our findings. In addition, if the different PROX1 constructs were expressed at lower levels via weaker promoters this would help address this issue for the deletion mutants. Identifying which domains result in specific PROX1 localization in the nucleus could help elucidate novel nuclear binding partners that have a crucial role in controlling PROX1 mediated cell cycle regulation.

To establish which domains were involved in activation of the *Ccne1* promoter, we performed luciferase reporter gene assays with a variety of PROX1 deletion versions. We observed that deletion of the nuclear receptor boxes (dblNRΔ) or deletion of the homeodomain (HDΔ) had no significant effect on activation of the 1 kb *Ccne1* promoter. We established that the HDPD2Δ version activated the *Ccne*1 promoter but not to the same extent as the WT PROX1 version. We were also intrigued that the PD2 domain deletion induced a reduced level of *Ccne1* activation. This suggests that the PD2 domain is required for the full activation of the *Ccne1* promoter by PROX1. It is possible that the PD2 domain, as well as being involved in DNA-binding, is crucial for binding to other co-factors required for PROX1's role at the *Ccne1* promoter. This hypothesis will be interesting to explore in the future and may contribute to our understanding the exact mechanism of PROX1 activation of *Ccne1* transcription. These findings support the hypothesis that PROX1 mediated activation of the *Ccne1* promoter is via a DNA-binding independent mechanism.

2. The PD1 domain mediates PROX1 subcellular localization.

Interestingly, we noted that the PD1Δ version of PROX1 was localized not only to the nucleus, but also to the cytoplasm in both HEK 293 and U2OS cell types. To determine if this mislocalization was due to a defect in nuclear protein import or nuclear protein export, we treated U2OS cells with a nuclear protein export inhibitor, leptomycin B (LMB). We observed that following the addition of LMB, PD1Δ was again found to predominantly nuclearly localized, indicating that the protein is being rapidly shuttled out of the nucleus due to a defect in nuclear protein export. A potential explanation for this finding is that the PD1 domain functions as a nuclear export signal (NES) mask. In *Drosophila*, the PD2 domain of the PROX1 ortholog Prospero masks a NES located in the HD which prevents nuclear export. This NES is conserved in PROX1 and could be masked by either the PD1 or the PD2 domains. This is the first instance in which a function for the recently characterized PD1 domain has been demonstrated.

We compared the sequence of the PD1 domain with other constructs that had been previously generated in our lab and determined that there was another version of PROX1, QrichΔ, in which residues 211-260 in the PD1 domain were deleted. The activity, expression and localization of this version of PROX1 was identical to WT PROX1 (Bocangel 2006). To refine the region of the PD1 domain that is responsible for controlling PROX1 nuclear localization, we generated two additional versions of PROX1 which deleted the two regions of the PD1 domain located on either side of Qrich region. We then used immunocytochemistry, western blotting, and luciferase

assays in HEK 293 and U2OS cells to compare the subcellular localization, expression levels, and activity of these two new versions with WT and PD1Δ PROX1. We observed that the CterPD1Δ was localized to the nucleus similar to the WT protein whereas the NterPD1Δ was localized to both the nucleus and the cytoplasm similar to the PD1Δ version. With respect to activation of *FGFR-3* promoter, the NterPD1Δ and PD1Δ did not induce activation to the same extent as either the WT or CterPD1Δ versions of PROX1 in HEK 293 cells. Interestingly, in U2OS cells, both NterPD1Δ and CterPD1Δ significantly activated the 220 bp *FGFR-3* promoter (Figure 14). This difference could be due to the presence of cell type specific co-factors in U2OS cells that compensate for deletion of the N-terminal region of the PD1 domain, but are not present in HEK 293 cells. Identifying these co-factors will be useful to elucidate the precise mechanism by which PROX1 up-regulates transcription of *FGFR-3* and *Ccne1*. By comparing the features of these two PD1 deletion mutants, we have identified that the key sequence required for PROX1 to be retained in the nucleus is located in the region between residues 158 and 211 which was deleted by the NterPD1Δ. Further studies with the NterPD1Δ version of PROX1 will elucidate the mechanism by which PROX1 is transported in and out of the nucleus. Interestingly, there are many conserved predicted phosphorylation sites found in this region. Phosphorylation can modulate subcellular localization and influence protein-protein interactions. Kinases can be localized to specific cellular sub-compartments, which provides a new layer of regulation. For a target protein to be successfully phosphorylated, it needs to be properly localized to the same intercellular compartment as its kinase. With respect to nuclear cytoplasmic shuttling,

phosphorylation is involved in proper recognition by the nuclear import and nuclear export machinery (Guo *et al.* 2012). It is interesting that the PD1 domain contains the majority of the predicted phosphorylation sites, which could indicate a role for PROX1 phosphorylation in mediating nuclear export. We did not examine if nuclear protein import was affected by deletion of the PD1 domain. Oxidative stress has been shown to prevent nuclear protein import (Kodiha *et al.* 2004) and incubating cells in culture with hydrogen peroxide is a common model used to block nuclear import. It will be important to further characterize these sites and determine if some or all are involved in mediating PROX1 subcellular localization.

3. PROX1 activates *Ccne1* transcription via a DNA-binding independent mechanism.

We had established through luciferase assays in HEK 293 cells with our two different DNA-binding version of PROX1 that PROX1 activated the *Ccne1* promoter in a DNA-binding independent manner. However, another group had generated a DNA-binding domain mutant version of PROX1 that apparently supported a DNA-binding dependent mechanism of action (Petrova *et al.* 2002). Petrova *et al.* performed luciferase reporter gene assays using the same 1 kb *Ccne1* promoter in U2OS cells instead of HEK 293 cells. They did not see a significant activation of the promoter by their DNA-binding domain mutant. To elucidate the cause for this discrepancy, we generated their DNA-binding domain mutant and compared it in parallel with our DNA-binding domain mutant in both HEK 293 and U2OS cells. We observed that in HEK 293 cells, both DNA-binding domain mutant versions of PROX1 significantly

activated the promoter to the same extent as the WT protein, but in U2OS cells, only the ^{623}WF**EE**FR^{628} mutant but not the ^{623}WFS**A**F**A**^{628} mutant significantly activated the promoter. To ensure that this difference wasn't an artifact, our next goal was to establish that the ^{623}WF**EE**FR^{628} DNA-binding domain mutant was in fact unable to bind DNA and function as expected. We used EMSA with probes containing the putative PROX1 binding sites from the *FGFR-3* promoter, a known DNA-binding dependent target of PROX1 (Shin *et al.* 2006), to determine if this protein was able to directly bind to DNA. As expected, we observed that only the WT PROX1 protein bound the probes and that neither the ^{623}WF**EE**FR^{628} or HDΔ versions of PROX1 bound the probe. To further support this, we performed luciferase reporter assays using a 220 bp *FGFR-3* promoter with the WT, HDΔ and ^{623}WF**EE**FR^{628} versions of PROX1. Again, we observed that only the WT PROX1 version of PROX1 significantly activated this promoter and we were confident that our constructs were in fact unable to bind DNA and that PROX1 activated the *Ccne1* promoter in a DNA-binding independent manner.

With this issue clarified, we moved onto exploring potential causes for the differences we had observed between the two DNA-binding mutant versions. We started by performing immunocytochemistry and western blotting to compare the subcellular localization and protein expression levels of the two proteins, respectively, in both HEK 293 and U2OS. To our surprise, we observed that 20% of U2OS cells the ^{623}WFS**A**F**A**^{628} DNA-binding domain PROX1 mutant was localized to both the nucleus as well as the cytoplasm. Mislocalization of this protein to the wrong cellular compartment could result in decreased induction of luciferase activity since the

protein in the cytoplasm will be unable to reach its target genes. We also observed that the ^{623}WFS**A**F**A**^{628} mutant protein had a decreased apparent molecular weight as compared to WT PROX1 or the ^{623}WF**EE**FR^{628} version of PROX1. This decrease is likely due to the absence of a post-translational modification which will be discussed further in the following section. Lack of a modification or alterations to the protein's overall stability and folding will have an effect on the ^{623}WFS**A**F**A**^{628} protein's function and could contribute to the observed differences. As well, the two cell types may have different co-factors available to function together with PROX1 to activate the 1 kb *Ccne1* promoter which could account for the differences in activity we observed. Taken together, we established that the discrepancy observed between our results and the Petrova group's results was likely due to the mislocalization and lack of post-translational modification of the DNA-binding domain mutant version of PROX1 that they used in their study (Petrova *et al.* 2002).

4. PROX1 is a phosphoprotein

When determining molecular weight by SDS-PAGE and western blotting, one must consider different parameters. Factors such as the hydrophobicity, charge and efficiency of SDS binding, amino acid sequence and the presence of post-translational modifications can affect the positioning of a protein on an SDS-PAGE gel. Taking these factors into consideration, we sought to identify the cause of the molecular weight discrepancy that we observed between the two different DNA-binding domain mutant constructs used in our study. To identify if the PROX1

proteins were phosphorylated, we treated whole cell lysates with a protein phosphatase and processed the samples for western blotting. If the shift in molecular weight was due to lack of a phosphorylation event, we should be able to reproduce this shift with phosphatase treatment. Following lambda phosphatase treatment of transduced HEK 293 and U2OS cells, we observed a shift in the predicted molecular weights of both WT and ^{623}WF**EE**FR^{628}, but only a minor shift in the predicted molecular weight of the ^{623}WFS**A**F**A**^{628} mutant. This indicates that the difference in molecular weight between the ^{623}WFS**A**F**A**^{628} mutant and WT PROX1 was likely due to decreased phosphorylation of the mutant protein. The WT sequence from amino acids 623 to 628 (WFSNFR) does not contain any predicted phosphorylation sites and we did not mutate or remove any sites to create either of the DNA-binding domain mutant proteins. However, we did replace a Ser residue with a Glu residue in our mutation which functions as a phosphomimetic. It will be important to determine if this sequence is in fact phosphorylated. Likely the ^{623}WFS**A**F**A**^{628} mutation changed the global folding or stability of the protein which altered its availability to the kinases responsible for its normal phosphorylation as well as altered access to sequences controlling nuclear protein import or export. This mechanism remains to be further characterized and could lead to further knowledge of PROX1's structure and biology.

We next wanted to determine if phosphorylation of PROX1 occurred in endothelial cells. We again noted that following lambda phosphatase treatment, we observed a shift in the apparent molecular weight of the exogenous PROX1 protein. Interestingly, the molecular weight of the HDPD2Δ protein was also shifted upon lambda phosphatase treatment. This indicates that PROX1 is being phosphorylated

in the N-terminus region of the protein. However, the HDPD2 region may be phosphorylated as well.

Finally, we sought to establish if endogenous PROX1 is phosphorylated. To this end, we treated whole cell lysates from primary LECs and HepG2, a hepatocellular carcinoma cell line that expresses high levels of PROX1 with protein lambda phosphatase. We observed a shift in the apparent molecular weight of PROX1 in both cell types indicating that endogenous PROX1 is phosphorylated. We used two online search engines (MotifScan and Scansite) and compared the results obtained with those from a mass spectrometry analysis of phospho-proteins in the mouse liver (Villen *et al.* 2007) to search for predicted phosphorylation sites in the PROX1 protein sequence. We found a large number of potential sites, and noted that many of them were clustered in the conserved PD1 domain. Upon deletion of the PD1 domain, we observed localization of the protein to the nucleus as well as the cytoplasm, but in contrast to the ^{623}WFS**A**F**A**^{628} mutant protein, this occurred in all transfected cells, not just 20%. We also noted that the protein was expressed as a doublet following western blotting and when we treated the cell lysate with protein lambda phosphatase, we observed that we could resolve the doublet into one band. This suggests that there are multiple phosphorylation sites in PROX1, since deleting the PD1 domain does not abolish phosphorylation. Furthermore, phosphorylation could occur in a specific location in the cell (either in the nucleus or the cytoplasm) and could be important for mediating PROX1 subcellular localization. We also observed when using HepG2 and LECs the presence of a larger molecular weight band around 125 kDa. Two groups have previously identified a SUMOylation site

(K556) in PROX1 and this band may represent SUMO-PROX1. Phosphorylation and SUMOylation have been shown to function together (Guo *et al.* 2012) and it will be interesting to further explore the role of these two modifications on the overall function of PROX1. The prediction searches also highlighted some potential protein kinases that may be responsible for PROX1 phosphorylation, many of which are involved in cell growth and cell cycle progression. Further study will allow us to establish links between PROX1 and known signaling pathways involved in cell cycle progression and growth and further elucidate PROX1's role in the lymphatic endothelial cell cycle. This is the first instance in which PROX1 has been shown to be phosphorylated in lymphatic endothelial cells.

5. PROX1 mediated activation of *Ccne1* and its role in mediating the lymphatic endothelial cell cycle.

We next investigated PROX1's role in activating transcription of the *Ccne1* promoter and regulating the lymphatic endothelial cell cycle. It has been previously shown that PROX1 significantly activates a 6xE2F promoter (Petrova *et al.* 2002). The *Ccne1* promoter is primarily regulated by two E2F binding sites located on either side of the transcriptional start site: the upstream E2FI-Sp1 site and the downstream E2FX site. We sought to determine if PROX1 could activate the promoter through one of these two sites. To accomplish this, we mutated each of the sites individually. We chose mutations that had been previously published and shown to inactivate both the E2F and Sp1 binding site portions of the upstream site and the E2F binding and AT-rich regions in the downstream site (Le Cam *et al.* 1999). We observed that upon

mutation of each site individually, there was no significant activation of the promoter by PROX1. This demonstrates that PROX1 requires both of these E2F sites to activate transcription of the *Ccne1* gene.

We further looked at the protein levels of CCNE1 in gain of function and loss of function systems to determine the role of PROX1 on CCNE1 levels in endothelial cells. In HUVECs, we observed that as predicted by our luciferase results, there was a significant increase in the amount of CCNE1 protein levels following infection with adenovirus encoding either WT or HDPD2Δ PROX1 when compared to an EGFP control. In contrast, we noted a significant decrease in CCNE1 protein levels in LECs following transfection with Prox1 siRNA when compared to control siRNA. These results indicate that PROX1 increases CCNE1 protein levels in endothelial cells, which correspond to the luciferase reporter gene assay results we obtained in HEK 293 and U2OS cells.

Finally, because PROX1 has an effect on CYCLIN E1, which is a key regulator of the G_1/S transition in the cell cycle, we wanted to examine the overall effect of PROX1 gain of function and loss of function on the lymphatic endothelial cell cycle. In HUVECs, we did not observe a significant increase in the proportion of S phase cells following infection with adenovirus encoding WT PROX1, but interestingly, we noted a significant decrease in the proportion of S phase cells following infection with adenovirus encoding HDPD2Δ PROX1 and an accumulation of cells in G_1 phase. This finding indicates that although CYCLIN E1 protein levels are increasing following HDPD2Δ expression, cells are not progressing from G_1 to S phase. A possible cause of this effect could be that the HDPD2Δ version of PROX1 is functioning as a

dominant negative in this setting and although it can increase transcription of the *Ccne1* gene, it cannot bind to the other co-factors or binding partners required for PROX1 mediated G_1 to S transition. This could have interesting applications in future studies to elucidate how PROX1 functions at the G_1 to S border. Alternatively, this indicates that PROX1 may be interacting with other cell cycle regulators involved in the G_1 to S transition such as D-type Cyclins or Cyclin dependent kinase inhibitors $p27^{kip1}$ and $p57^{kip2}$. The HDPD2Δ version of PROX1 is not capable of binding directly to DNA and although PROX1 regulates transcription of the *Ccne1* promoter using a DNA-binding independent mechanism, it may employ DNA-binding dependent mechanisms to regulate transcription of other genes involved in the G_1 to S transition. This would account for why HDPD2Δ up-regulated protein levels of CCNE1, but did not promote cell cycle progression in HUVECs. In contrast, following knockdown of PROX1 in LECs, we observed that there was a significant decrease in the number of S phase cells and a significant accumulation of cells in G1 phase. We further corroborated these results by BrdU labeling. This gave us a more accurate picture of the S phase proportion of cells and we observed a similar pattern, in which HUVECs infected with WT had no increase in the portion of S phase cells, and HDPD2Δ infected cells and LECs that had been transfected with PROX1 siRNA had a significant decrease in the proportion of S phase cells. We also observed similar results following PCNA staining and BrdU immunocytochemistry. Taken together, we propose a model in which following mitogen stimulation by pro-lymphangiogenic molecules such as VEGF-C/D or bFGF, PROX1 promotes cell cycle progression and the number of cells increases. Alternatively, in the absence of PROX1 following

siRNA knockdown, LECs do not enter the cell cycle and the number of progenitor cells is reduced (Figure 30).

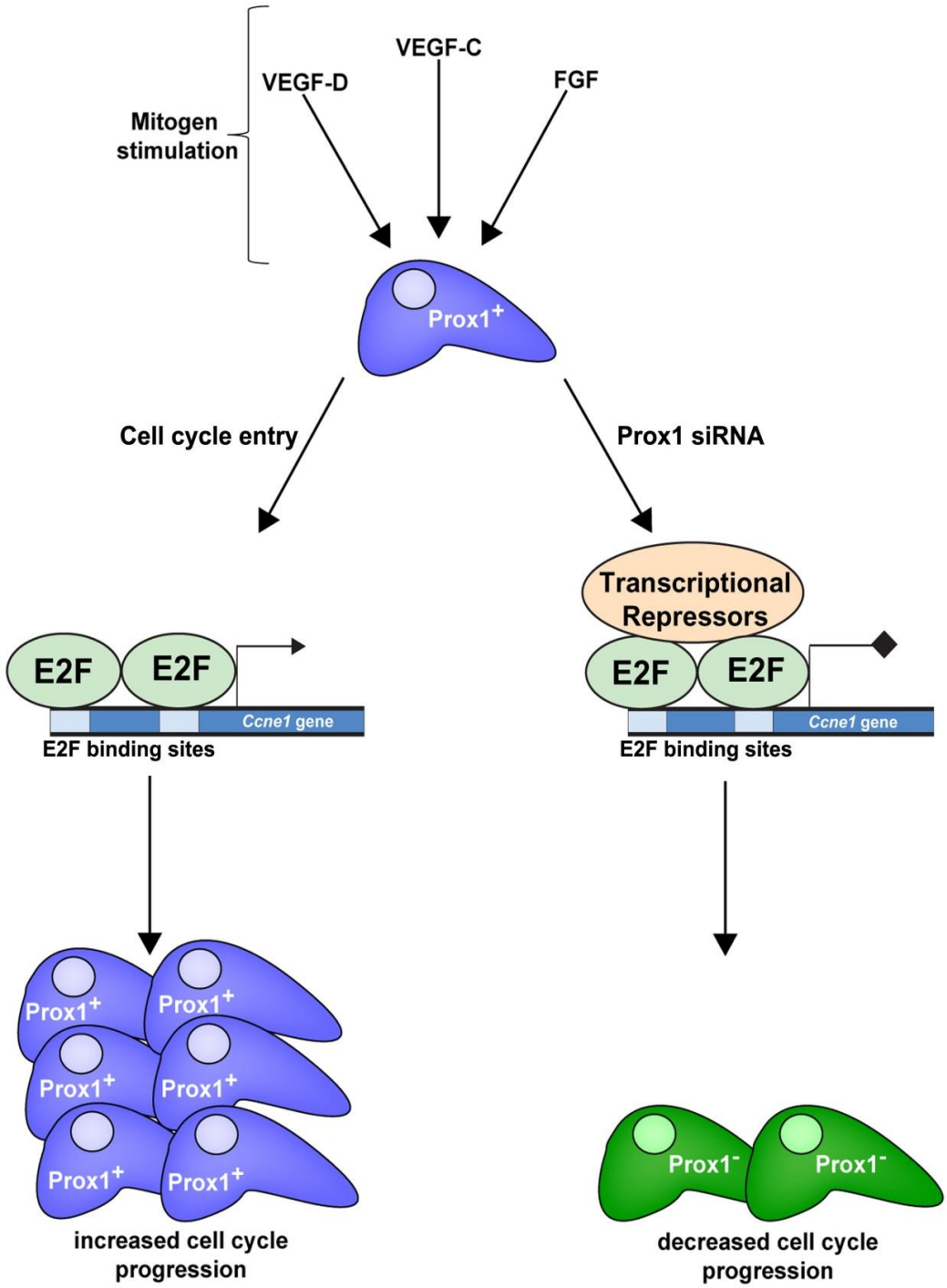
VEGF-C
VEGF-D
FGF
Mitogen stimulation
Prox1+
Cell cycle entry
Prox1 siRNA
Transcriptional Repressors
E2F
E2F
Ccne1 gene
E2F binding sites
E2F
E2F
Ccne1 gene
E2F binding sites
Prox1+
Prox1+
Prox1+
Prox1+
Prox1+
Prox1+
increased cell cycle progression
Prox1-
Prox1-
decreased cell cycle progression

Figure 30: Proposed model of PROX1's role in controlling the lymphatic endothelial cell (LEC) cycle. Based on the presented results, we propose that following pro-lymphangiogenic stimulation by mitogens such as vascular endothelial growth factors C or D (VEGF-C, VEGF-D) or basic fibroblast growth factor (FGF), PROX1 promotes transcription of the *Ccne1* promoter through binding indirectly to other co-factors already bound to the E2F sites located in the promoter. This promotes entry into the cell cycle, progression from G_1 to S phase, and increased cell cycle progression. In cells lacking PROX1, the repression on the *Ccne1* promoter is not relieved which results in a lack of cell cycle progression and, as such, decreased cell numbers.

VIII. CONCLUSIONS

I. PROX1 activates transcription of the *Ccne1* promoter via a DNA-binding independent mechanism.

II. The Prospero domain 1 (PD1) is important in controlling PROX1 subcellular localization.

III. PROX1 mediated transcriptional activation of the *Ccne1* promoter requires both E2F binding sites located on either side of the transcriptional start site.

IV. PROX1 is phosphorylated in a variety of cell types.

V. PROX1 knockdown in LECs significantly decreased CYCLIN E1 protein levels and the proportion of cells in S phase of the cell cycle.

VI. PROX1 over-expression in HUVECs significantly increased CYCLIN E1 protein levels.

VII. Expression of HDPD2Δ blocked endothelial cell cycle progression.

VIII. PROX1 controls the lymphatic endothelial cell cycle by promoting progression through the G_1/S border into the cell cycle.

IX. FUTURE DIRECTIONS

We have shown that loss of PROX1 in lymphatic endothelial cells results in reduced cell cycle progression. It has also been shown that PROX1 has a role in cell cycle regulation in a variety of other cell types (Dyer *et al.* 2003; Shimoda *et al.* 2006; Kamiya *et al.* 2008; Misra *et al.* 2008; Petrova *et al.* 2008; Foskolou *et al.* 2012). Further studies into the exact mechanism of how PROX1 controls the lymphatic endothelial cell cycle will be important and could potentially lead to novel strategies to either promote or inhibit LEC growth. Interestingly, we observed that the HDPD2Δ version of PROX1 in lymphatic endothelial cells blocks progression from G_1 to S phase of the cell cycle in HUVECs despite activating CYCLIN E1 to a similar level as compared to wild-type Prox1. This result indicates that CYCLIN E1 that other targets are regulated by PROX1, which are essential to promote cellular proliferation. Using WT and this DNA-binding deficient versions of PROX1, we will be able to determine which other mediators of the G_1 to S transition, such as other G_1 cyclins or cyclin dependent kinase inhibitors such as $p21^{cip1}$, $p27^{kip1}$ or $p57^{kip2}$, are dysregulated by its expression.

Identification of PROX1 as a phosphoprotein is an exciting and novel finding. There is much to explore in this area and further study will lead to understanding the role of phosphorylation in controlling PROX1 function. Specifically, it will be interesting to identify the sites that are phosphorylated in the context of lymphatic endothelial cells. This can be done through the use of samples enriched in PROX1 expression such as *in vitro* cultured primary lymphatic endothelial cells or tissues rich in lymphatic vessels such as the mesentery. A specific PROX1 antibody can be used

to immunoprecipitate and thereby enrich the samples for PROX1. Half of the sample can be treated with lambda phosphatase to remove phosphate groups from the protein and the entire sample can then be sent for liquid chromatography/mass spectrometric analysis (LC-MS/MS) using a titanium dioxide column. The spectra will then be compared and any mass difference of 98 or 80 Da represents a potential serine/threonine or tyrosine phosphorylation site respectively. The western blotting done in this study shows a large shift in the apparent molecular weight of PROX1 upon lambda phosphatase treatment, which indicates that PROX1 is likely phosphorylated at multiple sites. There are many predicted phosphorylation sites in the protein and determining which ones are biologically relevant in LECs could lead to identifying signaling pathways, which may regulate PROX1 function. We will also be able to use site directed mutagenesis to determine the effect of lack of phosphorylation on PROX1's function. A caveat is that some of these sites may be functionally redundant and therefore it may be necessary to mutate multiple sites in order to alter PROX1 activity. PROX1 is SUMOylated and we have observed a high molecular weight band in both LECs and HepG2 cells. It will be interesting to determine whether PROX1 SUMOylation is regulated by PROX1 phosphorylation or *vice versa*. SUMOylation and phosphorylation have been shown to work synergistically to alter the function of a target protein and in general post-translational modifications are very important for successful progression through the cell cycle. Taken together, this is an exciting finding that is only the first step into a new area of lymphatic biology.

XI. REFERENCES

Abtahian, F., A. Guerriero, *et al*. (2003). "Regulation of blood and lymphatic vascular separation by signaling proteins SLP-76 and Syk." Science **299**(5604): 247-51.

Baluk, P., J. Fuxe, *et al*. (2007). "Functionally specialized junctions between endothelial cells of lymphatic vessels." J Exp Med **204**(10): 2349-62.

Barneda-Zahonero, B. and M. Parra (2012). "Histone deacetylases and cancer." Mol Oncol.

Baxter, S. A., D. Y. Cheung, *et al*. (2011). "Regulation of the lymphatic endothelial cell cycle by the PROX1 homeodomain protein." Biochim Biophys Acta **1813**(1): 201-12.

Bertozzi, C. C., A. A. Schmaier, *et al*. (2010). "Platelets regulate lymphatic vascular development through CLEC-2-SLP-76 signaling." Blood **116**(4): 661-70.

Bocangel, P. (2006). Regulation of Cyclin E1 transcription by the Prox1 homeodomain transcription factor. Biochemistry and Medical Genetics. Winnipeg, University of Manitoba**:** 101.

Chang, T. M. and W. C. Hung (2012). "Transcriptional repression of TWIST1 gene by Prospero-related homeobox 1 inhibits invasiveness of hepatocellular carcinoma cells." FEBS Lett.

Chen, X., J. R. Taube, *et al*. (2008). "Dual roles for Prox1 in the regulation of the chicken betaB1-crystallin promoter." Invest Ophthalmol Vis Sci **49**(4): 1542-52.

Choksi, S. P., T. D. Southall, *et al*. (2006). "Prospero acts as a binary switch between self-renewal and differentiation in Drosophila neural stem cells." Dev Cell **11**(6): 775-89.

Christiansen, A. and M. Detmar (2011). "Lymphangiogenesis and cancer." Genes Cancer **2**(12): 1146-58.

Chu-Lagraff, Q., D. M. Wright, *et al*. (1991). "The prospero gene encodes a divergent homeodomain protein that controls neuronal identity in Drosophila." Development **Suppl 2**: 79-85.

Clasper, S., D. Royston, *et al*. (2008). "A novel gene expression profile in lymphatics associated with tumor growth and nodal metastasis." Cancer Res **68**(18): 7293-303.

Clurman, B. E., R. J. Sheaff, *et al*. (1996). "Turnover of cyclin E by the ubiquitin-proteasome pathway is regulated by cdk2 binding and cyclin phosphorylation." Genes Dev **10**(16): 1979-90.

Cobrinik, D. (2005). "Pocket proteins and cell cycle control." Oncogene **24**(17): 2796-809.

Colonques, J., J. Ceron, *et al*. (2011). "A transient expression of Prospero promotes cell cycle exit of Drosophila postembryonic neurons through the regulation of Dacapo." PLoS One **6**(4): e19342.

Cook, T., F. Pichaud, *et al*. (2003). "Distinction between color photoreceptor cell fates is controlled by Prospero in Drosophila." Dev Cell **4**(6): 853-64.

Cormier, J. N., R. L. Askew, *et al*. (2010). "Lymphedema beyond breast cancer: a systematic review and meta-analysis of cancer-related secondary lymphedema." Cancer **116**(22): 5138-49.

Cui, W., S. I. Tomarev, *et al*. (2004). "Mafs, Prox1, and Pax6 can regulate chicken betaB1-crystallin gene expression." J Biol Chem **279**(12): 11088-95.

Dagenais, S. L., R. L. Hartsough, *et al*. (2004). "Foxc2 is expressed in developing lymphatic vessels and other tissues associated with lymphedema-distichiasis syndrome." Gene Expr Patterns **4**(6): 611-9.

Demidenko, Z., P. Badenhorst, *et al*. (2001). "Regulated nuclear export of the homeodomain transcription factor Prospero." Development **128**(8): 1359-67.

Downes, M., M. Francois, *et al*. (2009). "Vascular defects in a mouse model of hypotrichosis-lymphedema-telangiectasia syndrome indicate a role for SOX18 in blood vessel maturation." Hum Mol Genet **18**(15): 2839-50.

Dulic, V., E. Lees, *et al*. (1992). "Association of human cyclin E with a periodic G1-S phase protein kinase." Science **257**(5078): 1958-61.

Dumont, D. J., L. Jussila, *et al*. (1998). "Cardiovascular failure in mouse embryos deficient in VEGF receptor-3." Science **282**(5390): 946-9.

Duong, T., P. Koopman, *et al*. (2012). "Tumor lymphangiogenesis as a potential therapeutic target." J Oncol **2012**: 204946.

Dyer, M. A., F. J. Livesey, *et al*. (2003). "Prox1 function controls progenitor cell proliferation and horizontal cell genesis in the mammalian retina." Nat Genet **34**(1): 53-8.

Erickson, R. P., S. L. Dagenais, *et al*. (2001). "Clinical heterogeneity in lymphoedema-distichiasis with FOXC2 truncating mutations." J Med Genet **38**(11): 761-6.

Fang, J., S. L. Dagenais, *et al*. (2000). "Mutations in FOXC2 (MFH-1), a forkhead family transcription factor, are responsible for the hereditary lymphedema-distichiasis syndrome." Am J Hum Genet **67**(6): 1382-8.
Fasanaro, P., M. C. Capogrossi, *et al*. (2009). "Regulation of the endothelial cell cycle by the ubiquitin-proteasome system." Cardiovasc Res **85**(2): 272-80.

Flister, M. J., A. Wilber, *et al*. (2010). "Inflammation induces lymphangiogenesis through up-regulation of VEGFR-3 mediated by NF-kappaB and Prox1." Blood **115**(2): 418-29.

Ford, H. L., E. Landesman-Bollag, *et al*. (2000). "Cell cycle-regulated phosphorylation of the human SIX1 homeodomain protein." J Biol Chem **275**(29): 22245-54.

Forster, R., A. C. Davalos-Misslitz, *et al*. (2008). "CCR7 and its ligands: balancing immunity and tolerance." Nat Rev Immunol **8**(5): 362-71.

Foskolou, I. P., D. Stellas, *et al*. (2012). "Prox1 suppresses the proliferation of neuroblastoma cells via a dual action in p27-Kip1 and Cdc25A." Oncogene.

Francois, M., A. Caprini, *et al*. (2008). "Sox18 induces development of the lymphatic vasculature in mice." Nature **456**(7222): 643-7.

Frogne, T., K. B. Sylvestersen, *et al*. (2012). "Pdx1 is post-translationally modified in vivo and serine 61 is the principal site of phosphorylation." PLoS One **7**(4): e35233.

Gareau, J. R. and C. D. Lima (2010). "The SUMO pathway: emerging mechanisms that shape specificity, conjugation and recognition." Nat Rev Mol Cell Biol **11**(12): 861-71.

Glotzer, M., A. W. Murray, *et al*. (1991). "Cyclin is degraded by the ubiquitin pathway." Nature **349**(6305): 132-8.

Glover-Collins, K. and M. E. Thompson (2008). "Nuclear export of BRCA1 occurs during early S phase and is calcium-dependent." Cell Signal **20**(5): 958-68.

Griffiths, R. L. and A. Hidalgo (2004). "Prospero maintains the mitotic potential of glial precursors enabling them to respond to neurons." Embo J **23**(12): 2440-50.

Guo, M. and B. X. Huang (2012). "Integration of phosphoproteomic, chemical and biological strategies for the functional analysis of targeted protein phosphorylation." Proteomics.

Guo, Z., J. Kanjanapangka, *et al*. (2012). "Sequential posttranslational modifications program FEN1 degradation during cell-cycle progression." Mol Cell. **47**(3): 444-56.

Hanahan, D. and R. A. Weinberg (2011). "Hallmarks of cancer: the next generation." Cell **144**(5): 646-74.

Harvey, N. L., R. S. Srinivasan, *et al*. (2005). "Lymphatic vascular defects promoted by Prox1 haploinsufficiency cause adult-onset obesity." Nat Genet **37**(10): 1072-81.

Hashiya, N., N. Jo, *et al*. (2004). "In vivo evidence of angiogenesis induced by transcription factor Ets-1: Ets-1 is located upstream of angiogenesis cascade." Circulation **109**(24): 3035-41.

Hassan, B., L. Li, *et al*. (1997). "Prospero is a panneural transcription factor that modulates homeodomain protein activity." Proc Natl Acad Sci U S A **94**(20): 10991-6.

Hirakawa, S., Y. K. Hong, *et al*. (2003). "Identification of vascular lineage-specific genes by transcriptional profiling of isolated blood vascular and lymphatic endothelial cells." Am J Pathol **162**(2): 575-86.

Hollenhorst, P. C., A. A. Shah, *et al*. (2007). "Genome-wide analyses reveal properties of redundant and specific promoter occupancy within the ETS gene family." Genes Dev **21**(15): 1882-94.

Hong, Y. K. and M. Detmar (2003). "Prox1, master regulator of the lymphatic vasculature phenotype." Cell Tissue Res **314**(1): 85-92.

Horton, R. M., H. D. Hunt, *et al*. (1989). "Engineering hybrid genes without the use of restriction enzymes: gene splicing by overlap extension." Gene **77**(1): 61-8.

Huntington, G. M., CFW (1910). "The anatomy and development of the jugular lymph sac in the domestic cat (Felis domestica)." Am J Anat(10): 177-312.

Irrthum, A., K. Devriendt, *et al*. (2003). "Mutations in the transcription factor gene SOX18 underlie recessive and dominant forms of hypotrichosis-lymphedema-telangiectasia." Am J Hum Genet **72**(6): 1470-8.

Johnson, N. C., M. E. Dillard, *et al*. (2008). "Lymphatic endothelial cell identity is reversible and its maintenance requires Prox1 activity." Genes Dev **22**(23): 3282-91.

Joyce, J. A. and J. W. Pollard (2009). "Microenvironmental regulation of metastasis." Nat Rev Cancer **9**(4): 239-52.

Kamiya, A., S. Kakinuma, *et al*. (2008). "Prospero-related homeobox 1 and liver receptor homolog 1 coordinately regulate long-term proliferation of murine fetal hepatoblasts." Hepatology **48**(1): 252-64.

Karkkainen, M. J., P. Haiko, *et al*. (2004). "Vascular endothelial growth factor C is required for sprouting of the first lymphatic vessels from embryonic veins." Nat Immunol **5**(1): 74-80.
Kerjaschki, D., H. M. Regele, *et al*. (2004). "Lymphatic neoangiogenesis in human kidney transplants is associated with immunologically active lymphocytic infiltrates." J Am Soc Nephrol **15**(3): 603-12.

Kodiha, M., A. Chu, *et al*. (2004). "Multiple mechanisms promote the inhibition of classical nuclear import upon exposure to severe oxidative stress." Cell Death Differ **11**(8): 862-74.

Kojima, K., M. Konopleva, *et al*. (2007). "Mitogen-activated protein kinase kinase inhibition enhances nuclear proapoptotic function of p53 in acute myelogenous leukemia cells." Cancer Res **67**(7): 3210-9.

Kume, T. (2010). "Specification of arterial, venous, and lymphatic endothelial cells during embryonic development." Histol Histopathol **25**(5): 637-46.

Le Cam, L., J. Polanowska, *et al*. (1999). "Timing of cyclin E gene expression depends on the regulated association of a bipartite repressor element with a novel E2F complex." Embo J **18**(7): 1878-90.

Lee, S., J. Kang, *et al*. (2009). "Prox1 physically and functionally interacts with COUP-TFII to specify lymphatic endothelial cell fate." Blood **113**(8): 1856-9.

Li, L. and H. Vaessin (2000). "Pan-neural Prospero terminates cell proliferation during Drosophila neurogenesis." Genes Dev **14**(2): 147-51.

Lim, H. Y., J. M. Rutkowski, *et al*. (2009). "Hypercholesterolemic mice exhibit lymphatic vessel dysfunction and degeneration." Am J Pathol **175**(3): 1328-37.

Mann, M., S. E. Ong, *et al*. (2002). "Analysis of protein phosphorylation using mass spectrometry: deciphering the phosphoproteome." Trends Biotechnol **20**(6): 261-8.

McEwen, D. G., R. P. Green, *et al*. (1999). "Fibroblast growth factor receptor 3 gene transcription is suppressed by cyclic adenosine 3',5'-monophosphate. Identification of a chondrocytic regulatory element." J Biol Chem **274**(43): 30934-42.

Misra, K., H. Gui, *et al*. (2008). "Prox1 regulates a transitory state for interneuron neurogenesis in the spinal cord." Dev Dyn **237**(2): 393-402.

Mouta, C. and M. Herault (2003). "Inflammatory triggers of lymphangiogenesis." Lymphat Res Biol **1**(3): 201-18.

Norman, S. A., A. R. Localio, *et al*. (2009). "Lymphedema in breast cancer survivors: incidence, degree, time course, treatment, and symptoms." J Clin Oncol **27**(3): 390-7.

Oliver, G., B. Sosa-Pineda, *et al*. (1993). "Prox 1, a prospero-related homeobox gene expressed during mouse development." Mech Dev **44**(1): 3-16.

Pan, M. R., T. M. Chang, *et al*. (2009). "Sumoylation of Prox1 controls its ability to induce VEGFR3 expression and lymphatic phenotypes in endothelial cells." J Cell Sci **122**(Pt 18): 3358-64.

Paskett, E. D., J. A. Dean, *et al*. (2012). "Cancer-Related Lymphedema Risk Factors, Diagnosis, Treatment, and Impact: A Review." J Clin Oncol.

Petrova, T. V., T. Karpanen, *et al*. (2004). "Defective valves and abnormal mural cell recruitment underlie lymphatic vascular failure in lymphedema distichiasis." Nat Med **10**(9): 974-81.

Petrova, T. V., T. Makinen, *et al*. (2002). "Lymphatic endothelial reprogramming of vascular endothelial cells by the Prox-1 homeobox transcription factor." Embo J **21**(17): 4593-9.

Petrova, T. V., A. Nykanen, *et al*. (2008). "Transcription factor PROX1 induces colon cancer progression by promoting the transition from benign to highly dysplastic phenotype." Cancer Cell **13**(5): 407-19.

Pfarr, K. M., A. Y. Debrah, *et al*. (2009). "Filariasis and lymphoedema." Parasite Immunol **31**(11): 664-72.

Pistocchi, A., S. Bartesaghi, *et al*. (2008). "Identification and expression pattern of zebrafish prox2 during embryonic development." Dev Dyn **237**(12): 3916-20.

Podgrabinska, S., P. Braun, *et al*. (2002). "Molecular characterization of lymphatic endothelial cells." Proc Natl Acad Sci U S A **99**(25): 16069-74.

Podgrabinska, S., O. Kamalu, *et al*. (2009). "Inflamed lymphatic endothelium suppresses dendritic cell maturation and function via Mac-1/ICAM-1-dependent mechanism." J Immunol **183**(3): 1767-79.

Polanowska, J., E. Fabbrizio, *et al*. (2001). "The periodic down regulation of Cyclin E gene expression from exit of mitosis to end of G(1) is controlled by a deacetylase- and E2F-associated bipartite repressor element." Oncogene **20**(31): 4115-27.

Pytowski, B., J. Goldman, *et al*. (2005). "Complete and specific inhibition of adult lymphatic regeneration by a novel VEGFR-3 neutralizing antibody." J Natl Cancer Inst **97**(1): 14-21.

Qiao, C. X., X. F. Zhai, *et al*. (2012). "Health-related quality of life evaluated by tumor node metastasis staging system in patients with hepatocellular carcinoma." World J Gastroenterol **18**(21): 2689-94.

Qin, J., D. M. Gao, *et al*. (2004). "Prospero-related homeobox (Prox1) is a corepressor of human liver receptor homolog-1 and suppresses the transcription of the cholesterol 7-alpha-hydroxylase gene." Mol Endocrinol **18**(10): 2424-39.

Quick, C. M., A. M. Venugopal, *et al*. (2007). "Intrinsic pump-conduit behavior of lymphangions." Am J Physiol Regul Integr Comp Physiol **292**(4): R1510-8.

Reed, S. I. (2003). "Ratchets and clocks: the cell cycle, ubiquitylation and protein turnover." Nat Rev Mol Cell Biol **4**(11): 855-64.
Rossi, A., E. Weber, *et al*. (2007). "Mechanotransduction in lymphatic endothelial cells." Lymphology **40**(3): 102-13.

Ryter, J. M., C. Q. Doe, *et al*. (2002). "Structure of the DNA-binding region of prospero reveals a novel homeo-prospero domain." Structure **10**(11): 1541-9.

Sabin, F. (1902). "On the origin of the lymphatic system from the veins and the development of the lymph hearts and the thoracic duct in the pig." Am J Anat(1): 367-89.

Sahai, E. (2007). "Illuminating the metastatic process." Nat Rev Cancer **7**(10): 737-49.

Schnerch, D., J. Yalcintepe, *et al*. (2012). "Cell cycle control in acute myeloid leukemia." Am J Cancer Res **2**(5): 508-28.

Shan, S. F., L. F. Wang, *et al*. (2008). "Modulation of transcriptional corepressor activity of prospero-related homeobox protein (Prox1) by SUMO modification." FEBS Lett **582**(27): 3723-8.

Shimoda, M., M. Takahashi, *et al*. (2006). "A homeobox protein, prox1, is involved in the differentiation, proliferation, and prognosis in hepatocellular carcinoma." Clin Cancer Res **12**(20 Pt 1): 6005-11.

Shin, J. W., M. Min, *et al*. (2006). "Prox1 promotes lineage-specific expression of fibroblast growth factor (FGF) receptor-3 in lymphatic endothelium: a role for FGF signaling in lymphangiogenesis." Mol Biol Cell **17**(2): 576-84.

Silberschmidt, D., A. Rodriguez-Mallon, *et al*. (2011). "In vivo role of different domains and of phosphorylation in the transcription factor Nkx2-1." BMC Dev Biol **11**: 9.

Siu, K. T., M. R. Rosner, *et al*. (2012). "An integrated view of cyclin E function and regulation." Cell Cycle **11**(1): 57-64.

Sleeman, J. P. and W. Thiele (2009). "Tumor metastasis and the lymphatic vasculature." Int J Cancer **125**(12): 2747-56.

Song, K. H., T. Li, *et al*. (2006). "A Prospero-related homeodomain protein is a novel co-regulator of hepatocyte nuclear factor 4alpha that regulates the cholesterol 7alpha-hydroxylase gene." J Biol Chem **281**(15): 10081-8.

Sosa-Pineda, B., J. T. Wigle, *et al*. (2000). "Hepatocyte migration during liver development requires Prox1." Nat Genet **25**(3): 254-5.

Spiegel, R., A. Ghalamkarpour, *et al*. (2006). "Wide clinical spectrum in a family with hereditary lymphedema type I due to a novel missense mutation in VEGFR3." J Hum Genet **51**(10): 846-50.

Srinivasan, R. S., X. Geng, *et al*. (2010). "The nuclear hormone receptor Coup-TFII is required for the initiation and early maintenance of Prox1 expression in lymphatic endothelial cells." Genes Dev **24**(7): 696-707.

Srinivasan, R. S. and G. Oliver (2011). "Prox1 dosage controls the number of lymphatic endothelial cell progenitors and the formation of the lymphovenous valves." Genes Dev **25**(20): 2187-97.

Steffensen, K. R., E. Holter, *et al*. (2004). "Functional conservation of interactions between a homeodomain cofactor and a mammalian FTZ-F1 homologue." EMBO Rep **5**(6): 613-9.

Tammela, T. and K. Alitalo (2010). "Lymphangiogenesis: Molecular mechanisms and future promise." Cell **140**(4): 460-76.

Tammela, T., G. Zarkada, *et al*. (2008). "Blocking VEGFR-3 suppresses angiogenic sprouting and vascular network formation." Nature **454**(7204): 656-60.

Van den Eynde, M. (2009). "Treatment of colorectal liver metastases: a review." Rev Recent Clin Trials **4**(1): 56-62.

Villen, J., S. A. Beausoleil, *et al*. (2007). "Large-scale phosphorylation analysis of mouse liver." Proc Natl Acad Sci U S A **104**(5): 1488-93.

Walsh, C. T., S. Garneau-Tsodikova, *et al*. (2005). "Protein posttranslational modifications: the chemistry of proteome diversifications." Angew Chem Int Ed Engl **44**(45): 7342-72.

Wang, J., G. Kilic, *et al*. (2005). "Prox1 activity controls pancreas morphogenesis and participates in the production of "secondary transition" pancreatic endocrine cells." Dev Biol **286**(1): 182-94.

Wang, Y. and G. Oliver (2010). "Current views on the function of the lymphatic vasculature in health and disease." Genes Dev **24**(19): 2115-26.

Warren, A. G., H. Brorson, *et al*. (2007). "Lymphedema: a comprehensive review." Ann Plast Surg **59**(4): 464-72.

Wigle, J. T., K. Chowdhury, *et al*. (1999). "Prox1 function is crucial for mouse lens-fibre elongation." Nat Genet **21**(3): 318-22.

Wigle, J. T., N. Harvey, *et al*. (2002). "An essential role for Prox1 in the induction of the lymphatic endothelial cell phenotype." Embo J **21**(7): 1505-13.

Wigle, J. T. and G. Oliver (1999). "Prox1 function is required for the development of the murine lymphatic system." Cell **98**(6): 769-78.

Won, K. A. and S. I. Reed (1996). "Activation of cyclin E/CDK2 is coupled to site-specific autophosphorylation and ubiquitin-dependent degradation of cyclin E." Embo J **15**(16): 4182-93.

Wu, X. and N. F. Liu (2011). "FOXC2 transcription factor: a novel regulator of lymphangiogenesis." Lymphology **44**(1): 35-41.

Yamazaki, T., Y. Yoshimatsu, *et al*. (2009). "COUP-TFII regulates the functions of Prox1 in lymphatic endothelial cells through direct interaction." Genes Cells **14**(3): 425-34.

Yoshimatsu, Y., T. Yamazaki, *et al*. (2011). "Ets family members induce lymphangiogenesis through physical and functional interaction with Prox1." J Cell Sci **124**(Pt 16): 2753-62.

You, L. R., F. J. Lin, *et al*. (2005). "Suppression of Notch signalling by the COUP-TFII transcription factor regulates vein identity." Nature **435**(7038): 98-104.

Zhuo, S., J. C. Clemens, *et al*. (1993). "Expression, purification, crystallization, and biochemical characterization of a recombinant protein phosphatase." J Biol Chem **268**(24): 17754-61.